

# CEMENTING OF GEOTHERMAL WELLS

PROGRESS REPORT NO. 11  
OCTOBER - DECEMBER 1978

Contributors:

L.E. Kukacka	E.R. Fuller <sup>1</sup>
J. Fontana	A. Zeldin
T. Sugama	N. Carciello
T.J. Rockett <sup>2</sup>	W. Reams
R.S. Kalyoncu <sup>4</sup>	B.E. Simpson <sup>3</sup>
D.K. Curtice <sup>6</sup>	D.M. Roy <sup>5</sup>

NOTICE

This report was prepared as an account of work sponsored by the United States Government. Neither the United States nor the United States Department of Energy, nor any of their employees, nor any of their contractors, subcontractors, or their employees, makes any warranty, express or implied, or assumes any legal liability or responsibility for the accuracy, completeness or usefulness of any information, apparatus, product or process disclosed, or represents that its use would not infringe privately owned rights.

WORK PERFORMED FOR THE  
DIVISION OF GEOTHERMAL ENERGY  
U.S. DEPARTMENT OF ENERGY  
WASHINGTON, D.C. 20545

1. National Bureau of Standards
2. University of Rhode Island
3. Dowell Division of Dow Chemical

4. Battelle's Columbus Laboratories
5. Pennsylvania State University
6. Southwest Research Institute

M. STEINBERG, Head  
L.E. KUKACKA, Project Leader

PROCESS SCIENCES DIVISION  
DEPARTMENT OF ENERGY AND ENVIRONMENT

BROOKHAVEN NATIONAL LABORATORY  
UPTON, NEW YORK 11973

## **DISCLAIMER**

**This report was prepared as an account of work sponsored by an agency of the United States Government. Neither the United States Government nor any agency Thereof, nor any of their employees, makes any warranty, express or implied, or assumes any legal liability or responsibility for the accuracy, completeness, or usefulness of any information, apparatus, product, or process disclosed, or represents that its use would not infringe privately owned rights. Reference herein to any specific commercial product, process, or service by trade name, trademark, manufacturer, or otherwise does not necessarily constitute or imply its endorsement, recommendation, or favoring by the United States Government or any agency thereof. The views and opinions of authors expressed herein do not necessarily state or reflect those of the United States Government or any agency thereof.**

## **DISCLAIMER**

**Portions of this document may be illegible in electronic image products. Images are produced from the best available original document.**

## NOTICE

This report was prepared as an account of work sponsored by the United States Government. Neither the United States nor the United States Department of Energy (DOE), nor any of their employees, nor any of their contractors, subcontractors, or their employees, makes any warranty, express or implied, or assumes any legal liability or responsibility for the accuracy, completeness or usefulness of any information, apparatus, product or process disclosed, or represents that its use would not infringe privately owned rights.

Printed in the United States of America  
Available from  
National Technical Information Service  
U.S. Department of Commerce  
5285 Port Royal Road  
Springfield, VA 22161  
Price: Printed Copy \$8.00; Microfiche \$3.00

June 1979

540 copies

Table of Contents

	<u>Page</u>
Forward . . . . .	iv
Summary . . . . .	v
Introduction . . . . .	1
Program Management Plan . . . . .	3
Selection of Well Cementing Materials . . . . .	4
Polymer Cements . . . . .	4
Aggregate Composition . . . . .	14
Inorganic Cements . . . . .	25
Colorado School of Mines . . . . .	25
Dowell Division of Dow Chemical . . . . .	25
Battelle's Columbus Laboratories . . . . .	26
Pennsylvania State University . . . . .	28
Southwest Research Institute . . . . .	29
University of Rhode Island . . . . .	30
Mechanical, Physical, and Chemical Resistance Property Measurements . . . . .	30
Placement Technology . . . . .	32
Administrative . . . . .	32
References . . . . .	34
Appendices	
Appendix 1 - Fourth quarterly report, Dowell Division of Dow Chemical	
Appendix 2 - Fifth quarterly report, Battelle's Columbus Laboratories	
Appendix 3 - Fifth quarterly report, Pennsylvania State University	
Appendix 4 - Fifth quarterly report, Southwest Research Institute	
Appendix 5 - Sixth quarterly report, University of Rhode Island	

## Foreword

A coordinated program for the development of improved cements specifically designed for geothermal well applications was started in April 1976. Since that time an assessment of the state of the art of well cementing has been made, a management plan prepared, research on organic and inorganic cementing materials started and property verification tests initiated. One research study has been completed. Work accomplished during the period October 1 - December 31, 1978 is described in the current report.

### Summary

Work to implement the program plan for the development of improved high temperature cementing materials for geothermal wells is continuing. Research work is currently in progress at Brookhaven National Laboratory, Battelle's Columbus Laboratories, Dowell, Pennsylvania State University, Southwest Research Institute, University of Rhode Island and the National Bureau of Standards. Experimental work has been completed at the Colorado School of Mines and a final report is being prepared.

The second meeting of the American Petroleum Institute's Task Group on geothermal cements which serves as a review group for the DOE/DGE program, was scheduled for January 24-25, 1979.

Phase II of Dowell's program is continuing. Three, 6 and 24 mo field tests were started at East Mesa and approval was received to start tests at Niland. In a one month "shake-down" test at East Mesa, 32 cement formulations were exposed to flowing brine at 150°C and 95 psig. Based upon the results from this test, 15 formulations were selected for evaluation in a 2 year test.

Experimental work at Battelle's Columbus Laboratories indicates that none of the cements under consideration cause severe corrosion to steel casing. Compared with the possible corrosive attack on the steel casing by the geothermal environment, the corrosive effects of the cement are minimal.

A promising cementing composition has been sent to the National Bureau of Standards for additional tests, and at least one more composition will be submitted.

Pumpability tests performed on hydrothermal cements developed at Southwest Research Institute indicate several formulations that are pumpable for at least 2 hr at 316°C.

At BNL, polymer concrete samples containing 50 wt% styrene - 35 wt% acrylonitrile - 5 wt% acrylamide - 10 wt% divinyl benzene have not shown any reduction in strength after exposure to 25% brine at 240°C for 8 months. This is the highest strength formulation to date and is the first formulation that has not exhibited any strength reduction after brine exposure. Strengths of 204 MPa and 162 MPa were measured at 20° and 150°C, respectively, after 8 months in brine.

## Cementing of Geothermal Wells

Progress Report No. 11

October - December 1978

### Introduction

The Division of Geothermal Energy of the U.S. Department of Energy, is sponsoring a research program to develop improved cementing materials for use in the completion of geothermal wells. The motivation for the program stems from an assessment that the economics of geothermal power could be improved significantly if better materials are developed.

It is estimated that for use in geothermal wells, cementing materials with the following characteristics are needed:

1. Compressive strength, > 1000 psi 24 hours after placement.
2. Permeability to water, < 0.1 milli Darcy.
3. Bond strength to steel casing, > 10 psi.
4. Stability, no significant reduction in strength or increase in permeability after prolonged exposure at 400°C to 25% brine solutions, flashing brine, or dry steam.
5. Placement ability, capable of 3 to 4 hr retardation at expected placement temperatures.
6. Compatibility of the cement with drilling mud.
7. Noncorrosive to steel well casing.

The Process Sciences Division of the Department of Energy and Environment at BNL is assisting the Division of Geothermal Energy (DGE) in developing and managing a program that will result in the development of materials meeting the criteria listed above. The program represents an integrated approach to the definition, development, and implementation of the work. A successful development of improved materials will lead to a major advance in the technology required to economically utilize geothermal energy.



The goals for the overall program are as follows:

1. Preparation of an integrated research and development plan for the investigation of new well-cementing materials specifically designed for geothermal well applications.
2. Establishment of the technical basis for the development, testing, and practical demonstration of high-temperature cementing materials for geothermal wells.
3. Rapid transfer and implementation of the technology in the private sector.

The program goals are being achieved by performance of the following tasks: 1) development of well-cementing materials capable of withstanding the environmental conditions in geothermal wells, 2) performance of pilot-scale testing and analysis of the cementing materials at well down-hole conditions, 3) development of the technology required to mix, pump, and place the cementing materials, 4) demonstration of the process by the cementing of prototype wells, 5) performance of cost analyses to determine the economic viability of the cementing systems under investigation, 6) involvement of the well-cementing service industry and well owners in all phases of the program in order to provide a technical basis for the rapid implementation of the technology, and 7) preparation of a compressive, high-temperature geothermal well-cementing manual which will include details of down-hole equipment, pumps, cement properties, and field examples.

Planning work to organize and develop a management plan designed to meet the above objectives was started in April 1976. Experimental work was started in July 1976. The work at BNL involves in-house research on polymer concrete cementing materials as well as full management of an integrated program involving contract research and industrial participation.

This report constitutes the eleventh in a series of quarterly reports describing work on the program. Accomplishments during the period October-December 1978 are summarized below. During the quarter work has continued in Tasks 1, 2, 3, 4, and 7. Work on other tasks will commence as the research work progresses.

Task 1. Program Management Plan

The need for DOE to sponsor a program to develop improved geothermal cementing materials was ascertained by evaluating information obtained from well owners, cementing service companies, and governmental and private research organizations. The consensus of those contacted was that the program should be a cooperative one performed on a cost-sharing basis with well cementing service companies and well owners. It was also established that the focal point of the program should be a series of down-hole test facilities. The tests should be performed in several geothermal environments but the highest priority for near-term (approximately 10 yr) application should be given to medium salinity brines at temperatures up to 400°C.

In an earlier report,<sup>1</sup> an outline of the approved management plan was presented. The program consists of the following elements: problem definition, materials development, property verification, down-hole testing, and the use of the cements in completing demonstration wells. The problem definition element has been completed and work is progressing in the materials development and property verification phases. Pumpability tests have been performed on several promising cement systems. Plans are being formulated for down-hole testing. Organizations currently participating in the program are as follows:

Problem definition, Dowell Division of Dow Chemical Co.

Materials development, Battelle's Columbus Laboratories

Brookhaven National Laboratory

Colorado School of Mines

Dowell Division of Dow Chemical Co.

Pennsylvania State University

Southwest Research Institute

University of Rhode Island

Property verification, National Bureau of Standards

The experimental phase of the Colorado School of Mines program was completed in September 1978 and the final report is being written. All other parts in the materials development phase will be completed by September 30, 1979.

As a means of obtaining technical guidance for the overall program and to assist in the technology transfer process and in the establishment of standards, BNL organized a "Geothermal Well Cement Advisory Panel" which was subsequently affiliated with the American Petroleum Institute (API) as a Task Group of the Committee on Standardization of Oil Well Cements. The API Committee Chairman is Mr. H.J. Beach of the Gulf Research and Development Company. Mr. J.P. Gallus of Union Oil of California is Chairman of the Task Group. The second meeting of the Task Group will be in Houston, Texas on January 24-25, 1979.

## Task 2. Selection of Well Cementing Materials

Work is being performed in this task to identify, evaluate and select high temperature well cementing materials.

### 2.1 Polymer Cements

During the current report period work was started on the development of PC containing organosiloxane (OS) and work on the pumpability of crosslinked mixtures of styrene (St), acrylonitrile (ACN), acrylamide (Aa), and methacrylamide (MAa) was continued. Work to study interactions between polymers and inorganic fillers was also continued. Previous work indicated that significant improvements in properties could be obtained by the use of reactive filler materials.

Organosiloxanes are chemically resistant and can be made hydrothermally stable by crosslinking. Both properties are very important for geothermal applications.

In an earlier report<sup>2</sup> initial studies to determine the thermal and hydrolytic stability and strength of PC specimens containing organosiloxanes were described. Two organosiloxanes, Union Carbide Y-9208 and Rhodia Corporation RZ, were used in these tests. Based upon the encouraging results obtained, work to optimize the monomer and aggregate systems was started. The work performed to date is summarized below.

### Sand Particle Size

The particle size of the silica sand used in PC containing organosiloxanes has an effect on the properties of the composite and is dependent upon the viscosity of the monomer. The best results for the organic binders which have viscosities close to the viscosity of water, were obtained when a mixture of sand sizes was used. In this case, the low viscosity monomer could easily be mixed with the filler to wet the particles and to fill the voids in the aggregate. When the viscosity of the monomer mixture is increased, the percentage of filler that the monomer wets decreases. The result, therefore, is nonuniform polymer loading which decreases the durability and strength. The effect of sand particle size on the compressive strength of the organosiloxane PC is illustrated in Table 1.

For a 75 wt% organosiloxane - 25 wt% styrene mixture, decreasing the particle size from 600um to < 30 um resulted in an increase in strength from 4.7 to 41.6 MPa. The addition of portland cement to the aggregate results in further strength improvement. When 10 wt% Type III portland cement was added to the filler, the compressive strength increased to 85.2 MPa.

### Type of Cement

As was indicated above, the addition of cement significantly improves the strength and durability of siloxane PC composites. A study to determine the influence of various types of cement on the properties of PC is in progress. Four different commercially available types of cement which were included as a partial constituent of the aggregate were tested.

The properties of PC as a function of cement type are summarized in Table 2 for a 75 wt% Y-9208-25 wt% styrene monomer system and in Table 3 for 97 wt% RZ-3 wt% V47 system. PC samples containing Type I and II cements in conjunction with the Y-9208-styrene monomer system had high strengths (Figure 1). Type II cement used with the RZ-V47 system also yielded high strength (Figure 2). The sand-cement ratios were 90 to 10 and 95 to 5, respectively. The amount of water absorbed was lowest for samples containing Type III and V cement (Figure 1 and 2).

Table 1  
Compressive Strength of Organosiloxane as  
a Function of Sand Particle Size

Monomer composition, wt%		Aggregate composition		Compressive strength, MPa
OS	St	wt%	Sieve opening, $\mu\text{m}$	
75	25	100	< 30	41.6
75	25	100	150	12.5
75	25	100	600	4.7
75	25	90 10 Type III cement	< 30	85.2
75	25	90 10 Type III cement	150	31.6
75	25	90 10 Type III cement	600	21.8
75	25	36* 17 17 30 Type III cement	1180 600 150	40.3

OS, Organosiloxane

St, Styrene

\* Aggregate composition, used for organic systems.

Composite composition, 26 wt% monomer - 74 wt% aggregate.

Table 2  
Properties of Siloxane PC as a Function of Cement Type

Aggregate composition, wt%		Cement type	Boiling H <sub>2</sub> O absorption, %	Compressive strength, MPa	Modulus of elasticity, MPa
Sand <sup>a</sup>	Cement				
90	10	I	0.075	111.8	6500
		II	0.072	46.6	4301
		III	0.03	119.3	5175
		V	0.02	100.7	4825
80	20	I	0.12	66.2	--
		II	0.05	63.8	--
		III	0.06	42.5	--
		V	0.07	95.1	--
70	30	I	0.09	60	--
		II	0.08	105.3	--
		III	0.12	73.8	--
		V	0.05	104.2	--

Monomer composition, 75 wt% Y-9208 - 25 wt% styrene.  
 Curing agent, 1.0 wt% di-tert-butyl peroxide.  
 Curing condition, 110°C - 18 hr, 165°C - 4 hr.  
 a, particle size, sieve opening < 30 um.  
 Composite composition, 26 wt% monomer - 74 wt% aggregate.

Table 3  
Properties of Siloxane PC as a Function of Cement Type

Aggregate composition, wt%		Cement type	Boiling H <sub>2</sub> O absorption, %	Compressive strength, MPa	Modulus of elasticity, MPa
Sand <sup>a</sup>	Cement				
95	5	I	0.06	81	--
		II	0.09	111.2	--
		III	0.1	70.5	--
		V	0.09	49.1	--
90	10	I	0.07	106.9	6826
		II	0.08	101.6	--
		III	0.05	52.9	6791
		V	0.11	74.39	7526
85	15	I	0.11	86.1	--
		II	0.08	102.9	--
		III	0.08	72.2	--
		V	0.13	70.85	--
80	20	I	0.22	47.5	--
		II	0.12	71.6	--
		III	0.19	72.7	--
		V	0.14	68.2	--

a, particle size, sieve opening < 30 um.  
 Monomer composition, 97 wt% RZ - 3.0 wt% V47.  
 Curing agent, 1.0 wt% di-tert-butyl peroxide.  
 Curing condition, 110°C - 18 hr, 135°C - 3 hr, 170°C - 2 hr.  
 Composite composition, 26 wt% monomer - 74 wt% aggregate.

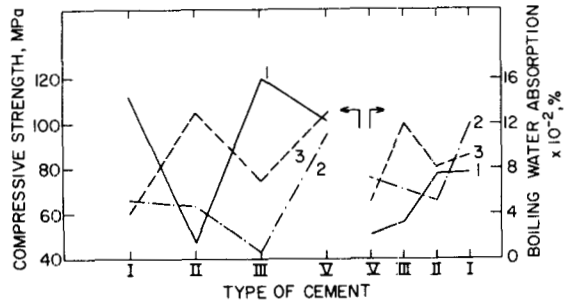


Figure 1. Compressive strength and boiling water absorption as a function of cement type. Monomer composition, 75 wt% Y-9208 - 25 wt% St. Sand-cement ratio, 1-90:10, 2-80:20, and 3-70:30.

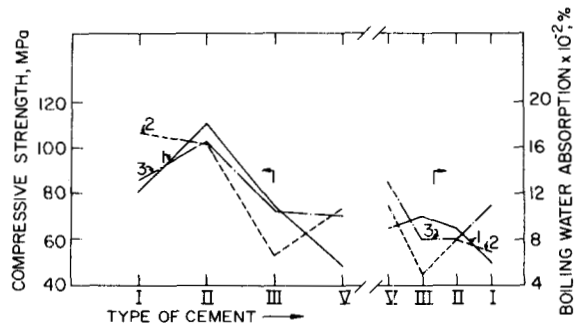


Figure 2. Compressive strength and boiling water absorption as a function of cement type. Monomer composition, 97 wt% RZ - 3 wt% V47. Sand-cement ratio, 1-95:5, 2-90:10, and 3-85:15.



Stress-strain curves (Figure 3 and 4) indicate that PC samples containing Type I and II cement are more brittle than PC containing the other cements. This brittleness can be reduced slightly using Type III cement. Greater reductions can be obtained using Type V cement. The reasons for this effect is probably due to the differences in the chemical composition of the cements.

Additional work is being performed to determine if the elasticity of the composite can be altered to the extent that the material will have elastomeric properties at high temperature. If so, applications as sealing materials are feasible.

#### Sand-Cement Ratio

Studies are also in progress to determine the optimum ratio of sand to cement that should be used in the composites. The results from compressive strength tests made before and after exposure of samples in autoclaves to brine at temperatures of 275°C and 300°C are summarized in Table 4.

The data indicate that PC samples containing cement up to a concentration of 15% are stable after exposure to brine at 275°C. Only the composites containing sand and cement in ratios of 95 to 5 and 90 to 10 showed stability at 300°C. Figure 5 shows several samples after exposure for 30 days in an autoclave at 300°C.

Infrared spectroscopy analyses (see Figure 6) and scanning electron microscopy studies of the structure of the PC before and after exposure to brine at 300°C did not indicate changes in structure and composition. The electron microscopy indicated fragments of resin adhering to the filler surfaces. These observations support the possibility of chemical bonding between the resin and the calcium silicate compounds of portland cement.

The results to date indicate that the optimum properties for either of the two organosiloxane systems tested (75 wt% Y-9208 - 25 wt% styrene or 97 wt% RZ-3 wt% V47) occur when an aggregate consisting of < 30 um silica flour is used in conjunction with Type II or III portland cement in a ratio of 90/10 or 95/5.

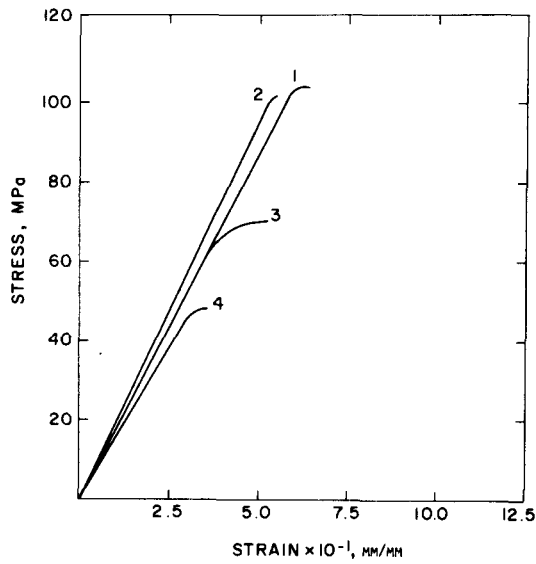


Figure 3. Compressive stress-strain curves for siloxane PC after preparation as a function of cement type. Monomer composition, 75 wt% Y-9208 - 25 wt% styrene. Aggregate composition, 90 wt% flour sand - 10 wt% cement. 1-Type I cement, 2-Type II cement, 3-Type III cement, and 4-Type V cement.

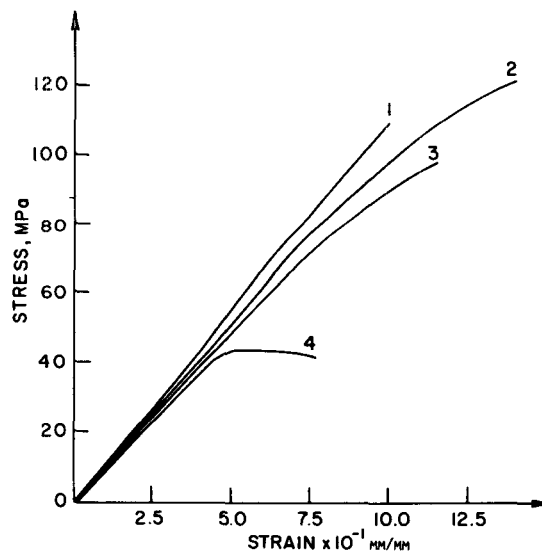


Figure 4. Compressive stress-strain curves for siloxane PC after preparation as a function of cement type. Monomer composition, 97 wt% RZ - 3 wt% V47. Aggregate composition, 90 wt% flour sand - 10 wt% cement. 1-Type I cement, 2-Type II cement, 3-Type III cement, and 4-Type V cement.

Table 4

Sand-Cement Ratio for System RZ-V47 (Ratio 97:3)

Aggregate ratio, wt%		Boiling water absorption, wt%	Compressive strength, MPa, after			Modulus of elasticity, MPa After exposure to hot brine for 30 days at 300°C
Sand <sup>a</sup>	Cement <sup>b</sup>		Boiling water	30 days in autoclave at 275°C	30 days in autoclave at 300°	
100	0	0.02	49.9	48.3	--	--
95	5	0.08	74.2	55.9	79.6	8845
90	10	0.07	90.2	69.7	57.1	7963
85	15	0.04	36.2	40.6	--	--
80	20	0.54	15.2	weak	--	--
70	30	0.69	34.2	weak	--	--
95 <sup>c</sup>	5	0.09	89.1	48.5	60.9	9100
90 <sup>c</sup>	10	0.12	46.4	107.2	62.8	5460

Initiator, 1/2 wt% DTBP, 1/2 wt% Silane A-174.

Curing condition, 125°C - 16 hr

150°C - 3 hr

180°C - 3 hr

a, particle size, sieve opening &lt; 30 um.

b, portland cement Type III.

c, These samples were made by using wetting agent.

Composite composition, 26 wt% monomer - 74 wt% aggregate.

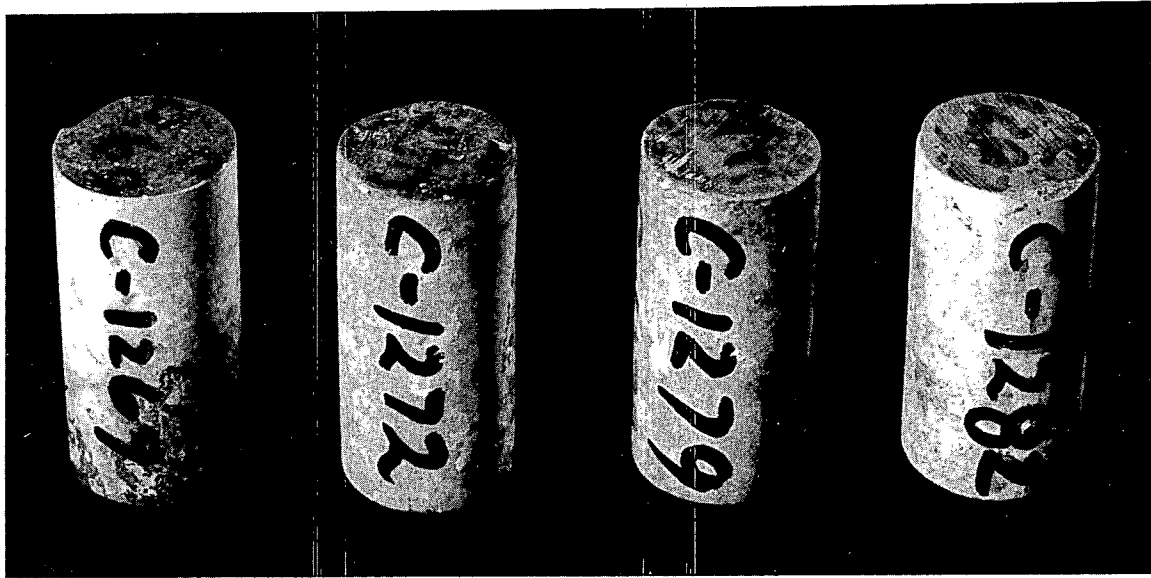


Figure 5. PC samples after exposure to brine at 300°C.

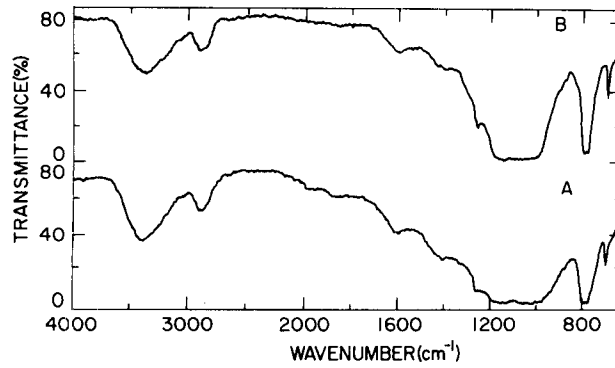


Figure 6. Infrared absorption spectra of siloxane PC samples before (A) and after (B) exposure to brine at 300°C.

## 2.2 Aggregate Composition

In the previous report,<sup>3</sup> initial results from a study to determine the effects of tricalcium silicate ( $C_3S$ ) on the thermal stability of condensation-type polymers such as phenol formaldehyde (PFR), epoxy and furan resins, were given. It was apparent from Differential Scanning Calorimeter (DSC) and Infrared (IR) spectroscopic analyses that  $C_3S$  has a significant effect on the thermal stability of PFR PC as a result of a reaction between the  $C_3S$  and the highly polar hydroxyl group in the PFR molecule. In addition, IR absorption bands of condensation - and vinyl addition - type PC after exposure to hot brine indicated that hydrated  $C_3S$  was produced.

During the current report period, the effect of  $C_3S$  on the thermal stability of PFR and vinyl-type copolymers was clarified further by mechanical and physical property measurements. Also, in order to obtain additional information regarding the hydration products of  $C_3S$  in PFR - and vinyl-type PC, X-ray diffraction and Scanning Electron Micrograph (SEM) measurements were performed on control samples and sections taken near the surface and of samples after exposure to 25% brine at 240°C for 10 days.

The compressive strength and changes in weight and diameter of PC containing three condensation-type polymers, after exposure to a 25% brine solution at 240°C for 30 days, are given in Table 5. Two aggregate additives,  $C_3S$  and silica flour, were evaluated.

Weight change data indicate that all of the systems tested except the PFR- $C_3S$  PC, exhibited losses after exposure to hot brine. The weight gain (2.96%) for the PFR- $C_3S$  suggests that hydrated  $C_3S$  was produced by reaction with the hot brine solution. Based upon the weight loss exhibited by the PFR-SiO<sub>2</sub> PC, it is probable that the resin exhibited some thermal degradation at the test conditions. However, the combination of slight polymer thermal degradation and  $C_3S$  hydration products resulted in a net weight increase. The increases in the diameter of the PFR samples that were noted, also indicate that some degradation of the resin occurred.

Table 5  
Stability of Condensation Polymer Concretes Containing C<sub>3</sub>S or SiO<sub>2</sub> After Exposure  
for 10 Days to 25% Brine at 238°C

Composition <sup>a</sup>	Change in		Compressive Strength <sup>b</sup> psi, (MPa)	
	Weight, %	Diameter, %	Before exposure	After exposure
24 wt% PFR-61 wt% S-15 wt% C <sub>3</sub> S	+ 2.96	+ 0.54	12,785 (84.0)	11,200 (77.2)
24 wt% PFR-61 wt% S-15 wt% SiO <sub>2</sub>	- 0.65	+ 0.29	6,950 (47.9)	4,031 (27.8)
22 wt% Epoxy-62 wt% S-16 wt% C <sub>3</sub> S	-11.46	--c	7,143 (49.2)	--c
20 wt% Epoxy-64 wt% S-16 wt% SiO <sub>2</sub>	-10.88	--c	7,345 (50.6)	--c
22 wt% Furan-62 wt% S-16 wt% C <sub>3</sub> S	- 2.39	- 0.21	1,220 ( 8.4)	456 ( 3.1)
22 wt% Furan-62 wt% S-16 wt% SiO <sub>2</sub>	- 0.41	- 0.42	1,626 (11.2)	764 ( 5.3)

- a, S = 50 wt% #16 sand (size, 1.16 mm) - 25 wt% #30 sand (size, 0.595 mm) - 25 wt% #100 sand (size, 0.149 mm); SiO<sub>2</sub> = silica flour.  
b, Specimens, 2.2-cm-diam. x 4.4-cm-long cylinders.  
c, Failed (large expansion) and removed from test.

Epoxy resin PC specimens failed in the test as a result of the large expansion produced by the thermal decomposition of the polymer. The furan resin PC samples showed shrinkage varying from 0.21 to 0.42%.

Interesting results were obtained from the compressive strength measurements. Tests performed on samples before exposure to the hydrothermal conditions, indicated that the addition of  $C_3S$  to PC containing epoxy or furan resins had no apparent effect on the compressive strength. The strength of the PFR PC containing  $C_3S$  was approximately 1.8 times greater (84 MPa vs 47.9 MPa) than the sample containing silica flour.

After exposure to the hot brine, the effect of the  $C_3S$  addition to the PFR was more apparent. The sample containing  $C_3S$  decreased in strength by approximately 12% compared to an approximate 42% decrease for silica flour-filled specimens.

Under the same test conditions, the furan samples had strength reductions varying from 53% to 63%, indicating severe decomposition of the polymer. The presence of  $C_3S$  did not appear to enhance the durability of the material. The epoxy samples yielded similar results. The samples were severely cracked during the exposure and it was not possible to measure their strength.

Based upon the results from the above tests, it appears that the use of  $C_3S$  as a means of enhancing the hydrothermal stability of PC containing condensation-type polymers, can only be used for resins such as PFR which contain a highly polar hydroxyl group in the molecular chain.

Since Type III portland cement contains 52% to 60%  $C_3S$ , it represents a possible low-cost source of the material. Therefore, a series of tests were performed to determine if  $C_3S$  added in this form yielded results similar to those obtained by the use of the pure compound.

The compressive strengths of PFR PC containing  $C_3S$  added in the form of Type III portland cement are summarized in Figure 7. For purposes of comparison, samples containing silica flour are also included.

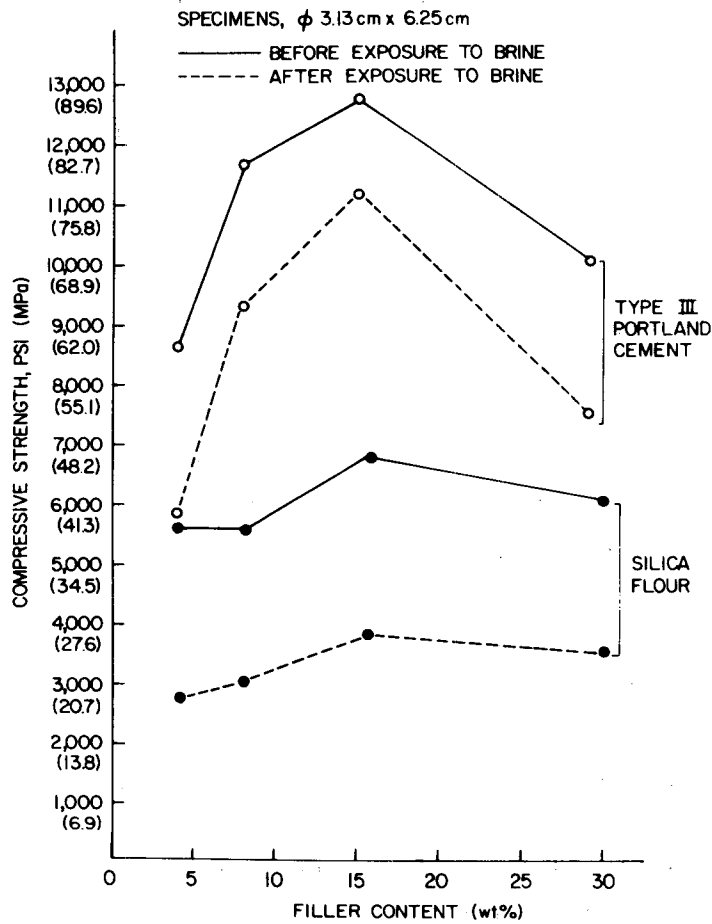


Figure 7. The effect of Type III portland cement on the compressive strength of PFR concrete specimens before and after exposure for 30 days to 25% brine at 240°C.



In the figure the compressive strength of PFR-PC containing Type III portland cement is shown to be considerably higher than for specimens containing silica flour. Similar trends were noted for samples exposed for 30 days to hydrothermal conditions. Specimens containing 15 wt% cement decreased in strength approximately 12% after 30 days in brine at 240°C, compared to a 44% decrease for samples containing 15 wt% silica flour. The concentration of silica flour in the PC had little effect on the compressive strength.

The condensation-type polymerization of PFR results in the formation of a porous material due to the by-products released during the curing process. When PFR is mixed with anhydrous cement to produce a PC which is subsequently exposed to hot water, only a part of this pore structure is filled by the hydration products. Therefore, before the composite can be used in high pressure hydrothermal processes, additional work to reduce the permeability is required. Studies to decrease permeability by further modification of the aggregate system and by co-polymerization of the PFR with other monomers, and to develop improved polymerization methods should be performed. These studies are currently in progress.

The results from compressive, bending and tensile strength measurements for vinyl-type PCs containing C<sub>3</sub>S, silica flour or calcium carbonate are given in Table 6. A mixture of vinyl-type monomers consisting of 55 wt% St, 36 wt% ACN, and 9 wt% trimethylolpropane trimethacrylate (TMPTMA) was used in the study. Polymerization was initiated by the use of 2 wt% benzoyl peroxide of 98% purity and subsequent heating at 85°C for 24 hr.

As indicated in Table 6, the compressive, bending and tensile strengths obtained by the addition of 17 wt% C<sub>3</sub>S to the PC were about 1.5 times higher than those obtained for specimens containing an equal amount of silica flour or calcium carbonate. Furthermore, the strength reductions for the C<sub>3</sub>S containing specimens, after exposure to hydrothermal conditions, were < 10%. Specimens containing silica flour and calcium carbonate had strength reductions > 40%.

Table 6

The Effect of  $C_3S$ ,  $SiO_2$  and  $CaCO_3$  on the Physical Properties of PC Before and After Exposure for 10 Days to 25% Brine at 240°C

Specimen No.	Composition <sup>a</sup>	Before Exposure to Brine				After Exposure to Brine			
		Compressive strength, psi (MPa) <sup>b</sup>	Bending strength, psi (MPa) <sup>c</sup>	Tensile strength, psi (MPa) <sup>b</sup>	Water Absorption, % <sup>d</sup>	Compressive strength, psi (MPa)	Bending strength, psi (MPa)	Tensile strength, psi (MPa)	Water Absorption %
1008	13% P-70% S-17% $C_3S$	16,487 (113.6)	3,900 (26.9)	1,614 (11.1)	0.89	15,426 (106.3)	3,563 (24.6)	1,588 (10.9)	1.22
1000	13% P-70% S-17% $SiO_2$	9,943 (68.5)	2,280 (15.7)	1,095 (7.5)	0.30	3,748 (25.8)	1,240 (8.5)	700 (4.8)	3.22
1012	13% P-70% S-17% $CaCO_3$	9,061 (62.4)	2,100 (14.5)	964 (6.6)	1.69	3,204 (22.1)	932 (6.4)	505 (3.5)	4.06

a, P = 55 wt% styrene-36 wt% acrylonitrile-9 wt% TMPTMA; S = 50 wt% #16 sand (size, 1.19 mm) - 25 wt% #30 sand (size, 0.595 mm) - 25 wt% #100 sand (size, 0.149 mm).

b, Specimens, 2.2-cm-diam. x 4.4-cm-long cylinders.

c, Specimens, 1.25-cm-square x 7.5-cm-long beams.

d, Water absorption in boiling water for 5 hours.

The water absorption of specimens containing 17 wt% C<sub>3</sub>S after exposure to hot brine was approximately 65% lower than those for specimens containing silica flour or calcium carbonate (see Table 6). This may be due to the hydration products of C<sub>3</sub>S formed during the brine exposure.

The results from stress-strain measurements performed on PC specimens before and after exposure to hot brine are given in Figure 8. The data indicate that unexposed specimens containing C<sub>3</sub>S had a high modulus of  $2.85 \times 10^4$  MPa and excellent ductility as indicated by the maximum strain of  $9.97 \times 10^{-3}$ . After exposure to the hydrothermal conditions, the curve is essentially a straight line, therefore indicating a brittle material. The maximum strain was reduced approximately 68%, compared to that before exposure. This indicates that the excellent ductility of the three dimensional copolymer structure used as a matrix is lost due to transformation of the polymer molecules during exposure to hot brine. The modulus of the C<sub>3</sub>S - filled specimens was observed to be almost the same value as that before exposure. This suggests that the presence of C<sub>3</sub>S may have two significant effects which tend to improve the strength and durability. The first is due to the hydration products of C<sub>3</sub>S formed during exposure to hydrothermal conditions and the second is the chemical interaction between the C<sub>3</sub>S and the polymer.

In order to determine if hydration products of C<sub>3</sub>S are formed in the hydrothermal environment, x-ray diffraction analyses were performed on sections taken near the surface of samples after exposure to hot brine. These results are given in Figures 9-11. Based upon the intense x-ray diffraction peaks at 3.03, 2.89, 2.82 and 2.08 Å, hydration products are apparent. The major hydration product of C<sub>3</sub>S appears to be  $3\text{CaO} \cdot \text{SiO}_2 \cdot 1.5 \text{H}_2\text{O}$  (abbreviated C<sub>3</sub>SH<sub>1.5</sub>). In addition, a small amount of  $\alpha\text{-C}_2\text{SH}$ , indicated by the weak peaks at 4.22, 3.27 and 2.41 Å is evident.

In the SEM study of PC containing C<sub>3</sub>S after exposure to hot brine, it appeared from the spiny network structure of hydrated C<sub>3</sub>S crystals

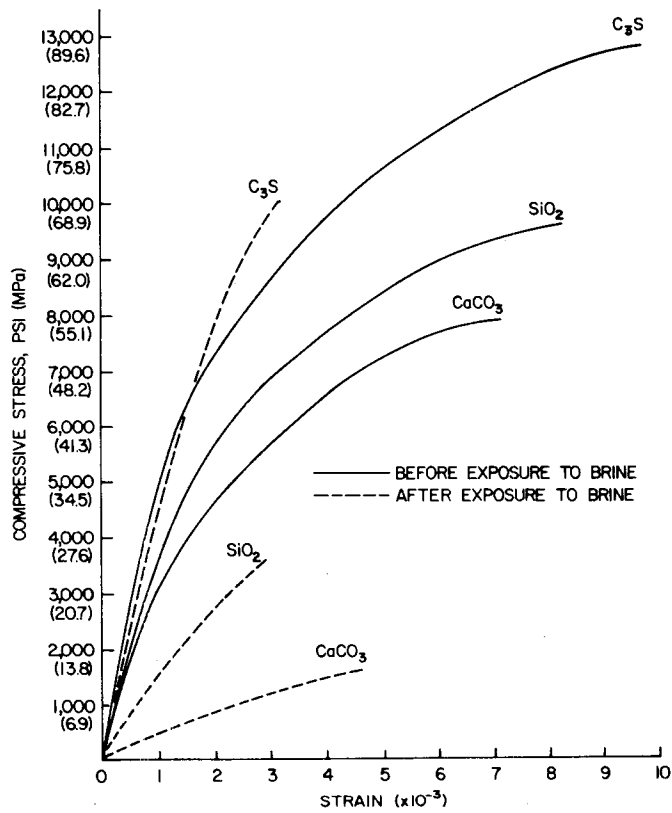


Figure 8. Stress-strain curves for PC containing C<sub>3</sub>S, SiO<sub>2</sub> and CaCO<sub>3</sub> before and after exposure to 25% brine at 240°C.

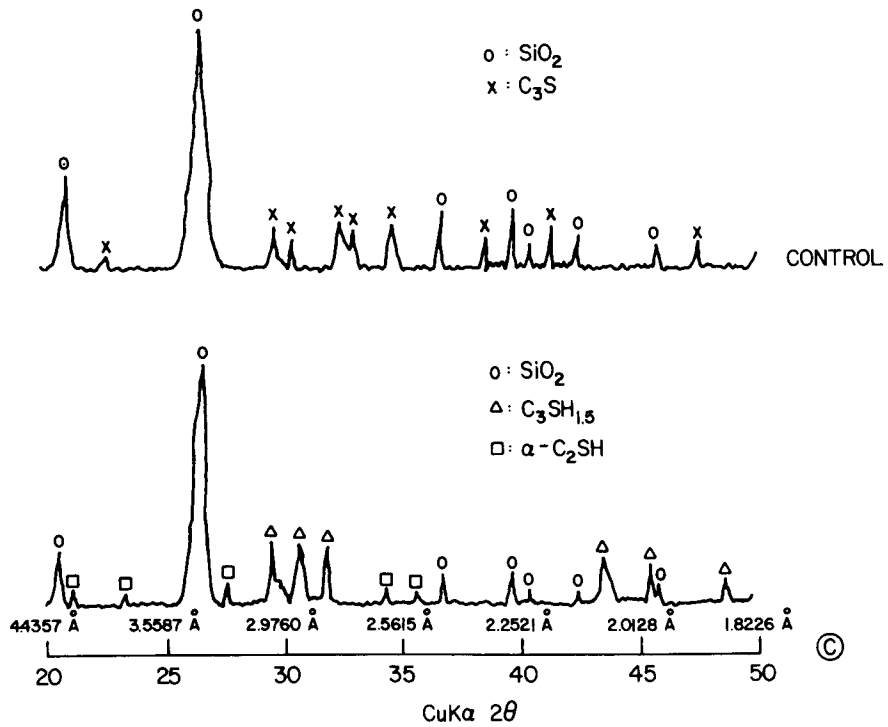


Figure 9. X-ray diffraction patterns for control and No. (C) samples.

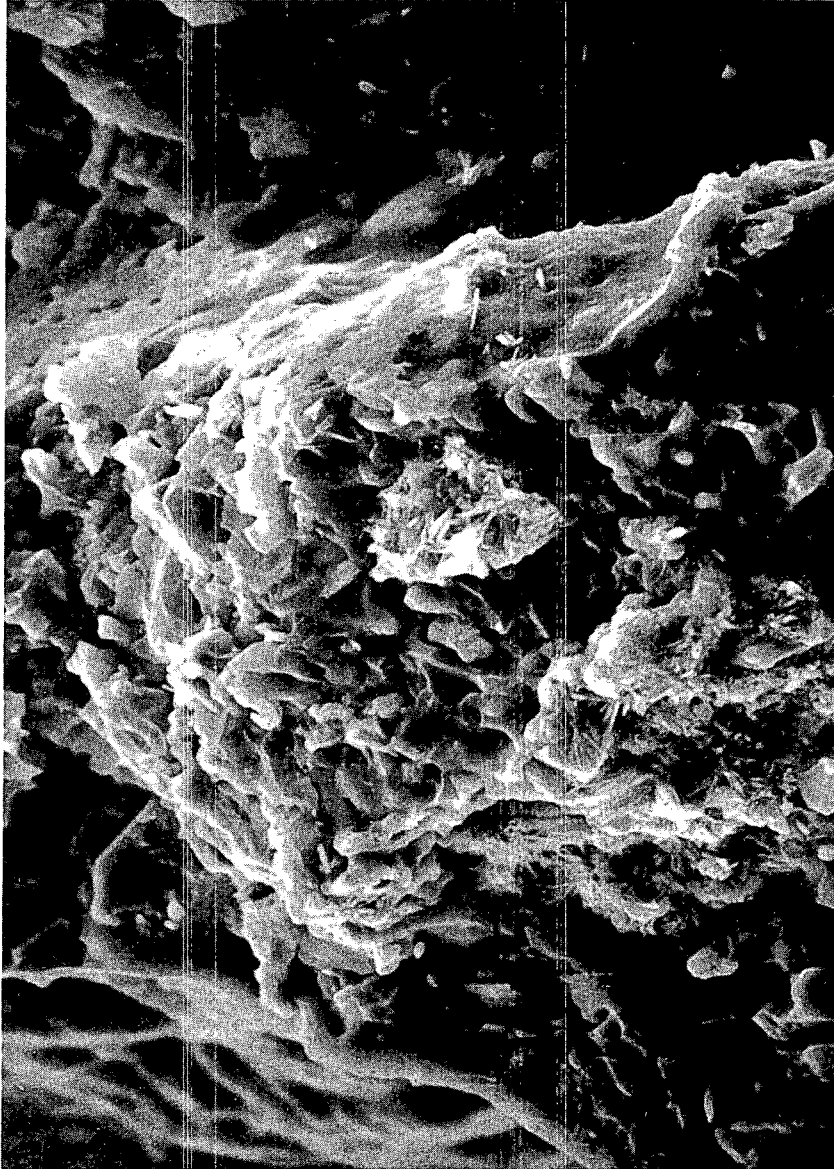


Figure 10. Low magnification scanning electron micrograph of PC showing hydration products of C<sub>3</sub>S.

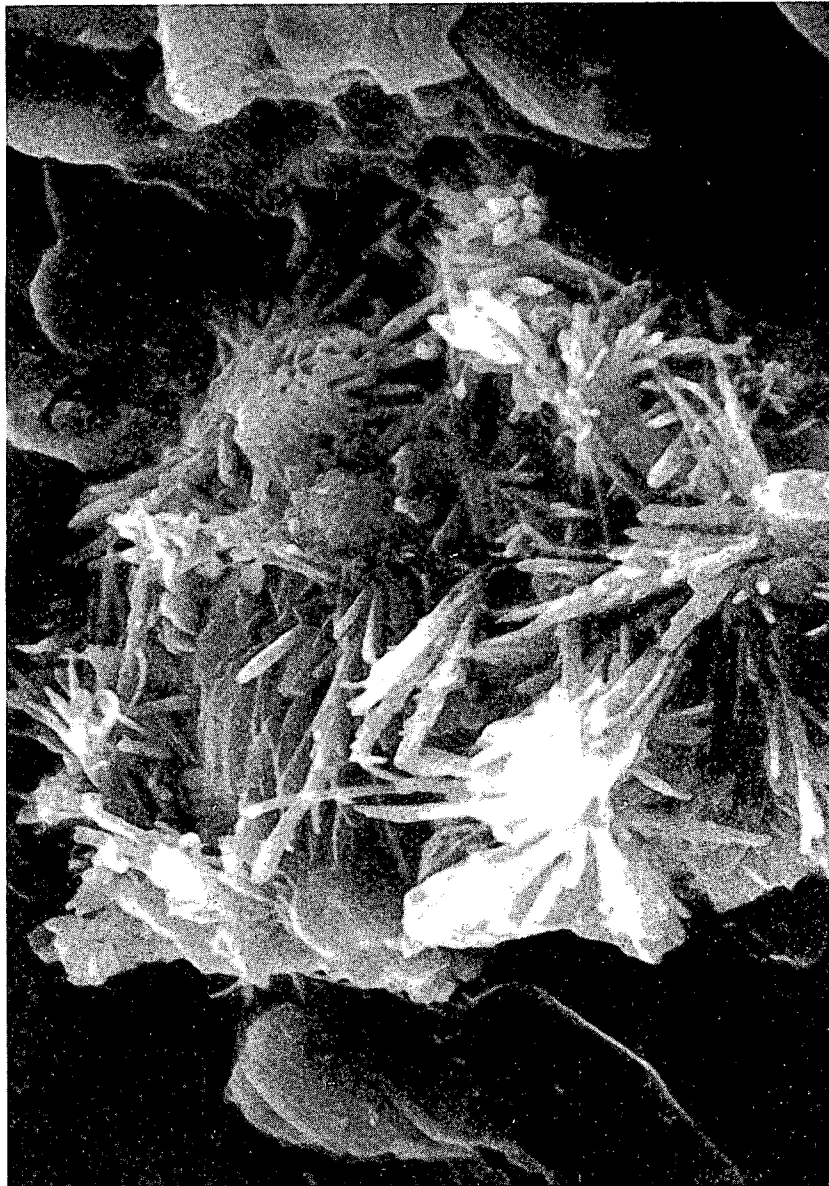


Figure 11. Higher magnification scanning electron micrograph of PC showing hydration products of  $C_3S$ .

that hydration products of  $C_3S$  were present in some places on the fractured surfaces of PC (see Figure 10). Figure 11 is an enlargement of the partial spiny network. As shown in Figure 11, the hydrated  $C_3S$  and polymer phase coexist. This can be seen from the picture where the hydrated  $C_3S$  crystals grow from the polymer phase as if from an arable land.

The results of studies on the bonding mechanism at the interface between polymer and calcium silicate compounds will be summarized in the next report.

### 2.3 Inorganic Cements

Research on high temperature cements has been completed at one institution and is in progress at five others. Short descriptions taken from the most recent progress report for each program are given below. The full reports are included in the Appendix.

#### Colorado School of Mines

G.L. Kalousek, Principal Investigator

Starting date, April 1977

Completion date, January 31, 1979

The most recent progress report was included in Report No. 9.<sup>4</sup> A final report for the program is nearing completion.

#### Dowell Division of Dow Chemical

B.E. Simpson, Principal Investigator

Starting date, July 1977

Completion date, July 1980

The Dowell effort is a three-phase program to develop completion systems for geothermal wells. In Phase I which has been completed,<sup>5</sup> a detailed definition of the problem was developed. Phase II is providing an evaluation of potential systems and the development of the best systems under the criteria developed in Phase I. The goal of Phase II is to develop a safe environmentally acceptable system which will provide both maximum energy recovery and well life. Materials are being examined to determine chemical composition and stability in relation to compressive strengths and permeabilities. Phase III will be the actual well testing of materials and systems developed in Phase II.



Phase II of the program has been continued during the quarter. Major progress has been made in several areas: mechanical property measurements, understanding of the polymerization reactions of furfuryl alcohol, completion of the dynamic brine exposure apparatus, studies on the effect of silica particle size on cement stability and commencement of field testing at East Mesa. Only minor progress was made in the chemical studies portion of the program due to problems encountered with new x-ray equipment. Also, written approval to test at the Nilands geothermal facility in Southern California has been obtained. The fourth progress report for this work is given in Appendix 1.

Battelle's Columbus Laboratories

R.S. Kalyoncu, Principal Investigator

Starting date, September 1977

Completion date, August 1979

The objectives of this research program are to evaluate the cementing materials currently used in geothermal applications and, based on the knowledge of this evaluation, to develop new materials which will meet the property requirements dictated by the thermal, mechanical and chemical environments encountered in geothermal wells.

The work plan of the research program comprises four phases, namely: (1) definition of the current state of knowledge regarding the cementing materials for geothermal applications and selection of materials and screening procedures for determination of the most promising cementing compositions; (2) selection of a list of materials, based on Phase I results, for laboratory evaluation and development and identification of material components most suitable in geothermal applications; (3) further evaluation and development of candidate materials through detailed studies of rheology, compressive strength, permeability, bond strength, compatibility with drilling muds, and characterization of the final products of hydration; and (4) preparation of a final report and the development of plans for further studies.

During the current report period compressive strength and cement-to-metal casing bond strength evaluations have essentially been completed. Occasional evaluations in these two tasks will be made on an as needed basis in the future.

Experimental efforts during the past 3 months have been concentrated on the evaluation of permeability of cements and corrosion of the metal casing by the cementing compositions. The permeability measurements were made starting at low pressure gradients (e.g. 172.4 KPa) and going to high values (689.5 KPa) and repeated on the same samples going from high (689.5 KPa) to low (172.4 KPa) pressure gradients. The purpose of determining the permeabilities in this manner was essentially to assess possible damage the high pressure gradient may cause to microstructure of the permeability specimens. The results (which are partially supported by preliminary microscopic observations) indicate that certain specimens do experience microstructural damage at 172.4 KPa pressure gradient. Based on the above observations the actual permeabilities of the cementing compositions are believed to be much lower than the experimentally determined values.

The corrosion behavior of the metal casing by the cementing media was studied through half-cell potential measurements and visual observations. Although the potential measurement technique does not provide useful qualitative data on the conditions (corrosive, non-corrosive) to which the steel casing is subjected, it does indicate that no severe corrosion to the steel casing is caused by the cementing medium. Compared with the possible corrosive attack on the steel casing by the geothermal environment, the corrosive effects of the cement are minimal.

A promising cementing composition has been sent to the National Bureau of Standards for additional tests, and at least one more composition will be submitted.

Most of the efforts for the duration of this program will be devoted to extensive characterization of the cementing compositions thus far studied. Those compositions which exhibited high strength, low permeability, and sufficiently long thickening times will be thoroughly characterized using SEM, DTA, light microscopy, and X-ray diffraction techniques. Details for these efforts are given in Appendix 2.

Pennsylvania State University

D.M. Roy, Principal Investigator

Starting date, September 1977

Completion date, September 1979

The objective of this research is to develop new high temperature cementing materials for geothermal wells. The work involves investigation of compositions which lie dominantly within the systems  $\text{CaO-Al}_2\text{O}_3\text{-SiO}_2\text{-H}_2\text{O}$  and  $\text{CaO-MgO-SiO}_2\text{-H}_2\text{O}$ .

The stabilities and phase equilibria of constituent phases for the above systems have been determined, using reaction times varying from two to 98 days, with temperatures in the range up to 300-400°C, and pressures from 1400-10,000 psi (9.6-68.9 MPa).

Xonotlite, anorthite, boehmite, hydrogarnets, wairakite, x-phase or hexagonal anorthite, and truscottite are among the phases present in the system  $\text{CaO-Al}_2\text{O}_3\text{-SiO}_2\text{-H}_2\text{O}$ . Xonotlite, truscottite, talc, chrysotile, monticellite, and diopside are formed in the  $\text{CaO-MgO-SiO}_2\text{-H}_2\text{O}$  system. In the latter compositions, reaction is slower, and thus attainment of equilibrium is more difficult.

Viscosities of slurries, studies of reaction rates, determination of strength and microhardness, permeability, bond strength to rock, corrosiveness, and the effect of saline solutions generally comprise the major parts of the study. Other characterization tools used are x-ray diffraction, optical microscopy, SEM, microprobe, DTA, TGA, thermal expansion, thermal conductivity, and other analytical techniques. Data obtained to date are given in Appendix 3.

Southwest Research Institute

D.K. Curtice, Principal Investigator

Starting date, October 1977

Completion date, October 1979

Hydrothermally cured cements are being developed for use in geothermal well completion systems. The cure of these cements is controlled by the ambient temperature with the initiation temperature and cure rate being controlled by the chemical composition. The cured cements have high strength, strong adhesion to steel, high temperature resistance, acid and general chemical resistance and other properties which distinguish them from portland or modified portland type cements.

The current program is to first optimize the existing cement formulations for the particular environmental conditions existing in geothermal wells, and then to provide the necessary laboratory test and evaluation program that is necessary to precede a field or downhole test program.

During the period of October 1 to December 31, 1978, various formulations of hydrothermal cements have been studied to optimize those which will be pumpable at temperatures up to at least 315°C or higher and set with good compressive and bond strengths. Physical tests and long-term aging have continued.

A short-term test program has been added, to determine the effects of thermal cycling on one of the SwRI 150°C hydrothermal cements. This cement is for possible use in the completion of a hot dry rock geothermal well at Fenton Hill, New Mexico. The data indicate that even through the bond might be broken during the cooling down and reheat of these wells, the SwRI formulation will reheat the bond, maintaining good adhesion to the casing formulation. Details for this work are given in Appendix 4.

University of Rhode Island

T.J. Rockett, Principal Investigator

Starting date, July 1977

Completion date, July 1979

The research plan is to develop unique phosphate cements which can be used to complete geothermal wells. Using two well proven cement technologies as a starting point, a glass frit is being developed which will react with a buffered phosphoric acid solution to form a calcium aluminophosphate cementing phase.

During the report period work was performed in two major task groups. The first set of tasks were related to the stability of silicate glasses in phosphate solutions, and the second set of tasks involved the equilibrium relationships in the system  $\text{CaO-Al}_2\text{O}_3\text{-P}_2\text{O}_5\text{-H}_2\text{O}$ .

These tasks were pursued to obtain basic information which will be used to design cement compositions to be tested for stability and strength at geothermal conditions. The overall goal is to generate a glass frit which when mixed with phosphoric acid will set to a cement. By understanding the corrosion of silicate glasses in phosphoric acid, a frit can be obtained which will interact at a controlled rate. By knowing the phases which form in the system  $\text{CaO-Al}_2\text{O}_3\text{-P}_2\text{O}_5\text{-H}_2\text{O}$  the composition of the glass may be tailored to yield a phase which when formed in the geothermal environment will remain stable. The sixth progress report for the project is given in Appendix 5.

Task 3. Mechanical, Physical and Chemical Resistance Property

Measurements

In conjunction with work performed in Task 2, tests to measure the mechanical, physical and chemical resistance properties of high temperature cementing materials are being conducted.

The results from compressive strength measurements made on PC specimens containing varying amounts of St, ACN, Aa and DVB after exposure to brine at  $238^\circ\text{C}$  for times up to 8 mo. are summarized in Table 7. Five compositions were evaluated. A PC containing a 50 wt% St,

Table 7

Compressive Strength of PC After Exposure to  
25% Brine at 238°C

Monomer composition, wt%				Compressive strength (MPa) after brine exposure, days						
<u>St</u>	<u>ACN</u>	<u>Aa</u>	<u>DVB</u>	<u>control</u>	<u>30</u>	<u>120</u>	<u>240</u>			
52.5	40	5	2.5	191.6 <sup>a</sup>	211.9 <sup>a</sup>	128.2 <sup>b</sup>	160.9 <sup>a</sup>	127.9 <sup>b</sup>	124.7 <sup>a</sup>	95.6 <sup>b</sup>
62.5	30	5	2.5	202.4	227.0	141.9	174.9	136.4	174.2	137.9
50	40	5	5	189.5	196.1	150.9	147.3	136.0	123.8	111.4
50	37.5	5	7.5	176.6	237.1	166.2	177.8	150.4	162.6	151.2
50	35	5	10	180.8	237.6	161.9 <sup>a</sup>	231.9	148.3	204.1	161.7

Composite composition, 11.5 wt% polymer - 88.5 wt% aggregate

St, styrene

ACN, acrylonitrile

Aa, acrylamide

DVB, divinyl benzene

a, tested at 20°C

b, tested at 150°C

each value is the average of 2 specimens

35 wt% ACN, 5 wt% Aa, 10 wt% DVB monomer mixture in conjunction with a 70 wt% sand, 30 wt% Type III portland cement aggregate exhibited the best durability. Compared to a control strength of 180.8 MPa, the compressive strength increased to 237.6 MPa after brine exposure for 30 days and has gradually decreased to 204.1 MPa after 240 days. Based upon studies on the effects of aggregate composition, the initial increase in strength upon brine exposure was probably due to C<sub>2</sub>S and C<sub>3</sub>S hydration products. The subsequent decrease is due to degradation of the polymer. This PC formulation has given the highest strength and durability to brine obtained to date.

Property verification tests on several candidate cements are in progress at the National Bureau of Standards. This work will serve to establish priorities for evaluation in proposed down-hole testing facilities. A progress report for this work was not prepared during the current period. The major effort during the period has been the preparation of recommended standardized test procedures for geothermal cements. These procedures will be reviewed at the API Task Group meetings scheduled for January and June 1979.

#### Task 4. Placement Technology

Pumpability tests performed on hydrothermal cements developed at Southwest Research Institute indicate several formulations that are pumpable for at least 2 hr at 316°C. This work is summarized in Appendix 4.

Studies to determine the pumpability of PC mixes are in progress at BNL. One St-ACN-Aa-DVB formulation appears pumpable at 75°C and 20.7 MPa pressure for 4 hr. Increasing the temperature to 80°C results in the formation of gell after approximately 3 hr.

#### Task 7. Administrative

During the current report period three "Project Status Reports" were submitted to DGE by each of the organizations participating in the program. A draft copy of Quarterly Progress Report No. 10<sup>3</sup> was prepared and circulated for review.

The following papers based upon the DOE/DGE national program were prepared for presentation at the meeting of the American Society of Petroleum Engineers of AIME scheduled for January 22-24, 1979 in Houston, Texas.

"Effect of Silica Particle Size on Degradation of Silica Stabilized Portland Cement" by L.H. Eilers and E.B. Nelson, Dowell Division of Dow Chemical.

"Potential New High Temperature Cements for Geothermal Wells" by D.M. Roy, E.L. White, C.A. Langton and M.W. Grutzeck, Pennsylvania State University.

A paper entitled "The Effect of Tricalcium Silicate on the Thermal Stability of Condensation-Type Polymer Concretes" by T. Sugama, L.E. Kukacka and W. Horn was submitted to the International Journal of Cement Composites for publication. Another paper, "High Temperature Polymer Concretes from Organosiloxane Resins" by A. Zeldin et al. has been accepted for publication by that journal.



#### References

1. Cementing of Geothermal Wells, Progress Report No. 2, July - September 1976, BNL 50578.
2. Alternate Materials of Construction for Geothermal Applications, Progress Report No. 16, April - September 1978, BNL 50925.
3. Cementing of Geothermal Wells, Progress Report No. 10, July - September 1978, BNL 50943.
4. Cementing of Geothermal Wells, Progress Report No. 9, April - June 1978, BNL 50911.
5. Cementing of Geothermal Wells, Progress Report No. 8, January - March 1978, BNL 50850.

Distribution

U.S. Department of Energy  
Division of Geothermal Energy

Bennie Dibona  
John Salisbury  
Morris Skalka  
Clifton McFarland  
Robert Reeber  
Barbara J. Mueller

Brookhaven National Laboratory

Kenneth C. Hoffman  
Lawrence Kukacka  
David Gurinsky  
David Schweller (DOE)  
Meyer Steinberg  
Warren E. Winsche  
Arkady Zeldin  
Robert Isler  
Daniel Van Rooyen  
Toshifumi Sugama

Battelle's Columbus Laboratories

Rustu S. Kalyoncu

Colorado School of Mines

George L. Kalousek

Dowell

B.E. Simpson

National Bureau of Standards

Edward R. Fuller

Pennsylvania State University

Della M. Roy

Southwest Research Institute

David K. Curtice

University of Rhode Island

Thomas J. Rockett

Los Alamos Scientific Laboratory

Roland A. Pettitt



APPENDIX 1



**DOWELL** DIVISION OF DOW CHEMICAL U.S.A.

COO/4190-5

DEVELOPMENT OF GEOTHERMAL WELL COMPLETION SYSTEMS

Phase II: Progress Report No. 4  
October - December, 1978

Contributors:

L. H. Eilers	E. B. Nelson
R. D. Foreman	L. B. Spangle
L. K. Moran	B. E. Simpson

work performed for the  
DIVISION OF GEOTHERMAL ENERGY  
U.S. DEPARTMENT OF ENERGY  
Washington, D.C. 20545

Dowell Division  
of Dow Chemical U.S.A.  
Tulsa, Oklahoma 74102

AN OPERATING UNIT OF THE DOW CHEMICAL COMPANY



## EXECUTIVE SUMMARY

Phase II of Dowell's DOE contract has continued this quarter. Major progress has been made in several areas: 1) continuing compressive strengths and bonding strengths as per the block diagram in Figure 1, 2) understanding the polymerization reactions of furfuryl alcohol, 3) completing the dynamic brine exposure testing apparatus (D-BETA), 4) expanding our knowledge of the effect of silica particle size on cement stability, and 5) completing the "shake-down" test portion of the East Mesa field study. Only minor progress has been made in the chemical studies portion of the program due to problems encountered with the new Philips x-ray equipment. Also, written approval to test at the Nilands geothermal facility in Southern California has been obtained.

## INTRODUCTION

Phase II of Dowell's contract research on behalf of the Department of Energy is continuing on schedule. This report documents work performed during the months October through December, 1978. Work is continuing on the Laboratory Screening Tests as per the block diagram in Figure 1 as well as on Stability Measurements and Chemical Measurements. Consideration is also being given to the idea of initiating tests to determine the ability of cements to withstand thermal shock. Other work included in this report are studies on furfuryl alcohol polymers. The furfuryl alcohol polymers fall into the category of non-portland systems. Once problems with these systems are overcome they will go through the Laboratory Screening Tests and Stability Measurements but presently they have not been able to pass the initial thickening time tests due to a tremendous exotherm.

## LABORATORY SCREENING PROGRAM (Figure 1)

Data generated this quarter is presented in data tables I, II, III, and IV. For a total understanding of what this data means a review of the previous reports would be needed. Thus, the reader is encouraged to compare the new results with those listed in previous progress reports.

## Compressive Strengths (Table I)

This series of data consists of 600°F tests cured in sealed pipe at 1500 psi and 400°F tests cured in water bath autoclaves with 2500 psi pressure. Both were cured 28 days. The tests at 500°F were conducted first due to test chamber availability. For this reason several low strength systems were not tested at 400°F. The 600° tests were preset 1-inch diameter cement cylinders (1-inch long) which were sealed in pipe nipples with enough water for steam saturation pressure. Six of the cements were cured with less than saturated steam due to leakage in one pipe at 600°F.

### Shear Bond (Table I)

Bonding between the cement systems and solvent cleaned smooth surface pipe was measured after 28 days curing at 400°F under water at 2500 psi. Two-inch pieces of lathe surfaced pipe were placed in the center of two-inch cube molds and cement was poured around and into the pipe. At the 28th day the samples were removed from curing chambers and tested for bond without stripping the molds. The first test measurement was to break the bond of the center cement plug from the pipe. Next the pipe to outer cement bond was measured. Photographs of these pipes were made to show surface adherence of cement after removal of the samples (Figure 2).

### X-ray Analysis (Table II)

Samples of the cement cured at 600°F were ground to finer than 200 mesh and rinsed with three acetone rinses. These were x-ray analyzed and the data is reported in Table II.

### Differential Thermal Analysis (Table III)

At the same time as the x-ray sampling, 60 to 200 mesh portions were taken and analyzed by DTA.

## DISCUSSION OF LABORATORY SCREENING PROGRAM

At this time the bulk of the screening data has been completed. There will be expansion tests conducted, hopefully next quarter which will include the systems showing good characteristics on previous tests. The expansions will be at high temperature and pressure and are expected to compliment the bond test results. Some unexpected results may appear on systems which will be still changing in compressive and shear strength when tested. Expansion is planned to be unrestrained in water bath curing. The erosion testing will be covered not under the Laboratory Screening Program but under the Stability Measurements section.

Cement systems being dropped from testing are those which fail in one or more significant test areas. Systems 14, 15, and 16 were dropped due to low strength. All three of these are Class J cement with bentonite. Since some tests overlap in termination dates, a failing system can sometimes be seen in several tests. Systems 14, 15, and 16 were tested for bond and can be seen in Table I to be unbonded for 15 and 16 and very little bond for system 14. X-ray indicates these systems have scawtite as a significant percentage of their crystalline composition.

The pipe usually slipped out of the cement without assistance in system 15 and 16. Also note the photographs of these showing no adherence of cement. Systems 18 and 19 of the Class J series

also failed due to low bond for system 18 and low strength for system 19. Note from the x-ray data scawtite is again a high percentage crystalline component. The three Class J systems passing these tests 12, 13, and 17 can be seen to have scawtite as a minor component in 12 and 17 and none indicated in system 13. The other systems tested for bonding were felt to be adequate. System 33 did show borderline bond to pipe but strength and other tests dictated further testing.

All silica-lime systems except 26 were dropped due to low strength. They were not tested for bond for that reason. System 35 was dropped due to low strength at 600°F but may be reconsidered since it is a highly extended system similar to system 4.

### STABILITY MEASUREMENTS

Stability measurements are proceeding along three different paths: 1) static testing, 2) laboratory dynamic testing, and 3) field dynamic testing.

#### Static Brine Testing

It was noted that some systems were not performing as expected when exposed to heavy brine. Last quarter it was speculated that the reason is a lower rate of solubility of silica in brine solutions. This quarter that theory was verified.

The stability of a silica stabilized Portland cement in geothermal brines was noted to depend to some degree on the particle size of the silica as reported previously. Tests were conducted to determine the rate of solubility of silica in 3% and 37% sodium chloride brines at 260°C (500°F). Silica flour dissolved more rapidly than the coarser 70-200 mesh silica as would be expected. Also the 3% sodium chloride brine dissolved silica 2.5 to 3 times as fast as the 37% brine. This was in line with the observation that about 100 parts of 70-200 mesh silica instead of 35 parts are required to stabilize Portland cement in heavy geothermal brines. Robert Fournier of U.S. Geological Survey, Menlo Park, California, indicated they found 4N sodium chloride brine to dissolve silica considerably slower at elevated temperatures than 2N sodium chloride. We also found that the addition of calcium hydroxide similar to that released by cement increased the rate of solubility of silica in a brine (See Table IV). This data should conclude the static portion of the Stability Measurements.

#### Laboratory Dynamic Testing

Studies on cement systems for geothermal wells require extensive testing at down hole conditions. In order to meet these conditions in the lab an apparatus for this specific purpose was designed. The equipment was called a "Dynamic Brine Exposure Testing Apparatus" and was to be completed by January 1, 1979.

D-BETA, as it is referred to, will flow hot brine past the cement samples at specific conditions (up to 700°F and 3100 psi).

This project was completed on time and is in running condition. Tests are now being prepared for evaluation in D-BETA. The systems being evaluated at East Mesa, California, will be evaluated in the D-BETA under the same conditions of temperature and pressure along with a simulated East Mesa brine.

#### Field Dynamics Testing

During this quarter the one month "shake-down" test at East Mesa test facility has been completed. During this test period well 6-1 experienced a severe scale problem and the tests were moved to well 6-2. The tests were on well 6-1 for 375 hours and on well 6-2 for 297 hours. The test conditions on both wells were 300°F and 95 psig. The chemical analysis of the brines are given in Tables V and VI. Thirty-two systems (Table VII) were exposed to these brines and after exposure these thirty-two systems were evaluated in the laboratory (Table VIII). From these thirty-two systems fifteen were picked for evaluation in a two year exposure test. A sixteenth system not in the shake-down test was formulated because it was felt a system composed of truscotite should be in this test program. The sixteen systems now being evaluated are listed in Table IX. These tests were placed on well 8-1 whose brine analysis is given in Table X.

Also during this past quarter written approval to test at the Nilands facility in Southern California has been given. This testing will consist of bolting a wire basket inside of a flasher so that cement cubes can be exposed to the flashing brine. The test basket has been prepared and testing should begin in March of 1979.

#### CHEMICAL STUDIES

The chemical studies portion of Dowell's contract research effort continued this quarter with work concerning two subjects. First, silica stabilized Portland cements were analyzed by x-ray diffraction in an effort to relate phase composition with strength and silica particle size. Second, further work was performed to identify the cause for the occurrence of the anomalous 3.50Å peak that is often observed with geothermally cured cements. The pace of the chemical studies research was hindered somewhat by installation difficulties encountered with the new x-ray diffractometer.

Last quarter the relationship between degradation of silica-stabilized Portland cements and the particle size of the silica was reported. In general, when cured in the presence of geo-



thermal brines, cements stabilized with silica in the 3 to 44  $\mu\text{m}$  particle size range will retain their integrity, while cements using silica greater than 44  $\mu\text{m}$  in size tend to weaken and become excessively permeable. It was felt that this behavior was due to the rate of solution of silica. Slurries with coarse silica became silica deficient in the aqueous phase; as a result, the hydration products are also silica-deficient and weak.

Table XI illustrates the differences in phase composition of set cements cured under geothermal conditions with varying sizes of added silica. The weaker silica deficient cements are composed primarily of the phase Kilchoanite (c/s = 1.50), while the stronger binders are mostly xonotlite (c/s = 1.00).

Work continued to identify the cause of the anomalous 3.50 $\text{\AA}$  peak often observed on x-ray diffraction patterns of geothermally cured cements. In earlier reports it was stated that xonotlite was always present when the 3.50 $\text{\AA}$  peak was observed. This quarter the extraneous peak was found with a sample composed of tobermorite, truscotite, and calcio-chondroite. The original slurry contained a silica-rich extender as have all the others. This data establishes that the 3.50 peak is definitely not due to enhancement of the xonotlite 002 peak and also lends credence to the theory that the presence of a silica-rich extender is required.

Testing is currently in progress to determine whether the 3.50 $\text{\AA}$  phase may be obtained by during these extenders hydrothermally with geothermal brines. Also, more cements are being evaluated in an effort to better determine the curing conditions required to reproducibly obtain the 3.50 $\text{\AA}$  phase.

#### NON-PORTLAND SYSTEMS

Coal filled furfuryl alcohol cement tests are being run on an accelerating rate calorimeter (ARC) with various combinations of furfuryl alcohol to determine at what temperatures reactions takes place and how much heat is evolved. In an acid catalyzed, coal filled, furfuryl alcohol resin there were up to four peaks (four different reactions) noted between 50 and 300°C. Powdered coal will catalyze the polymerization of furfuryl alcohol producing at least two reactions. The addition of one part fine coal to one part furfuryl alcohol appears to control heat evolution sufficiently for most cementing operations.

BIBLIOGRAPHY

1. Development of Geothermal Well Completion Systems, Phase I Report, July-September, 1977, COO/4190-1.
2. Development of Geothermal Well Completion Systems, Phase II Progress Report No. 1, October, 1977 - March, 1978, COO/4190-2.
3. Development of Geothermal Well Completion Systems, Phase II Progress Report No. 2, April - June, 1978, COO/4190-3.
4. Taylor, H. F. W., Personal Correspondence with E. B. Nelson, October, 1978.
5. Kalousek, G. L., Personal Communication with E. B. Nelson, October, 1978.
6. Kalousek, G. L. and Nelson, E. B., Cement and Concrete Research, Vol. 8 (1978), pp. 283-290.

ADDITIVE CODES

<u>Code</u>	<u>Material</u>
ALOH	Aluminum hydroxide, $\text{Al}(\text{OH})_3$
BENT	Bentonite
COAL	Powdered coal
DE	Diatomaceous earth
FA/L	La Due fly ash
FA/N	Needles fly ash
ILLM	Ilmenite, $\text{FeTiO}_3$
PERL	Expanded perlite
PP	Plaster of paris, $\text{CaSO}_4 \cdot 1/2 \text{H}_2\text{O}$
R1	Retarder - proprietary blend of sugar and lignin derivatives
R2	Retarder - proprietary blend of lignin and inorganic salts
SF	Silica flour - $\leq 10 \mu\text{m}$ avg.
SAND	Medium fine silica - $\leq 100 \mu\text{m}$ avg.
SR	Sugar retarder
SSS	Sodium metasilicate, solid
GIL	Gilsonite
MgO	Magnesium oxide

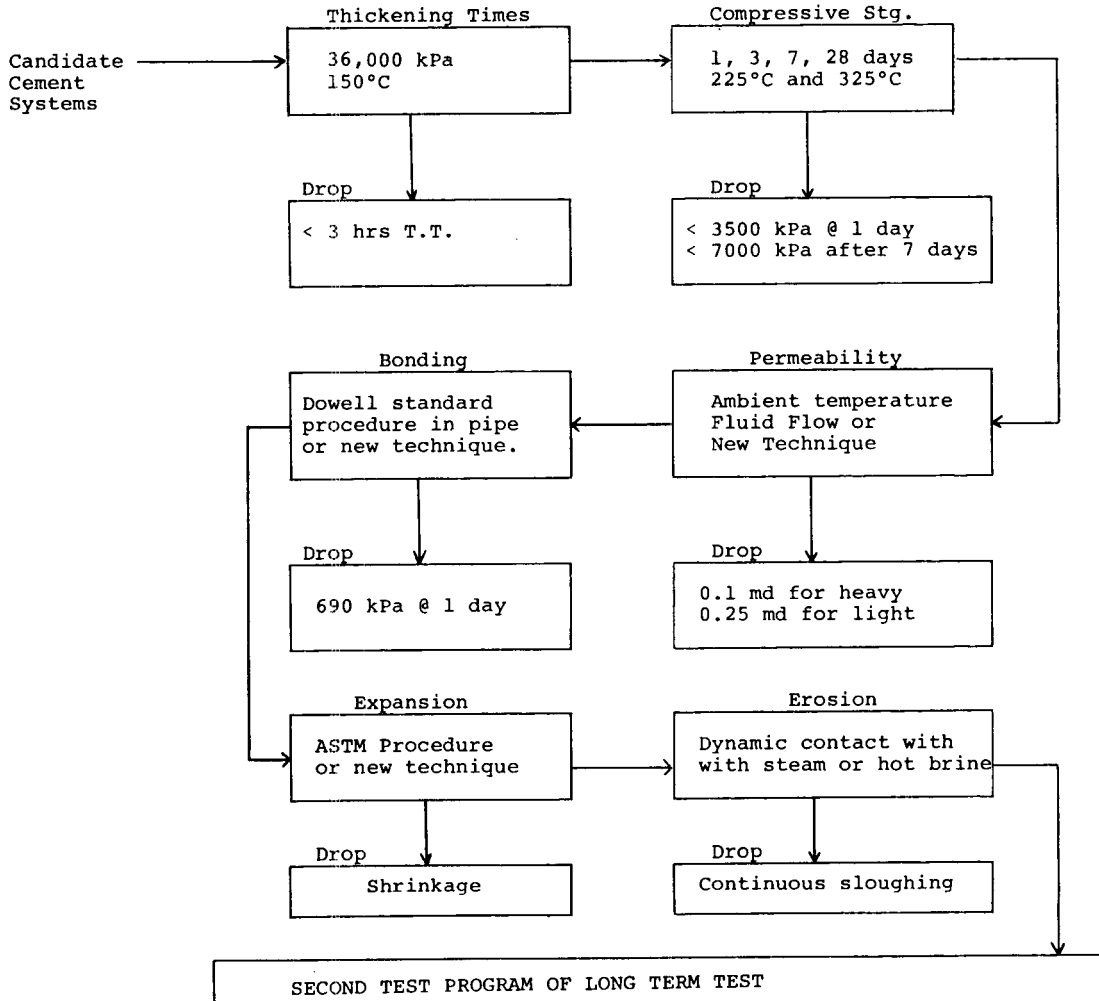


Figure 1.



LABORATORY  
SCREENING PROGRAM  
DATA TABLES AND FIGURES

TABLE 1

Compressive and Shear Bond Strength  
4th Quarter, 1978, for Laboratory Screening Program

\* Percent by weight of water

(L) Leak

System #	Cement Type	Additives (% BWO)			% Water	Retarder Code %	Comp. Str. 227°C 316°C		Shear Bond Strength 204°C, 28 Day, 2500 psi	
		Code %	Code %	Code %			28 Days	28 Days	Inside Pipe	Outside Pipe
1	Permanente "G"	Sand	35		54	1 1.0	4350	5600(L)	1500	150
2	Permanente "G"	SF	35		54	1 1.0	2750	6875(L)	2400	450
3	Permanente "G"	SF	35	FA-N 79	52	1 1.0	5000	2925	2350	850
4	Permanente "G"	SF	35	PERL 8.5 BENT 2.0	116	1 1.0	775	1800	700	150
5	Permanente "G"	SF	35	NaCl 37*	54	1 1.0	1300	4325	1200	225
6	Permanente "G"	SF	35	NaCl 10*	54	1 1.0	2250	7950	2450	250
7	Permanente "G"	SF	35	KCl 37*	54	1 1.0	2750	4775	2500	425
8	Permanente "G"	SF	35	KCl 10*	54	1 1.0	2300	5800	525	250
9	Permanente "G"	SF	35	DE 8.9	91	1 1.0	2300	5600	850	100
10	Permanente "G"	SF	35	COAL 27	63	1 1.0	2750	5425	1275	500
11	Permanente "G"	SF	35	GIL 27	63	1 1.0	2625	2875	1775	650
12	Unadeep "J"				44	1 0.4	3225	4025	1725	375
13	Unadeep "J"	FA-N	79		75	1 0.4	3350	3200	675	175
14	Unadeep "J"	PERL	8.5	BENT 2.0	106	1 0.4	575	500	350	25
15	Unadeep "J"	BENT	4.0		65	1 0.4	1650	425	700	0
16	Unadeep "J"	BENT	8.0		86	1 0.4	1675	650	--	0
17	Unadeep "J"	NaCl	37*		44	1 0.2	2650	4775(L)	1250	475
18	Unadeep "J"	KCl	10*		44	1 0.2	1400	2175	300	25
19	Unadeep "J"	SSS	2		90	1 0.2	4125	775	1550	150
20	Fondu				50	1/2 1.5/1.5	3350	1975	1600	600
21	Fondu	FA-N	85		81	1/2 "	1200	1100	250	200
22	Slag Cement	SF	35		56	1 1.25	2400	3750(L)	>2500	300
23	Slag Cement	SF	35	FA-N 79	93	1 1.25	2425	2293(L)	1900	--
24	Slag Cement	SF	35	SSS 1.5	122	1 1.25	3450	1200	1075	450
25	Slag Cement	SF	35	PP 10	74	1 1.25	2625	2750	1750	450
26	Lime:Silica (1:1)				96	1 0.7	3650	1275	1875	600
27	Lime:Silica (1:1)	ALOH	7.0		96	1 1.0	--	575	--	--
28	Lime:Silica (1:1)	PERL	8.5	BENT 2.0	110	1 0.7	--	450	--	--
29	Lime:Silica (1:1)	FA-N	79		130	1 1.0	--	250	--	--
30	Lime:Silica (1:1)	FA-N	79		130	1 1.0	--	575	--	--
31	Lime:Silica (1:0.4)				142	1 0.7	--	325	--	--
32	Millwhite Pozz:Lime (1:0.42)				142	1 0.7	--	575	--	--
33	"B"	SAND	35		56	1 1.2	600	7400	375	25
34	"B"	SF	35		56	1 1.5	1350	6550	100	75
35	"B"	SF	35	PERL 8.5 BENT 2.0	118	1 0.6	2275	700(L)	1100	275
36	"B"	SF	35	KCl 37*	56	1 1.0	2500	5425	2075	350
37	"B"	SF	35	NaCl 37*	56	1 1.0	4375	4150	1450	750
38	"B"	SF	35	FA-L 79	120	1 1.0	375	2800	350	100

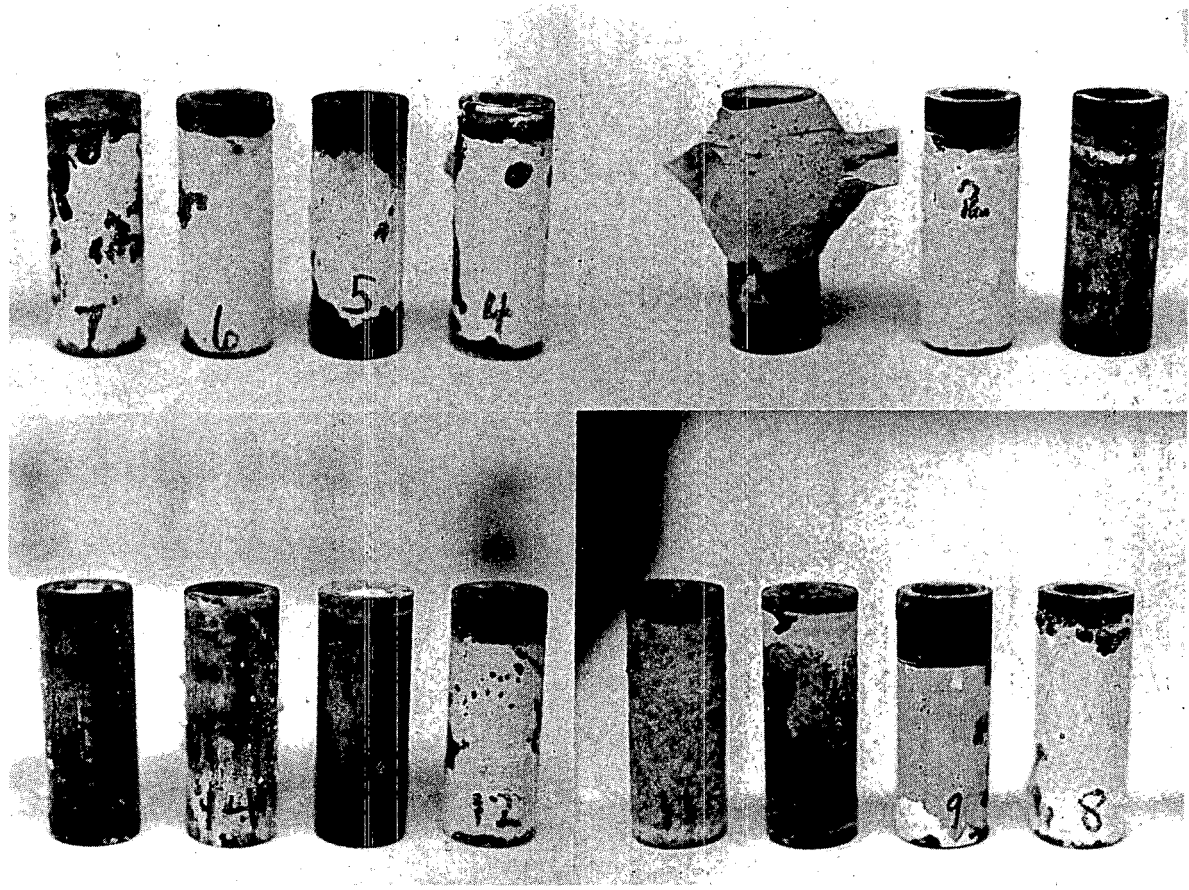


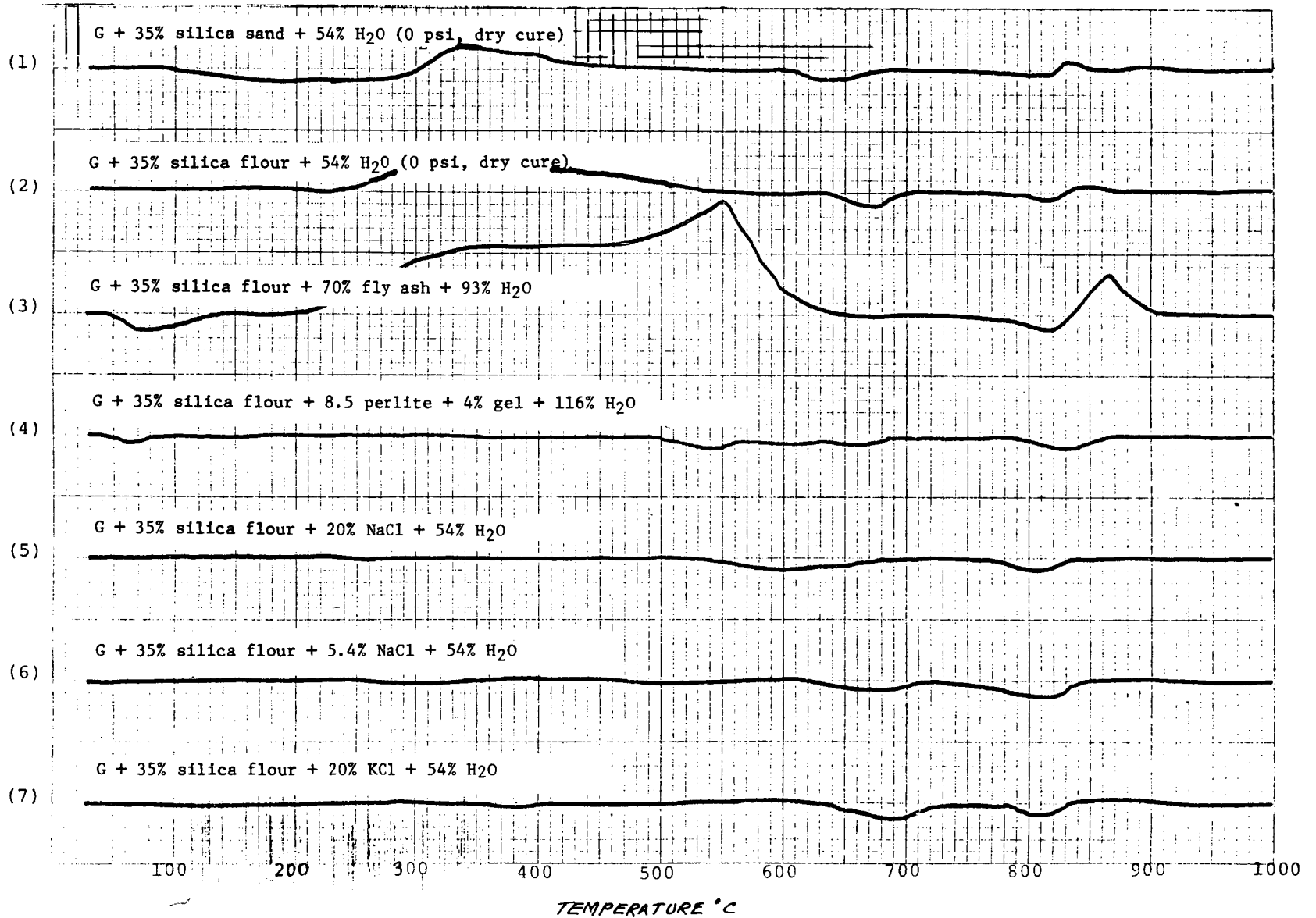
Figure 2.

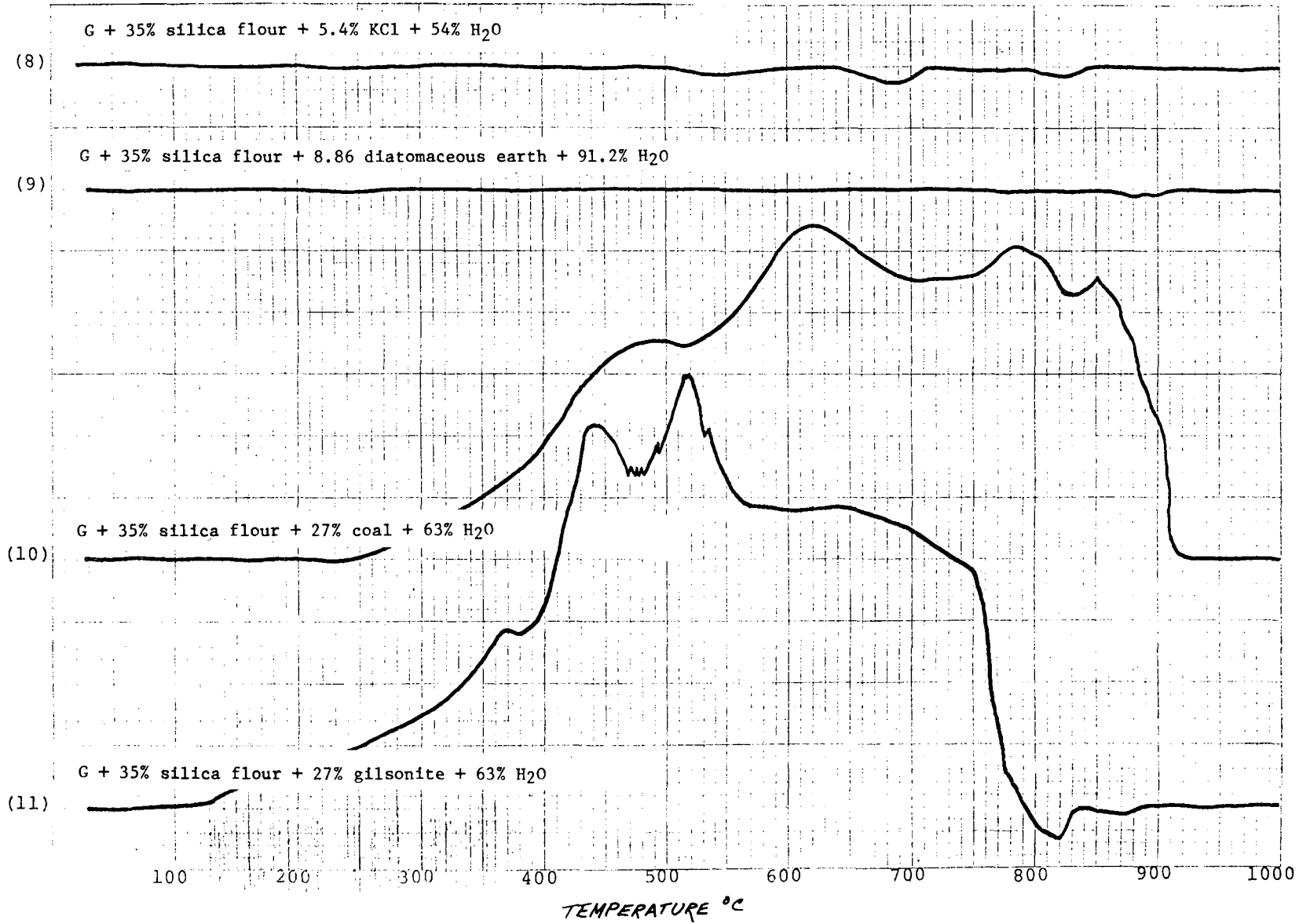


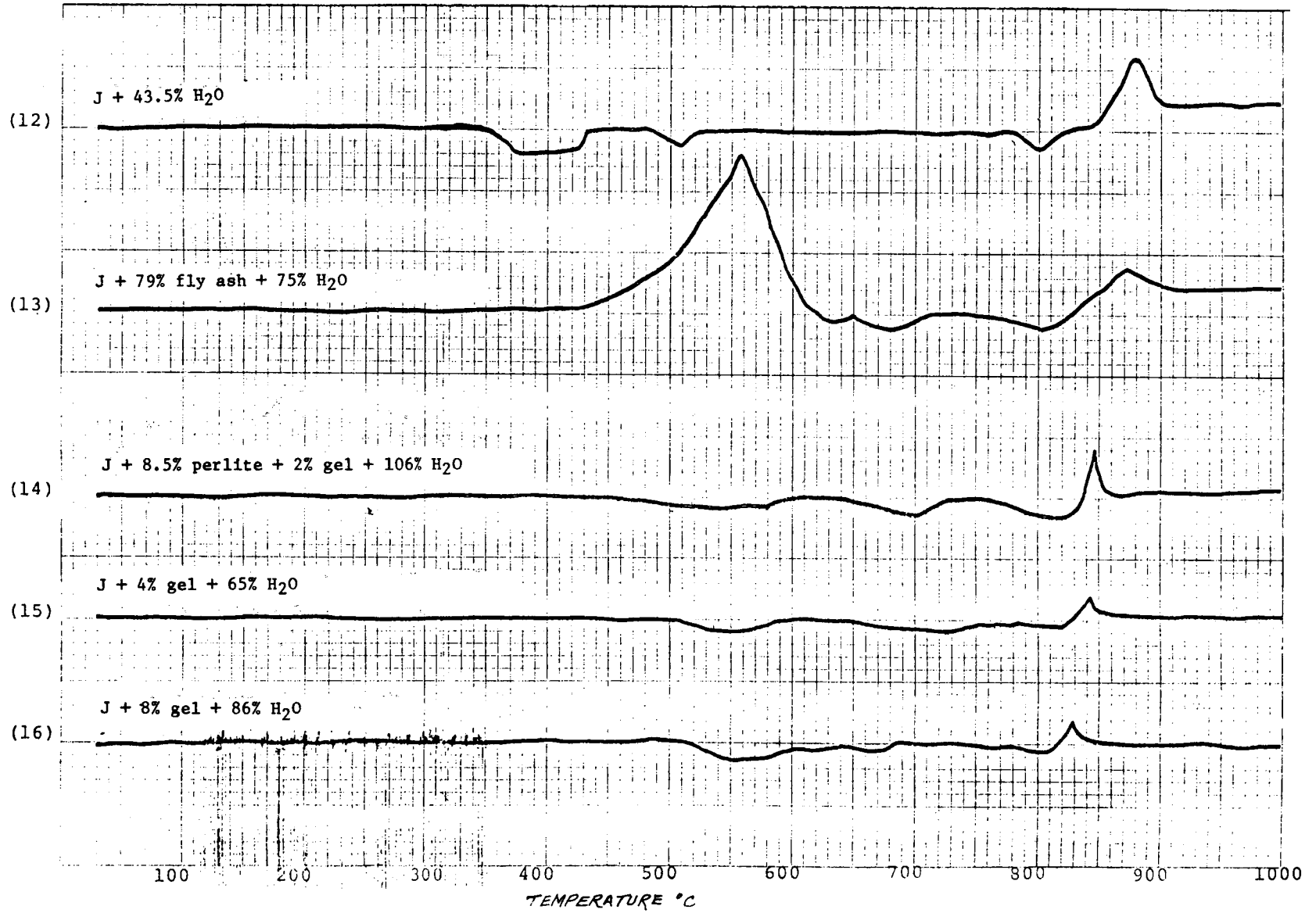
TABLE II  
 X-ray Analysis of Laboratory Screening Program  
 28 Day Compressive Strength Samples - Cured at  
 316°C and Saturated Steam Pressure

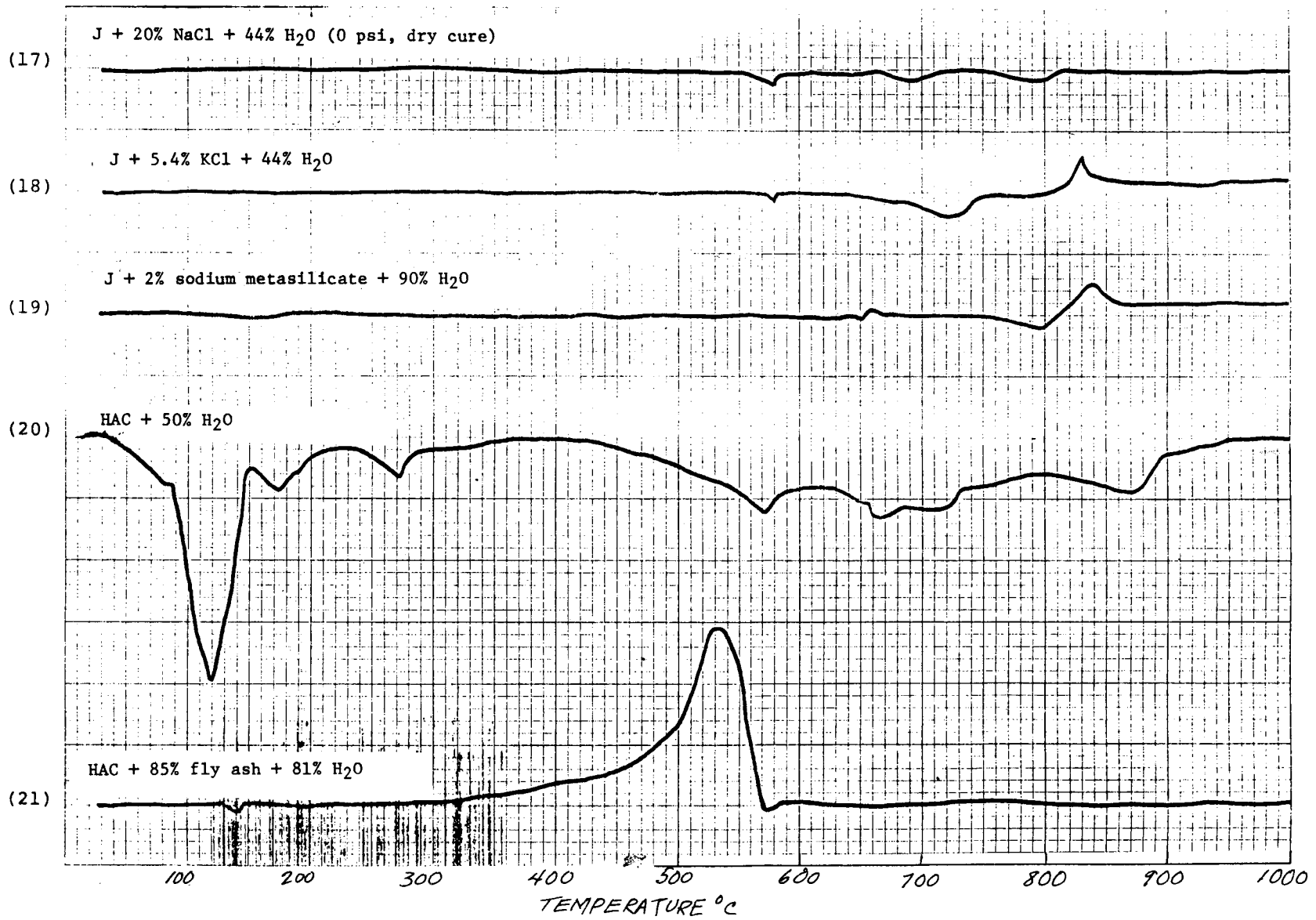
System #	Major	Minor	Low
1	-----	Xonotlite	Rustumite
2	Xonotlite	-----	Calcite
3	Tobermorite	-----	Rosenhahnite
4	Xonotlite	-----	Calcite
5	Xonotlite	-----	Calcite
6	Xonotlite	-----	-----
7	Xonotlite	-----	Calcite
8	Xonotlite	-----	Calcite
9	Xonotlite	-----	Calcite
10	Xonotlite	-----	Calcite
11	Xonotlite	-----	Calcite
12	Quartz	-----	Calcite, scawtite, truscotite, xonotlite
13	Calcium, analcite	Reyerite	-----
14	Scawtite	-----	Truscotite
15	Scawtite	-----	Quartz, xonotlite, truscotite
16	-----	-----	Quartz, xonotlite, scawtite
17	-----	Xonotlite	Quartz, scawtite
18	-----	-----	Quartz, scawtite, xonotlite, truscotite
19	-----	Scawtite, truscotite	Xonotlite
20	$Ca_2Al_2SiO_7 \cdot H_2O$	-----	Plaster of paris, ettringite
21	$Ca_3Fe_2Si_3O_{12}$	-----	Plaster of paris, $Ca_2Al_2Si_7H_2O$
22	Xonotlite	-----	-----
23	Tobermorite	-----	Calcium analcite
24	-----	Xonotlite, truscotite	-----
25	Xonotlite	-----	Scawtite
26	Xonotlite	-----	Calcite, Quartz
27	Xonotlite	-----	-----
28	-----	Quartz	Xonotlite, scawtite, truscotite
29	-----	-----	Truscotite, xonotlite, tobermorite
30	Xonotlite	-----	Quartz, truscotite
31	Tobermorite	-----	Rosenhahnite, calcite
32	-----	-----	Truscotite, calcite
33	Xonotlite	-----	Calcite
34	Xonotlite	-----	Calcite
35	Xonotlite	-----	Calcite
36	Xonotlite	-----	Calcite
37	Xonotlite	-----	Calcite
38	-----	Tobermorite	Truscotite

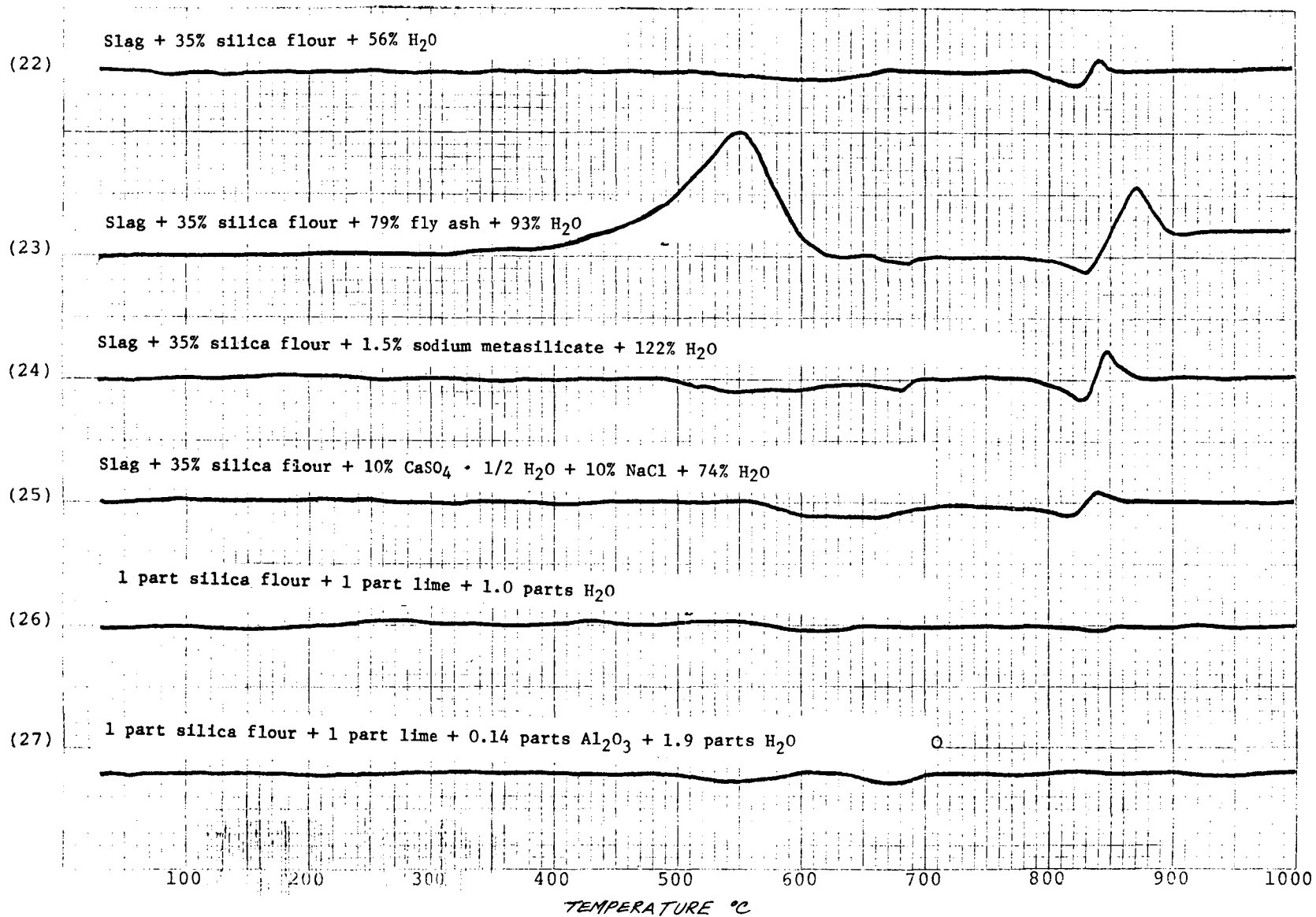
TABLE III  
 Differential Thermal Analysis of Cement Cured 28 Days at 600°F  
 All Systems Retarded For Placement Time  
 Deltatherm D2000, Heat Rate = 10°C/Min., ΔT = 1°C/25.4mm (1/2 scale simulated thermograms), 11-1-78

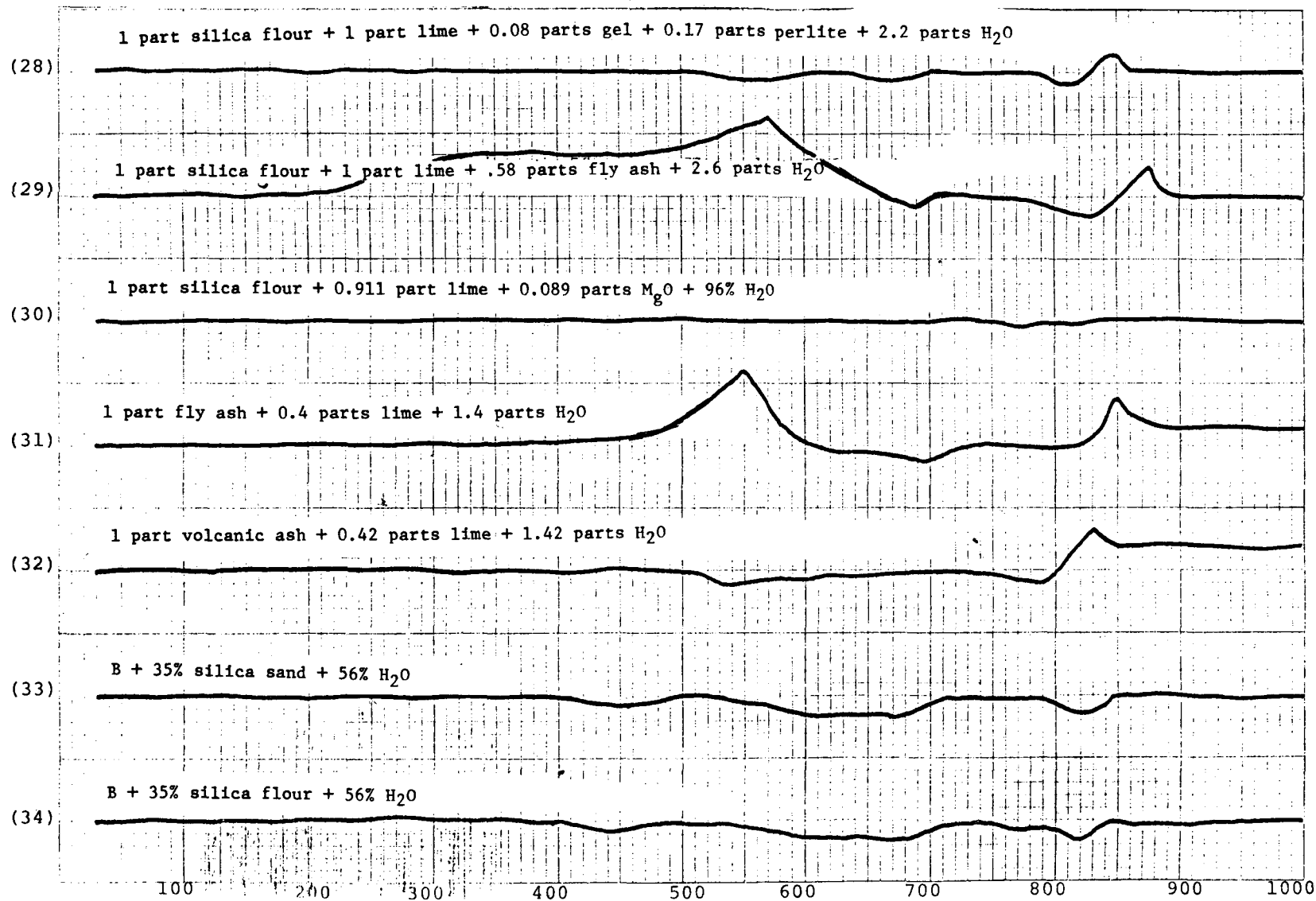


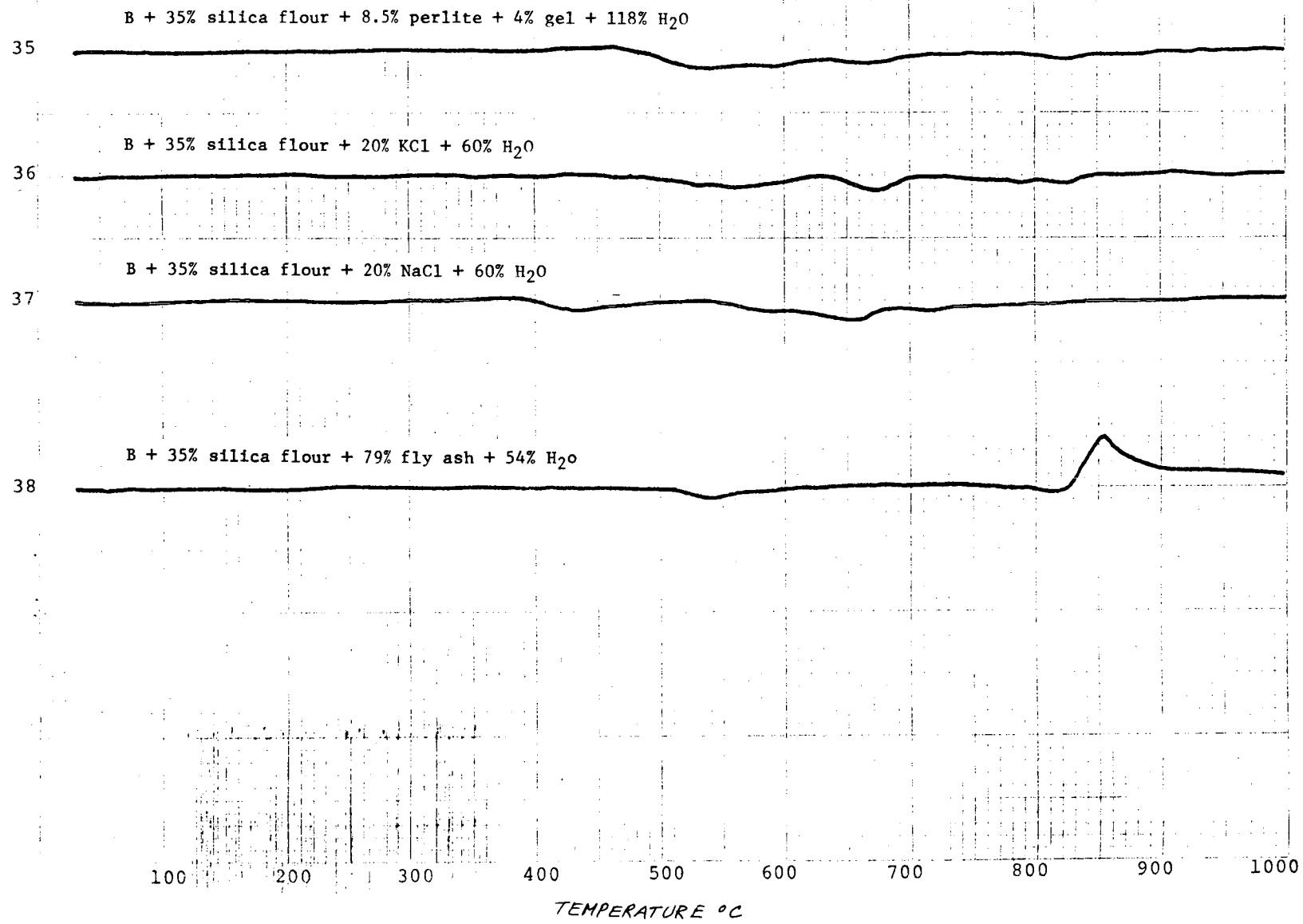
















S T A B I L I T Y   M E A S U R E M E N T S  
D A T A   T A B L E S

TABLE IV

RATE OF SOLUTION OF SILICA IN BRINES  
 200 GMS SILICA ROTATED AT 35RPM IN A BAROID MUD AGING CELL  
 AT 260°C (500°F)\*  
 SILICA DETERMINATIONS IN BRINE MADE BY PLASMA EMISSION SPECTROMETRY

MIX 1		MIX 2		MIX 3		MIX 4	
Silica Flour In 37% NaCl		70-200 Mesh Silica In 37% NaCl		70-200 Mesh Silica In 37% NaCl		70-200 Mesh Silica In 37% NaCl 0.01% Ca(OH) <sub>2</sub>	
Time Hrs.	Silica Mg/l	Time Hrs.	Silica Mg/l	Time Hrs.	Silica Mg/l	Time Hrs.	Silica Mg/l
1.1	10	1.2	7.7	1.3	2.2	1.0	2.5
2.6	27**	3.1	30	3.0	12	2.5	22
-	--	6	48	6	20	3.7	25

\* Approximately one hour estimated for sample to reach temperature. First reading reflects heat up time.

\*\* Silica flour tests run on separate samples since fine silica plugged valve allowing fluid to escape.

TABLE V  
 MESA 6-1 WELLHEAD UNFLASHED  
 June 9, 1976  
 Geothermal Resource Investigations  
 Imperial Valley, California

Chloride (Cl <sup>-</sup> )	15,850	mg/l	Sulfide (S <sup>=</sup> )	3.0	mg/l
Conductivity (at 25°C)	40,000	umhos	Silica (SiO <sub>2</sub> )	320	mg/l
pH	5.45		<u>1/</u> Total Dissolved Solids (TDS)	26,300	mg/l
Titanium (Ti)	0.10	mg/l	Iron (Fe)	8.8	mg/l
Lithium (Li)	40.0	mg/l	Potassium (K)	1,050	mg/l
Copper (Cu)	0.10	mg/l	Magnesium (Mg)	17.2	mg/l
Molybdenum (Mo)	0.005	mg/l	Zinc (Zn)	0.07	mg/l
Manganese (Mn)	0.95	mg/l	Nickel (Ni)	0.10	mg/l
Barium (Ba)	14	mg/l	Bicarbonates (HCO <sub>3</sub> <sup>=</sup> )	202	mg/l
Carboniates (CO <sub>3</sub> <sup>=</sup> )	0.0	mg/l	Sulfate (SO <sub>4</sub> <sup>=</sup> )	42.8	mg/l
Fluoride (F)	0.99	mg/l	Nitrate (NO <sub>3</sub> <sup>=</sup> )	TRACE,	0.02
Phosphate (PO <sub>4</sub> ) Total	N.D.,	0.01	Cadmium (Cd)	N.D.,	0.01
Ammonia (NH <sub>4</sub> )	40.75	mg/l	Beryllium (Be)	N.D.,	0.02
Cesium (Ce)	2.75	mg/l	Bismuth (Bi)	3	mg/l
Mercury (Hg)	N.D.,	0.002	Arsenic (As)	0.26	mg/l
Selenium (Se)	N.D.,	0.1	Antimony (Sb)	5.5	mg/l
Tantalum (Ta)	0.14	mg/l	Niobium (Nb)	0.40	mg/l
Sodium (Na)	8,100	mg/l	Calcium (Ca)	1,360	mg/l
Strontium (Sr)	320	mg/l	Germanium (Ge)	N.D.,	0.1
Indium (In)	N.D.,	0.1	Gold (Au)	N.D.,	0.01
Palladium (Pd)	N.D.,	0.1	Platinum (Pt)	N.D.,	0.1
Cobalt (Co)	0.06	mg/l	Iridium (Ir)	N.D.,	0.1
Tungsten (W)	N.D.,	0.1	Aluminum (Al)	0.04	mg/l
Boron (B)	9.75	mg/l	Chromium (Cr)	N.D.,	0.01
Lead (Pb)	0.5	mg/l	Vanadium (V)	0.005	mg/l
Silver (Ag)	0.013	mg/l			

N.D. = None Detected  
 = Less Than  
1/ = Evaporated at 180°C

TABLE VI  
MESA 6-2 WELLHEAD UNFLASHED  
June 1976  
Geothermal Resource Investigations  
Imperial Valley, California

Chloride (Cl <sup>-</sup> )	2,142	mg/l	Sulfide (S <sup>=</sup> )	1.5	mg/l
Conductivity (at 25°C)	6,000	umhos	Silica (SiO <sub>2</sub> )	320	mg/l
pH	6.12		<u>1/</u> Total Dissolved Solids (TDS)	5,000	mg/l
Titanium (Ti)	0.10	mg/l	Iron (Fe)	0.10	mg/l
Lithium (Li)	4.0	mg/l	Potassium (K)	150	mg/l
Copper (Cu)	0.10	mg/l	Magnesium (Mg)	0.24	mg/l
Molybdenum (Mo)	0.005	mg/l	Zinc (Zn)	0.01	mg/l
Manganese (Mn)	0.05	mg/l	Nickel (Ni)	0.10	mg/l
Barium (Ba)	0.25	mg/l	Bicarbonates (HCO <sub>3</sub> <sup>=</sup> )	560	mg/l
Carbonates (CO <sub>3</sub> <sup>=</sup> )	0.0	mg/l	Sulfate (SO <sub>4</sub> <sup>=</sup> )	156	mg/l
Fluoride (F)	1.23	mg/l	Nitrate (NO <sub>3</sub> <sup>=</sup> )	0.1	mg/l
Phosphate (PO <sub>4</sub> ) <sup>4</sup> Total	0.2	mg/l	Cadmium (Cd)	N.D.,	0.01 mg/l
Ammonia (NH <sub>4</sub> ) <sup>4</sup>	14.7	mg/l	Beryllium (Be)	N.D.,	0.02 mg/l
Cesium (Ce)	0.38	mg/l	Bismuth (Bi)	N.D.,	0.005 mg/l
Mercury (Hg)	N.D.,	0.002 mg/l	Arsenic (As)		0.22 mg/l
Selenium (Se)	N.D.,	0.1 mg/l	Antimony (Sb)		0.90 mg/l
Tantalum (Ta)		0.17 mg/l	Niobium (Nb)		0.40 mg/l
Sodium (Na)	1,700	mg/l	Calcium (Ca)		16.4 mg/l
Strontium (Sr)		6.4 mg/l	Germanium (Ge)	N.D.,	0.1 mg/l
Indium (In)	N.D.,	0.1 mg/l	Gold (Au)	N.D.,	0.01 mg/l
Palladium (Pd)	N.D.,	0.1 mg/l	Platinum (Pt)	N.D.,	0.1 mg/l
Cobalt (Co)	N.D.,	0.01 mg/l	Iridium (Ir)	N.D.,	0.1 mg/l
Tungsten (W)	N.D.,	0.1 mg/l	Aluminum (Al)		0.03 mg/l
Boron (B)		7.45 mg/l	Chromium (Cr)	N.D.,	0.01 mg/l
Lead (Pb)		0.5 mg/l	Vanadium (V)		0.005 mg/l
Silver (Ag)		0.010 mg/l			

N.D. = None Detected  
= Less Than  
1/ = Evaporated at 180°C

TABLE VII

Initial Dynamic Field Exposure Systems East Mesa Test Facility, California

	Cement	Additives (% BWOC Unless Otherwise Indicated)								%H <sub>2</sub> O	
		Additive	%	Additive	%	Additive	%	Additive	%		
1	Kaiser G	SAND	35	SR	1	----	-	----	-	54	
2	Kaiser G	SF	35	SR	1	----	-	----	-	54	
3	Kaiser G	SF	35	SR	1	FA/N	79	----	-	52*	
4	Kaiser G	SF	35	SR	1	PERL	8.5	BENT	2	116	
5	Kaiser G	SF	35	SR	0.8	NaCl	37	----	-	54	
6	Kaiser G	SF	35	SR	1	NaCl	10	----	-	54	
7	Kaiser G	SF	35	SR	1	KCl	10	----	-	54	
8	Kaiser G	SF	35	SR	1	DE	8.86	----	-	91.2	
9	Kaiser G	SF	35	SR	1	COAL	27	----	-	62.9	
10	Unadeep J	SR	0.4	--	-	----	--	----	-	43.5	
11	Unadeep J	SR	0.4	FA/N	79	----	--	----	-	42*	
12	Unadeep J	SR	0.4	PERL	8.5	BENT	2	----	-	106	
13	Unadeep J	SR	0.4	BENT	4	----	--	----	-	65	
14	Unadeep J	SR	0.4	BENT	8	----	--	----	-	86	
15	Unadeep J	SR	0.2	NaCl	37	----	--	----	-	44	
16	Unadeep J	SR	0.2	KCl	10	----	--	----	-	44	
17	Unadeep J	SR	0.2	SSS	2	----	--	----	-	90	
18	(1:1)	Lime-Silica	SR	0.7	---	-	----	--	----	-	96
19	(1:1)	Lime-Silica	SR	1	Al <sub>2</sub> O <sub>3</sub>	7	----	--	----	-	96
20	(1:1)	Lime-Silica	SR	0.7	PERL	8.5	BENT	2	----	-	110
21	(1:1)	Lime-Silica	SR	1	FA/N	79	----	--	----	-	130
22	(0.4:1)	Lime:FA/N	SR	0.7	---	-	----	--	----	-	100
23	(0.4:1)	Lime:Pozz	SR	0.7	---	-	----	--	----	-	142
24	Ideal B	SAND	35	---	-	----	--	----	-	56	
25	Ideal B	SF	35	SR	1.5	----	--	----	-	56	
26	Ideal B	SF	35	SR	0.6	PERL	8.5	BENT	2.0	118	
27	Ideal B	SF	35	SR	1.0	KCl	37	----	-	60	
28	Ideal B	SF	35	SR	1.0	NaCl	37	----	-	60	
29	Ideal B	SF	35	SR	1.0	FA/L	79	----	-	54	
30	Kaiser G	SAND	35	SR	1.0*	FA/N	79	----	-	52	
31	Kaiser G	SAND	35	SR	1.0	PERL	8.5	BENT	4	116	
32	Ideal B	SAND	35	SR	0.6	PERL	8.5	BENT	4	118	

\* By weight of ash + cement

TABLE VIII

## Laboratory Evaluation of East Mesa "Shake-Down" Test Samples

System #	Water Permeability in Millidarcies	Compressive Strength In psi	X-ray Analysis		
			Major	Minor	Low
1	.03	2825	Non-crystalline	----	Quartz, calcite, $\text{CaH}_4\text{Si}_2\text{O}_7$
2	.01	1500	Non-crystalline	----	Quartz, calcite
3	.02	2250	Non-crystalline	Quartz	Calcite
4	.06	875	Non-crystalline	----	Calcite, quartz
5	.05	1250	Non-crystalline	----	Calcite, quartz
6	.01	1100	Non-crystalline	----	Calcite, quartz
7	.17	2800	Non-crystalline	----	Calcite, quartz
8	.06	2800	Non-crystalline	----	Calcite, quartz
9	.08	1725	Non-crystalline	----	Calcite, quartz
10	.18	2700	Non-crystalline	Calcite	Quartz
11	.10	1825	Non-crystalline	----	Quartz, calcite, tobermorite 11.3Å
12	.19	475	Calcite	----	Quartz
13	.94	1425	Calcite	Calcite	Quartz
14	.22	1250	Calcite	Calcite	Quartz
15	.04	2700	Calcite	Calcite	Quartz
16	.03	2025	Calcite	----	Quartz
17	Deteriorated	50	Calcite	Quartz	-----
18	Deteriorated	----	Calcite	----	Quartz
19	.43	100	Calcite	Quartz	-----
20	Deteriorated	25	Calcite	----	Quartz
21	.50	250	Quartz	Calcite	-----
22	.89	50	Calcite	----	Quartz
23	Deteriorated	50	Calcite	----	Quartz
24	.01	2500	Non-crystalline	----	Calcite, quartz
25	Broken	2025	Non-crystalline	----	Calcite, quartz
26	.20	700	Calcite	----	Quartz
27	.04	1825	Non-crystalline	Calcite	Quartz
28	.09	2825	Non-crystalline	----	Calcite, quartz
29	.08	1525	Non-crystalline	----	Calcite, quartz, tobermorite 11.3Å
30	.04	3575	Non-crystalline	----	Calcite, quartz, tobermorite 11.3Å
31	.16	775	Non-crystalline	Calcite	Quartz
32	.24	425	Calcite	----	Quartz

TABLE IX

Two Year Dynamic Field Exposure Systems East Mesa Test Facility, California

	Cement	Additives (% BWOC Unless Otherwise Indicated)						%H <sub>2</sub> O
		Additive	%	Additive	%	Additive	%	
1	Kaiser G	SAND	35	SR	1	----	-	54
2	Kaiser G	SF	35	SR	1	----	-	54
3	Kaiser G	SF	35	SR	1	FA/N	79	52*
4	Kaiser G	SF	35	SR	0.8	NaCl	37	54
5	Kaiser G	SF	35	SR	1	NaCl	10	54
6	Kaiser G	SF	35	SR	1	DE	8.86	91.2
7	Kaiser G	SF	35	SR	1	COAL	27	62.9
8	Unadeep J	SR	0.4	--	1	----	-	43.5
9	Unaddep J	SR	0.4	FA/N	79	----	-	42*
10	Ideal B	SAND	35	SR	1.2	----	-	56
11	Ideal B	SF	35	SR	1.5	----	-	56
12	Ideal B	SF	35	SR	1.0	KCl	37	60
13	Ideal B	SF	35	SR	1.0	NaCl	37	60
14	Ideal B	SF	35	SR	1.0	FA/L	79	54
15	Kaiser G	SAND	35	SR	1.0*	FA/N	79	52
16	Kaiser G	SF	100	SR	.75	----	-	72

\* By weight of ash + cement



TABLE X  
MESA 8-1 WELLHEAD UNFLASHED  
June 22, 1976  
Geothermal Resource Investigations  
Imperial Valley, California

Chloride (Cl <sup>-</sup> )		500	mg/l	Sulfide (S <sup>-</sup> )		1.0	mg/l
Conductivity (at 25°C)		3,200	umhos	Silica (SiO <sub>2</sub> )		389	mg/l
pH		6.27		<u>1/</u> Total Dissolved Solids (TDS)		1,600	mg/l
Titanium (Ti)		0.10	mg/l	Iron (Fe)		0.10	mg/l
Lithium (Li)		1.1	mg/l	Potassium (K)		70	mg/l
Copper (Cu)		0.10	mg/l	Magnesium (Mg)		0.05	mg/l
Molybdenum (Mo)		0.005	mg/l	Zinc (Zn)		0.01	mg/l
Manganese (Mn)		0.05	mg/l	Nickel (Ni)		0.10	mg/l
Barium (Ba)		0.15	mg/l	Bicarbonate (HCO <sub>3</sub> <sup>-</sup> )		417	mg/l
Carbonates (CO <sub>3</sub> )		0.0	mg/l	Sulfate (SO <sub>4</sub> <sup>=</sup> )		173	mg/l
Fluoride (F)		1.60	mg/l	Nitrate (NO <sub>3</sub> )		0.34	mg/l
Phosphate (PO <sub>4</sub> ) Total	N.D.,	0.1	mg/l	Cadmium (Cd)	TRACE,	0.01	mg/l
Ammonia (NH <sub>4</sub> )		4.95	mg/l	Beryllium (Be)	N.D.,	0.02	mg/l
Cesium (Ce)		0.14	mg/l	Bismuth (Bi)	N.D.,	0.005	mg/l
Mercury (Hg)		0.014	mg/l	Arsenic (As)		0.053	mg/l
Selenium (Se)		0.5	mg/l	Antimony (Sb)		1.2	mg/l
Tantalum (Ta)		0.12	mg/l	Niobium (Nb)		0.40	mg/l
Sodium (Na)		610	mg/l	Calcium (Ca)		8.5	mg/l
Strontium (Sr)		2.1	mg/l	Germanium (Ge)	N.D.,	0.1	mg/l
Gold (Au)		0.024	mg/l	Indium (In)			
Aluminum (Al)		0.02	mg/l	Paladium (Pd)			
Boron (B)		1.60	mg/l	Platinum (Pt)	N.D.,	0.1	mg/l
Chromium (Cr)	N.D.,	0.01	mg/l	Cobalt (Co)	N.D.,	0.01	mg/l
Lead (Pb)		0.5	mg/l	Iridium (Ir)	N.D.,	0.1	mg/l
Vanadium (V)		0.005	mg/l	Tungsten (W)	N.D.,	0.1	mg/l
Silver (Ag)		0.010	mg/l				

N.D. = None Detectable

= Less Than

1/ = Evaporated at 180°C

C H E M I C A L   S T U D I E S  
D A T A   T A B L E S

TABLE XI  
X-RAY ANALYSIS OF SILICA STABILIZED PORTLAND CEMENTS

Silica Size		Phases Detected		
Mesh	Micron	Major	Minor	Trace
70 - 100	175	-quartz scawtite	Kilchoanite	Xonotlite 3.50Å unident.
100 - 170	120	-quartz Kilchoanite	--	3.50Å unident.
170 - 325	60	Kilchoanite	--	Xonotlite
325	32	Xonotlite	--	-quartz
325	10.5	Xonotlite	--	Kilchoanite -quartz
325	3.2	Xonotlite	--	Scawtite
70 - 200	105	-quartz Kilchoanite	Calcio- chondroite	--
325	15	Xonotlite	--	Scawtite 3.50Å unident.

APPENDIX 2

Quarterly Technical Progress Report  
September-November, 1978

on

HIGH TEMPERATURE CEMENTING MATERIALS  
FOR COMPLETION OF GEOTHERMAL WELLS

to

BROOKHAVEN NATIONAL LABORATORY

December 15, 1978

by

Rustu S. Kalyoncu  
and  
M. Jack Snyder

Under Contract No. 420825-S

BATTELLE  
Columbus Laboratories  
505 King Avenue  
Columbus, Ohio 43201

TABLE OF CONTENTS

	<u>Page</u>
INTRODUCTION AND SUMMARY. . . . .	73
PROGRAM SCHEDULE. . . . .	74
Phase I: Define the Current State of Knowledge Regarding the Cementing of Geothermal Wells - Procedures and Materials. . . . .	75
Phase II: Select Cements, Additives, and Admixtures for the Laboratory Evaluation and Development and Use of Screening Procedures for Identifying the Most Promising Materials. . . . .	75
Phase III: Evaluate Cements Selected on the Basis of Their Performance in Phase II. . . . .	75
Task No. 1 - Thickening Time Measurements. . . . .	76
Task No. 2 - Compressive Strength Measurements . . . . .	85
Task No. 3 - Permeability Measurements . . . . .	85
Task No. 4 - Cement-to-Metal Casing Bond Strength. . . . .	87
Task No. 5 - Corrosion of Steel Casing by the Cementing Materials . . . . .	87
Task No. 6 - Characterization of Cementing Materials . . . . .	91

## NOMENCLATURE

I	- Type I Portland Cement
III	- Type III Portland Cement
V	- Type V Portland Cement
G	- Class G Oil Well Cement
H	- Class H Oil Well Cement
J	- Class J Oil Well Cement
SF	- Silica Flour
HL	- Hydrated Lime
BFS	- Blast Furnace Slag
AP	- Aluminum Phosphate
PT	- Perlite
P	- Pozzolan
CMC	- Carboxy Methyl Cellulose
CMHEC	- Carboxy Methyl Hydroxy Ethyl Cellulose
COT	- Cream of Tartar
CAL	- Calgon
BA	- Boric Acid
$t_T$	- Thickening Time
$t_s$	- Setting Time
W/C	- Water to Solids Ratio
Uc	- Unit of Consistency

NOMENCLATURE FOR NUMBERS FOR FIGURE 9

- |   |                         |
|---|-------------------------|
| 1 | J-40<br>SF-40<br>P-40   |
| 2 | J-30<br>SF-30<br>BFS-40 |
| 3 | J-30<br>SF-40<br>BFS-40 |
| 4 | J-30<br>BFS-60<br>SF-10 |
| 5 | J-30<br>P-60<br>BFS-30  |

HIGH TEMPERATURE CEMENTING MATERIALS  
FOR COMPLETION OF GEOTHERMAL WELLS

Quarterly Technical Progress Report  
September-November, 1978

INTRODUCTION AND SUMMARY

Compressive strength and cement-to-metal casing bond strength evaluations have been brought to completion for all intents and purposes. Occasional evaluations in these two tasks will be made on an as needed basis in the future.

During the past three months the efforts have essentially been concentrated on the evaluation of permeability of cements and corrosion of the metal casing by the cementing compositions. The permeability measurements were made starting at low pressure gradients (e.g. 25 psi) and going to high values (100 psi) and repeated on the same samples going from high (100 psi) to low (25 psi) pressure gradients. The purpose of determining the permeabilities in this manner was essentially to assess possible damage the high pressure gradient may cause to microstructure of the permeability specimens. The results (which are partially supported by preliminary microscopic observations) indicate that certain specimens somewhat do experience microstructural damage at 100 psi pressure gradient. Based on the above observations the actual permeabilities of the cementing compositions are believed to be much lower than the experimentally determined values.

The corrosion behavior of the metal casing by the cementing media was studied through half-cell potential measurements and visual observations. Although the potential measurement technique does not provide useful qualitative data on the conditions (corrosive, non-corrosive) to which the steel casing is subjected.



The half-cell potential values indicate that no severe corrosion is caused to the steel casing by the cementing medium. Compared with the possible corrosive attack by the geothermal environment on the steel casing through the annulus, the corrosive effects of the cement is minimal.

A promising cementing composition has been sent to Mr. Ed Fuller of the National Bureau of Standards for additional tests, and at least one more composition will be submitted.

Most of the efforts for the duration of this program will be devoted to extensive characterization of the cementing compositions thus far studied. Those compositions which exhibited high strength, low permeability, and sufficiently long thickening times will be thoroughly characterized using SEM, DTA, light microscopy, and X-ray diffraction techniques.

#### PROGRAM SCHEDULE

This laboratory research program is comprised of four main work phases, namely:

- Phase I Define the current state of knowledge regarding the cementing of geothermal wells-procedures and materials
- Phase II Select cements for the laboratory evaluation and develop and use screening procedures for identifying the most promising materials
- Phase III Evaluate cements selected on the basis of their performance in Phase II relative to performance criteria established by BNL/DOE
- Phase IV Prepare detailed final report of research procedures and findings and develop plans for further studies of potentially useful cements developed in the program.

The approach uses and builds upon existing knowledge in developing cementing materials with improved performance for the application of interest.

Phase I: Define the Current State of  
Knowledge Regarding the Cementing of  
Geothermal Wells - Procedures and Materials

The objective of this work phase was to identify, analyze, and document the experiences and research findings relating to the use of cementing materials for the completion of geothermal wells. The information and data of interest from the open literature and through telephone and personal interviews with knowledgeable individuals from oil and cement industries were summarized and presented in previous reports.

Phase II: Select Cements, Additives, and Admixtures for the  
Laboratory Evaluation and Development and Use of Screening  
Procedures for Identifying the Most Promising Materials

Based on our understanding of the research problem and guided by the results of the Phase I work, a number of cements, modifiers, and admixtures have been selected for evaluation. A large number of cementing compositions - literally hundreds of batches - have been formulated and screened on the basis of their rheological behavior and setting times.

Phase III: Evaluate Cements Selected on  
the Basis of Their Performance in Phase II

In the Phase III work, cementing materials selected on the basis of their performance in Phase II are subjected to a more detailed performance evaluation relating to their use in the lining of geothermal wells. Specifically, considerations are given to:

- Task No. 1 - Setting behavior of the cementing materials
- Task No. 2 - Strength of the cementing materials
- Task No. 3 - Permeability of the cementing materials
- Task No. 4 - Bond strength of the cementing materials to  
the steel casing
- Task No. 5 - Corrosion of the steel well casing by the  
cementing media
- Task No. 6 - Compatibility of cementing materials with  
drilling muds.

In all cases, the effect of prolonged exposure to the down-hole, geothermal well environment on the properties and behavior of interest are examined.

For this period the work was involved in various tasks of Phase III. Summary of progress follows.

#### Task No. 1 - Thickening Time Measurements

Additional thickening time experiments were carried out using the API High Temperature and Pressure Thickening Time Tester. Some of the data of this test are depicted in Figures 1 through 8 for a number of cementing compositions. The reported values of thickening times - at 400 F and 3000 psi - vary between a low of about 1 hour and a high of over 5 hours.

As the above numbers indicate the thickening times exhibit a wide range of values. The mechanistic effects of various additives (silica flour, pozzolan, and blast furnace slags) are not well understood at this stage; but it appears that, for example, blast furnace slags seem to lower the thickening times compared with the effects of silica flour and pozzolan, the increases in the additions of which appear to increase the thickening times of the cementing slurries. This, however, is only an empirical observation. The effects of one component, in turn, also depend on the nature and amounts of other additives. Blast furnace slag and pozzolan combinations, for example, yield shorter thickening times than blast furnace and silica flour combinations as evidenced by the data in Figures 1 and 4.

Based on limited efforts Carboxy Methyl Cellulose has been found to be the most effective retarder (single chemical) in this project. Unfortunately, elaborate development efforts of set retarders for geothermal cements would be beyond the scope of the present study. Such a study, however, in the near future, leading to the development of retarding admixtures to be used in various geothermal environments, would be very useful to the overall geothermal energy development program.

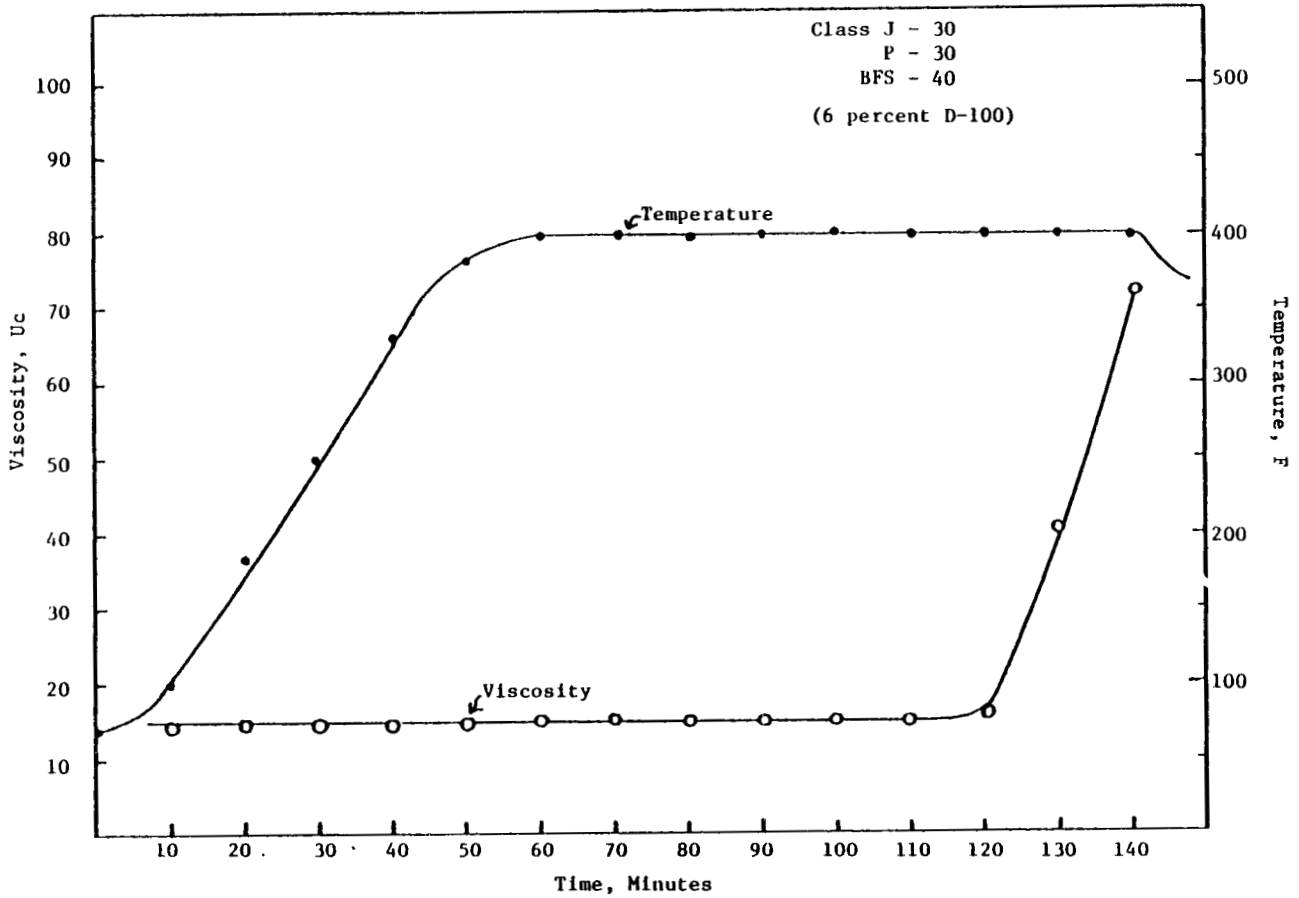


Figure 1. Temperature and viscosity profiles from the API high temperature consistometer.

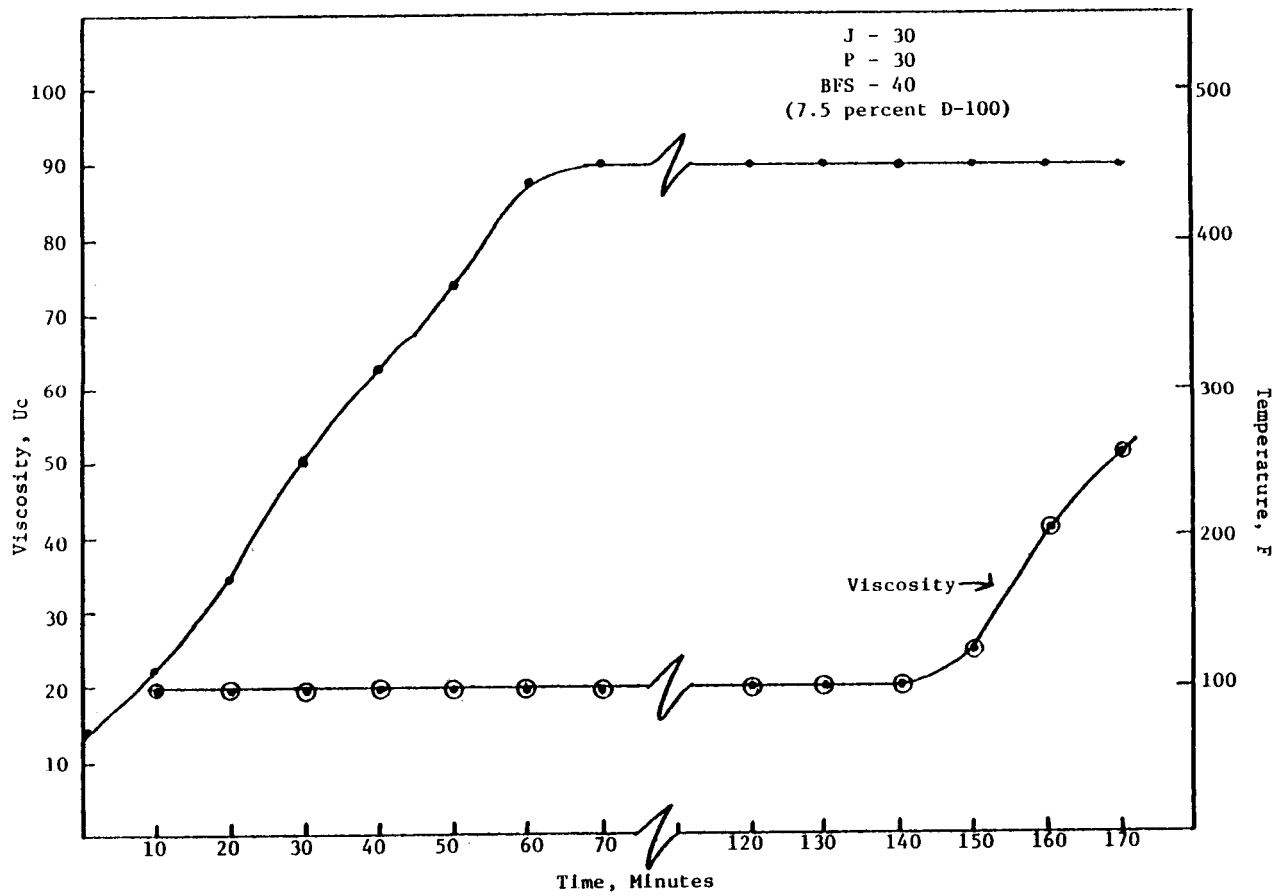


Figure 2. Temperature and viscosity profiles from the API high temperature consistometer.

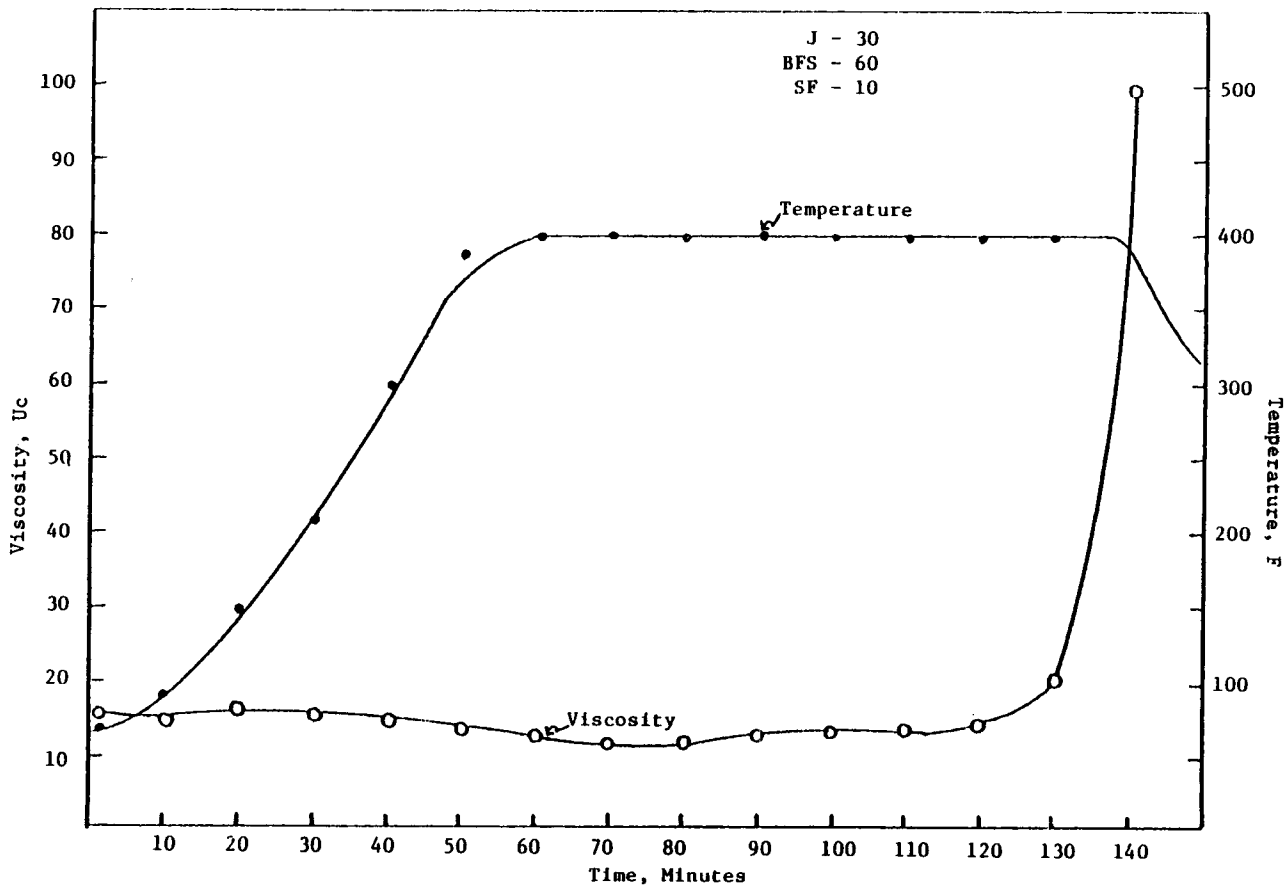


Figure 3. Temperature and viscosity profiles from the API high temperature consistometer.

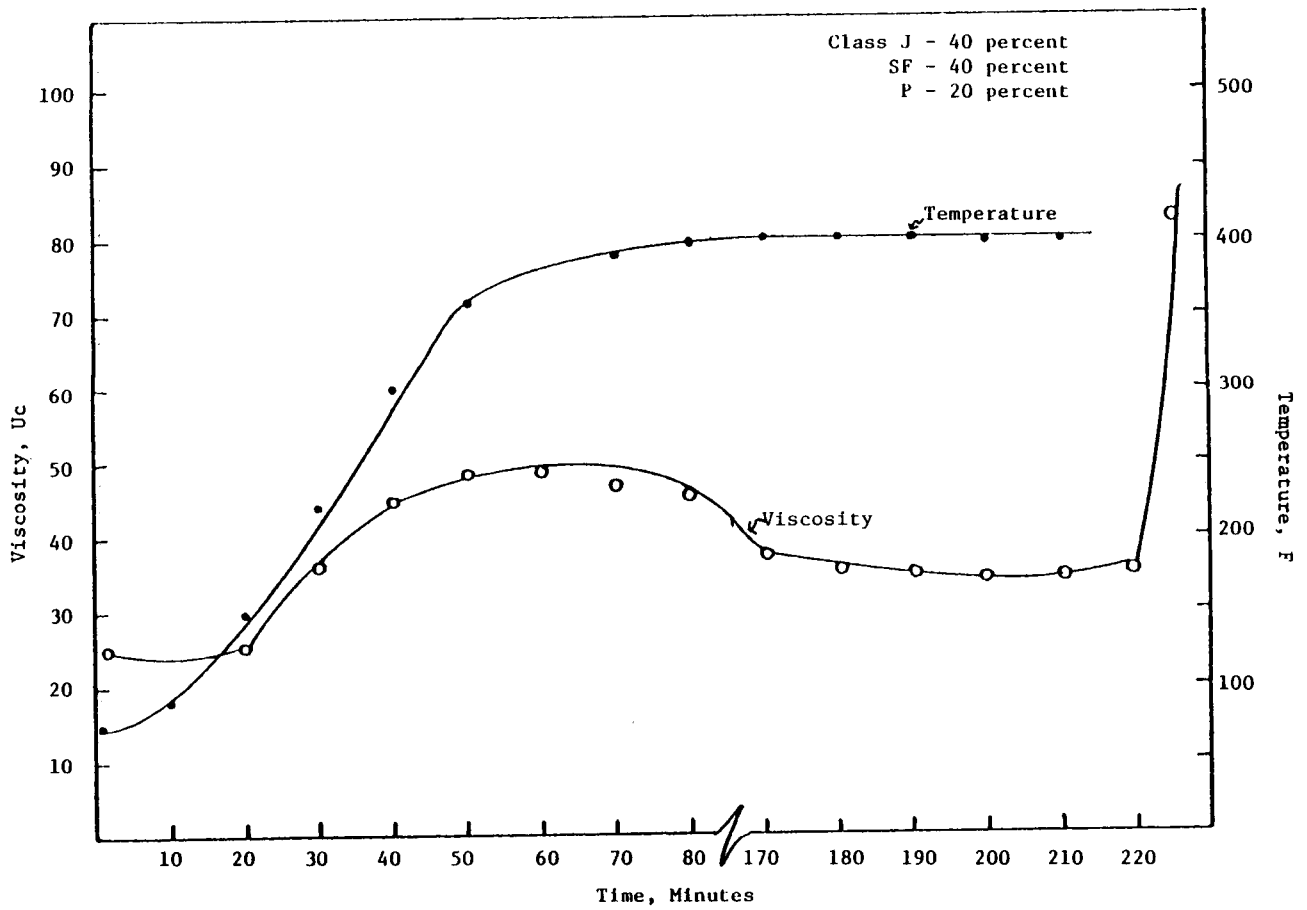


Figure 4. Temperature and viscosity profiles from the API high temperature consistometer.

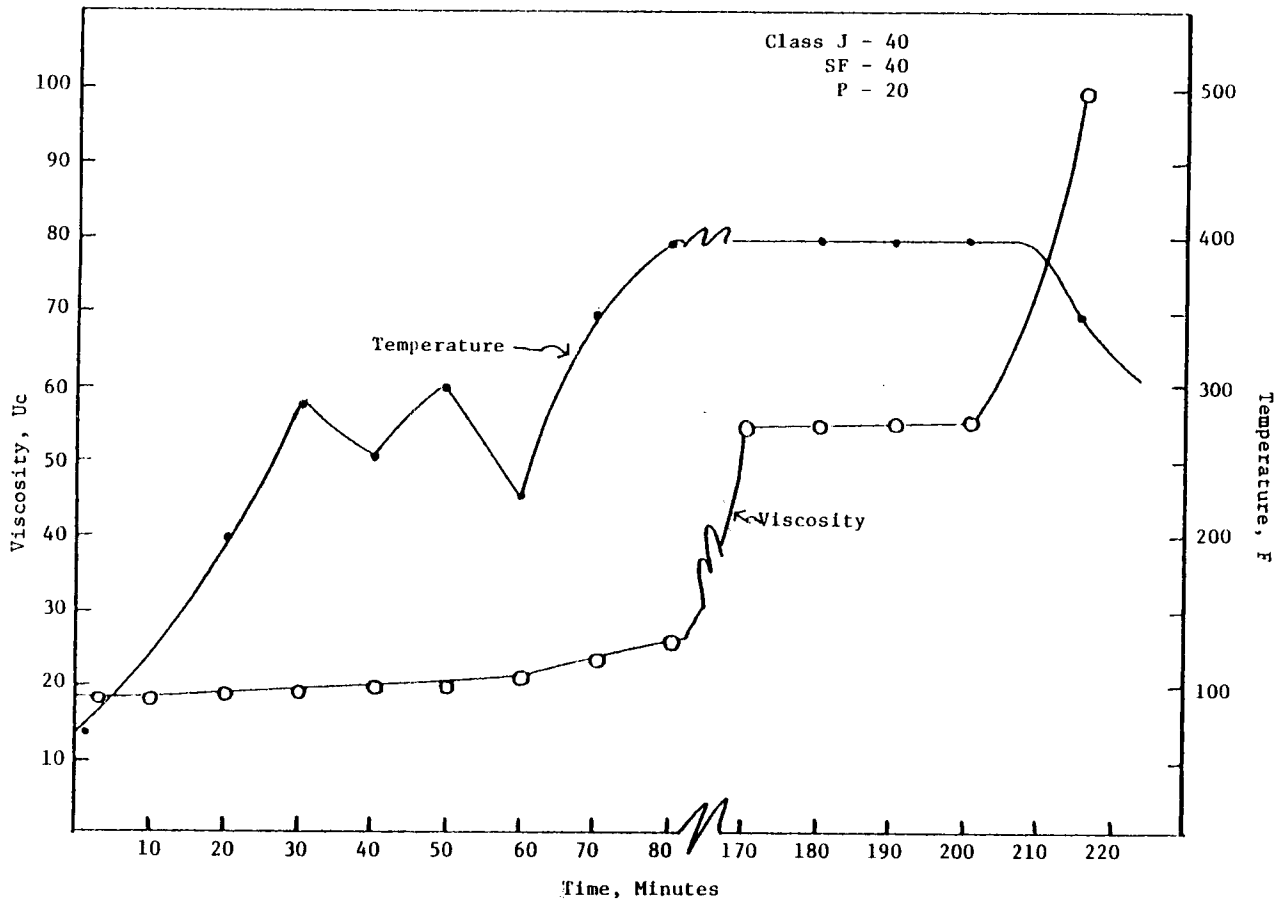


Figure 5. Temperature and viscosity profiles from the API high temperature consistometer.



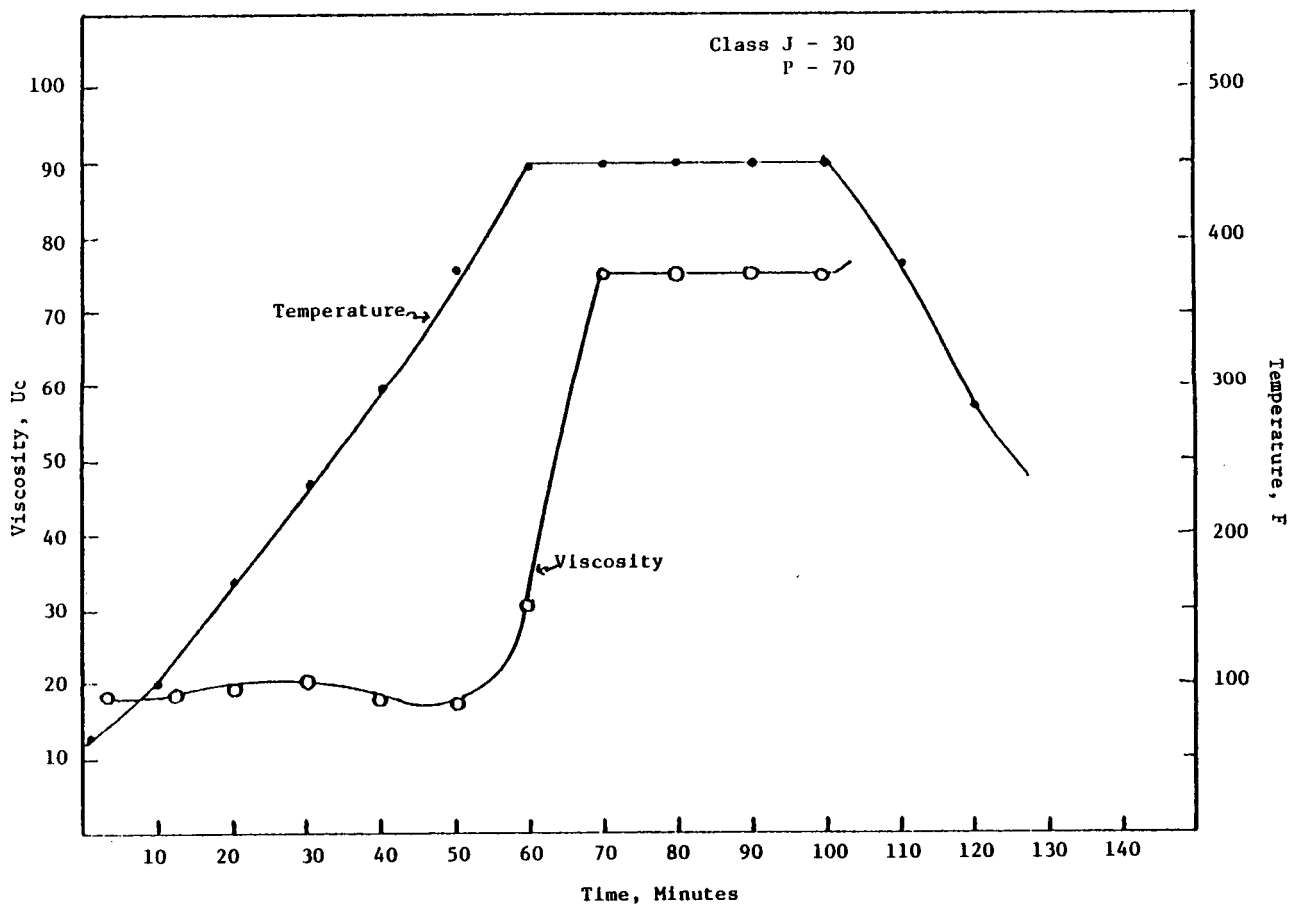


Figure 6. Temperature and viscosity profiles from the API high temperature consistometer.

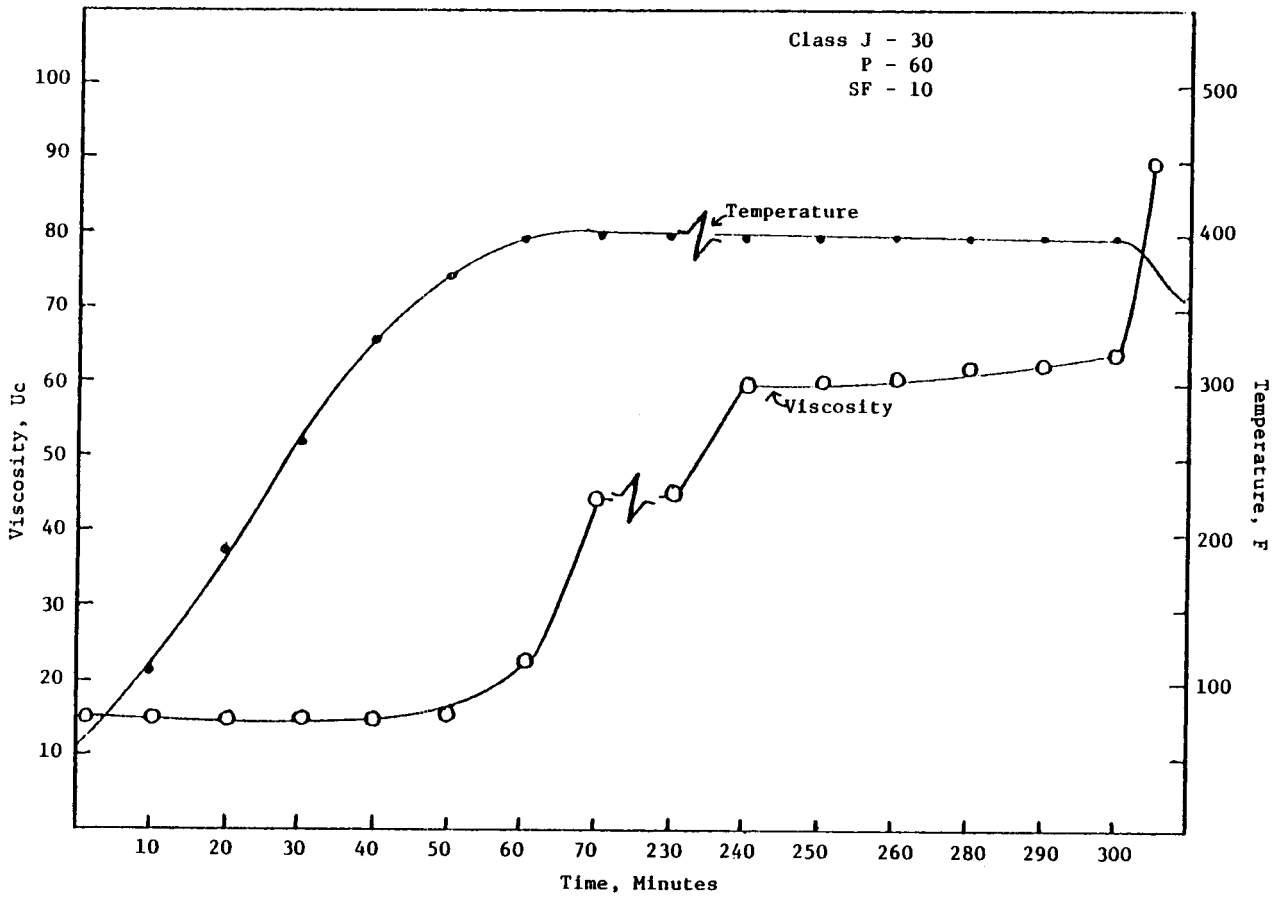


Figure 7. Temperature and viscosity profiles from the API high temperature consistometer.

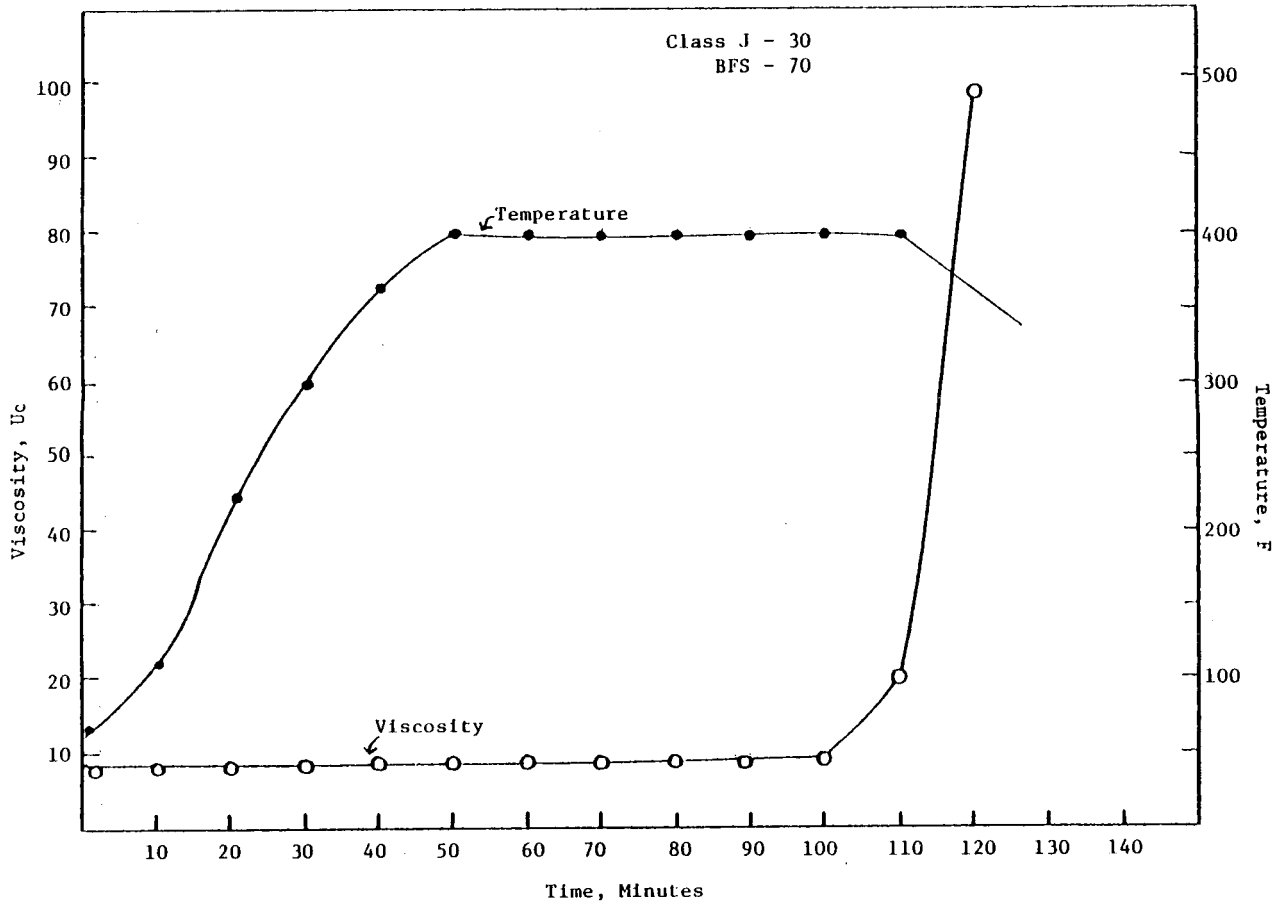


Figure 8. Temperature and viscosity profiles from the API high temperature consistometer.

## Task No. 2 - Compressive Strength Measurements

This task has essentially been completed. Compressive strength measurements on cementing compositions of interest were reported and analyzed in the Fourth Quarterly Technical Progress Report. No significant work had been done in this task since, and none is planned. From here on strength measurements will be limited to a few cement samples as are necessary to supplement existing data or as a possible verification of the past results.

## Task No. 3 - Permeability Measurements

All the necessary modifications of the permeability apparatus and procedures have now been made and reliable permeability data on a number of cementing compositions have been obtained.

Table 1 summarizes the permeability values. These values, as Table 1 depicts, are reported for pressure gradients of 25, 50, 75, and 100 psi, values for the first three pressure gradients being reported twice. The values were obtained using the same cement sample for all pressures. The first value was obtained at 25 psi; subsequent permeabilities were obtained at 25 psi increments up to 100 psi. Pressures, then, were lowered by 25 psi for the second set of values to 25 psi pressure gradients. The purpose of determining the permeabilities in this manner was to determine possible structural (micro or macro) damage to the permeability specimens by increased water pressures as well as to determine the variations in permeability as a function of pressure gradient.

Darcy's law assumes that no interaction (chemical or physical reaction) takes place between the porous medium and the fluid and that the fluid moves through the porous medium under the conditions of viscous flow. By viscous flow it is meant that the fluid flow velocity is low enough that the rate of flow is proportional to the pressure gradient across the permeability specimen. At high pressure gradients, however, depending on the pore shape and porosity distribution of the experimental specimen, the fluid movement through the solid will deviate from that of viscous flow,

TABLE 1  
 PERMEABILITY VALUES OF CEMENTS AS A  
 FUNCTION OF PRESSURE GRADIENT\* (md)

Composition	Experimental Pressure (psi)						
	25	50	75	100	75	50	25
SF-40 P-20	0.02	0.30	0.34	0.9	0.9	0.90	0.84
P-30 BFS-40	0.30	0.40	0.40	0.70	0.70	0.70	0.40
SF-35 BFS-30 B-5	0.09	0.10	0.10	0.30	0.24	0.24	0.24
BFS-70	1.60	2.02	1.45	2.02	3.4	3.4	1.65
P-70	0.40	0.51	0.67	0.90	0.90	0.90	0.90
BFS-60 SF-10	9.7	19.4	16.2	20.2	48.6	12.1	16.2
P-60 SF-10	0.54	0.90	0.60	0.50	0.45	0.24	0.40

\* Permeabilities were determined at pressures 25 through 100 psi and 100 through 25 psi using the same sample. Measurements were started at 25 psi then increased to 100 psi in increments of 25 psi.

that is, fluid flow velocity will no longer be directly proportional to pressure gradient. Under these conditions Darcy's law yields lower permeability values.

A close examination of the permeability values in Table 1, however, indicate higher permeabilities with increasing pressure gradients which is contrary to Darcy's equation. Cementing composition with 40 percent silica flour and 20 percent pozzolan, for example, exhibit permeability values between 0.02 md (for 25 psi pressure gradient) and 0.90 md (for 100 psi pressure gradient). The permeability value given in the last column, which is the value obtained at 25 psi pressure gradient after the sample has been exposed to 100 psi pressure, is higher than the value in the first column, which was also obtained at 25 psi, but before the sample had been subjected to 100 psi pressure gradient. Apparently, higher pressure gradients cause a somewhat permanent damage to the microstructure of the permeability specimens, especially at points with already existing flaws. Preliminary observation under the low power microscope lend support to the permeability data.

#### Task No. 4 - Cement-to-Metal Casing Bond Strength

Cement-to-metal casing bond strength tests were carried out both at room temperature and in the hot-can assembly on all the compositions of interest. The results were reported and discussed in the Fourth Quarterly Technical Progress Report. No cement-to-metal bond strength measurements are planned for the duration of this program unless necessitated by some future unforeseen factors.

#### Task No. 5 - Corrosion of Steel Casing by the Cementing Materials

The electrochemical nature of the corrosion process for steel in cement (or concrete) has allowed the development of techniques which can follow the progression of steel corrosion in a non-destructive fashion.

The great advantage of such techniques is that the onset and progress of the corrosive action of the cementing medium on steel can be determined before visual and structural manifestations, such as delamination, cracking, and spalling, due to stress development by expanding corrosion products.

Previous studies<sup>(1-3)</sup> have demonstrated that the half-cell potential of steel in concrete is a valid indicator of corrosion activity. The corrosion of steel in concrete probably, results from current flow between both macroscopically and microscopically separated anodes and cathodes. The anodes and cathodes can occur on the same steel reinforcing member (or steel casing in geothermal wells) or on widely separated steel members. In a geothermal well the part of the steel casing which is more exposed to a thermochemical environment (brine or flashing brine) would frequently act as an anode and the end that is relatively isolated from such environment would act as a large cathode.

Because of the macroscopic separation of anodes and cathodes, and the relatively high resistance of electrolyte (cement) path between them, the differing electrode potentials of the corroding (anodic) and non-corroding (cathodic) steel areas can be determined by using a reference electrode half-cell situated on the surface of the cement. By conducting a "scan" of the cement surface, the areas of active corrosion can be delineated. Potential measurement methods were utilized as the corrosion estimation technique in the present study.

- 
- (1) Tremper, B., Beaton, J. L., and Stratfull, R. F., Corrosion of Reinforcing Steel and Repair of Concrete in a Marine Environment, Part 2. HRB Bull. 182, 1957, pp. 18-41.
  - (2) Spellman, D. L., and Stratfull, R. F., Laboratory Corrosion Test of Steel in Concrete. Materials and Research Dept., California Division of Highways, Rept. M&R 635116-3, Sept. 1968.
  - (3) Spellman, D. L., and Stratfull, R. F., Chlorides and Bridge Deck Deterioration. Highway Research Record 328, 1970, pp. 38-49.

Corrosion data on five different cementing compositions are summarized in Figure 9. The band between -0.28 and -0.32 volts is considered to be a demarkation line between the corroding and noncorroding conditions. Half-cell potential values greater than -0.28 volt indicate the absence of any appreciable corrosion where as values below -0.32 volt (numerically greater) are an indication of significant corrosion.

Among the half-cell potential data on five cementing compositions in Figure 9 all but one show lower values - increased resistance to corrosion - with curing time. The potential values for these compositions are well above the critical value (-0.32 to -0.28 volt) at 21 day curing. The behavior of sample no. 4 (high point of -0.45 volt) at this time is not understood. After verifying this point an attempt will be made to explain this erroneous behavior with the help of characterization data.

Potential measurement methods are not without their problems, however, as the sole arbitrator of corrosion. The method, by its very nature, is a qualitative measurement which cannot be precisely related to a corrosion rate. The corrosion rate is the parameter which may need to be determined in geothermal wells. Nevertheless, the results of the laboratory work indicate that a non-destructive means for measuring or detecting corrosion activity of steel can be useful in evaluating cement and concrete structures exposed to aggressive environments. However, whenever the half-cell potential values are interpreted in terms of steel corrosion activity it is important to recognize that:

- (1) The half-cell potential of steel can only be empirically related on a statistical basis to cement failure under specific conditions.
- (2) The half-cell potential does not measure the physical condition of the cement medium, and
- (3) Any possible structural damage to the cement due to corrosion of the steel casing is related to cement strength, absorption, moisture content, other chemical species, stresses, and its thickness around the steel casing.



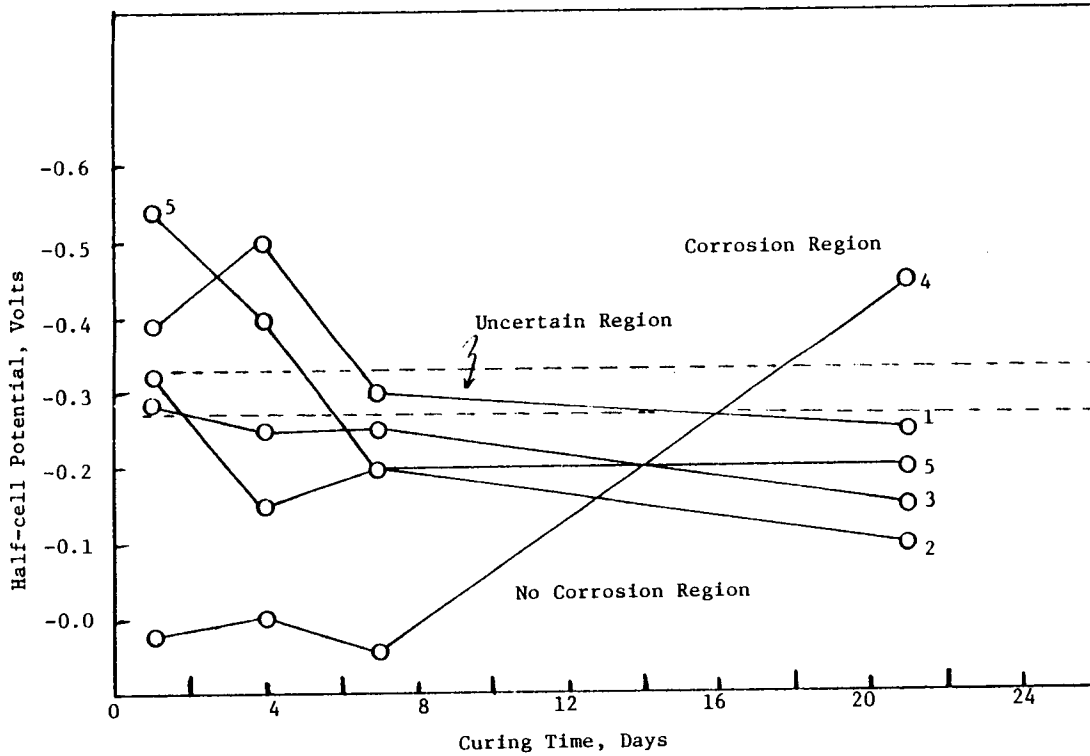


Figure 9. Half-cell potential values for various compositions.

In view of the fact that the steel casing in geothermal wells is exposed to cement on one side and a very aggressive geothermal environment on the other, the failure rate (or the life) of the casing will depend on the severity of the geothermal medium (brine, flashing brine, and steam) rather than the corrosion of the steel casing by the cementing medium. The corrosive action of the cement on the steel casing would be minimal compared to the corrosive effects of the geothermal environment.

Task No. 6 - Characterization of Cementing Materials

Characterization efforts on the cementing materials are presently underway. Various analytical techniques, such as DTA, XRD, SEM/EDAX will be employed in the execution of this task. Characterization studies will comprise the bulk of the efforts for the duration of this program.



APPENDIX 3

NEW HIGH TEMPERATURE CEMENTING MATERIALS FOR GEOTHERMAL WELLS:  
STABILITY AND PROPERTIES

A quarterly report to  
Brookhaven National Laboratory  
Upton, Long Island, New York 11973

for  
Contract No. 422272-S

Principal Investigator  
Della M. Roy  
Professor of Materials Science

for the period  
September 1 - November 30, 1978

December 1, 1978

Materials Research Laboratory  
The Pennsylvania State University  
University Park, Pennsylvania 16802

TABLE OF CONTENTS

	page
LIST OF FIGURES . . . . .	95
LIST OF TABLES . . . . .	96
KEY FOR TABLES . . . . .	97
ABSTRACT . . . . .	98
INTRODUCTION . . . . .	99
EXPERIMENTAL PROCEDURES . . . . .	102
Materials . . . . .	102
Methods . . . . .	102
RESULTS . . . . .	104
Stability Relationships . . . . .	104
Binary System CS(H) . . . . .	104
Ternary System CAS(H) . . . . .	107
Ternary System CMS(H) . . . . .	108
Viscosity of Slurries . . . . .	112
Properties . . . . .	115
Microhardness, Compressive Strength, and Permeability . . . . .	115
Cement-Rock Bonding . . . . .	115
PERSONNEL . . . . .	119
REFERENCES . . . . .	120

LIST OF FIGURES

FIGURE		page
1	Compositions of Starting Materials of the Product Phases for the CAS(H) System . . . . .	105
2	Compositions of Starting Materials of the Product Phases for the CMS(H) System . . . . .	105
3	Mats of Wollastonite Blades formed from 48% CaO, 52% SiO <sub>2</sub> Cured at 400°C and 68.9 MPa for 10 days . . . . .	116
4	Large Fibers of Foshagite Embedded in Fine Needles of Xonotlite Formed from 58% CaO, 42% SiO <sub>2</sub> Cured at 400°C, 68.9 MPa for 10 days . . . . .	116
5	Interlocking Needles of Xonotlite Formed from β-C <sub>2</sub> S + Tripoli at 48% CaO, 52% SiO <sub>2</sub> Cured at 350°C, 68.9 MPa for 10 days . . . . .	117
6	Hexagonal Plates of x-phase Formed from S Calcium Aluminate Cement and 5 μm Minusil, 13% CaO, 37% Al <sub>2</sub> O <sub>3</sub> , 50% SiO <sub>2</sub> Cured at 400°C, 68.9 MPa for 10 days . . . . .	117
7	Mostly Triclinic Anorthite and Some x-phase Formed from β-C <sub>2</sub> S, Metakaolinite, and Silica Cured at 400°C, 68.9 MPa, for 10 days . . . . .	118
8	Nearly Pure Diopside Formed from β-C <sub>2</sub> S and Calcined Chrsotile Paste Cured at 400°C, 68.9 MPa for 10 days . . . . .	118

LIST OF TABLES

TABLE		page
1	Runs used for Determinations of Phase Assemblages Crystallizing in a Portion of the Join $\text{CaO-SiO}_2\text{-H}_2\text{O}$ . . . . .	106
2	Runs used for Determination of Phase Assemblages Crystallizing in a Portion of the System $\text{CaO-Al}_2\text{O}_3\text{-SiO}_2\text{-H}_2\text{O}$ . . . . .	109
3	Runs used for Determination of Phase Assemblages Crystallizing in a Portion of the System $\text{CaO-MgO-SiO}_2\text{-H}_2\text{O}$ . . . . .	111
4	Compressive Strength and Microhardness Measurements for Modified Calcium Aluminate and Class J Oil Well Cement Samples . . . . .	114
5	Haake Rotoviscometer, RV3, Viscosity Measurements with a MK-50 Measuring Head and a Serrated Rotor Sensor System, SVIIP . . . . .	114
Key for Tables . . . . .		96

## KEY FOR TABLES

\*water/solid ratio = 0.45.

<sup>1</sup>All hydrothermally-cured samples crystallized in the presence of excess H<sub>2</sub>O

### <sup>2</sup>Starting Materials:

Oxides: reagent-grade oxides with Al<sub>2</sub>O<sub>3</sub> added as AlO(OH)  
R and S: calcium-aluminate commercial cements  
J: Class J oil well cement  
MK: metakaolinite (amorphous Al<sub>2</sub>Si<sub>4</sub>O<sub>11</sub>)  
Min: 5 μm Minusil (quartz)  
P: perlite--expanded volcanic glass (ca 73% SiO<sub>2</sub>, 18% Al<sub>2</sub>O<sub>3</sub>; 9% CaO)  
T: tripoli (amorphous silica)  
β-C<sub>2</sub>S: B<sub>2</sub>O<sub>3</sub> stabilized dicalcium silicate Ca<sub>2</sub>SiO<sub>4</sub>  
CC: calcined chrysotile

### <sup>3</sup>Product Phases:

AH = hexagonal anorthite CaAl<sub>2</sub>Si<sub>2</sub>O<sub>8</sub>  
AM = x-ray amorphous material  
AT = triclinic anorthite CaAl<sub>2</sub>Si<sub>2</sub>O<sub>8</sub>  
β-C<sub>2</sub>S = B<sub>2</sub>O<sub>3</sub> stabilized Ca<sub>2</sub>SiO<sub>4</sub>  
BI = bicchulite, Ca<sub>2</sub>Al<sub>2</sub>SiO<sub>7</sub>·H<sub>2</sub>O  
BO = boehmite, AlO(OH)  
CA = calcite, CaCO<sub>3</sub>  
CH = chrysotile, Mg<sub>3</sub>Si<sub>2</sub>O<sub>7</sub>·2H<sub>2</sub>O  
CO = corundum, Al<sub>2</sub>O<sub>3</sub>  
CR = cristobalite, SiO<sub>2</sub>  
DE = dellaite, Ca<sub>6</sub>Si<sub>3</sub>O<sub>11</sub>(OH)<sub>2</sub>  
DI = diopside, CaMgSi<sub>2</sub>O<sub>6</sub>  
F = foshagite, Ca<sub>4</sub>Si<sub>3</sub>O<sub>9</sub>(OH)<sub>2</sub>  
GR = grossular, Ca<sub>3</sub>Al<sub>2</sub>Si<sub>3</sub>O<sub>12</sub>  
HG = hydrogrossular: comp. varying between grossular and hibschite  
HI = hibschite, Ca<sub>3</sub>Al<sub>2</sub>Si<sub>2</sub>O<sub>8</sub>(OH)<sub>2</sub>  
MO = monticellite, CaMgSiO<sub>4</sub>  
Q = quartz, SiO<sub>2</sub>  
SC = scawtite, Ca<sub>7</sub>Si<sub>6</sub>(CO<sub>3</sub>)O<sub>18</sub>·2H<sub>2</sub>O  
TR = truscottite, Ca<sub>6</sub>Si<sub>10</sub>O<sub>24</sub>(OH)<sub>2</sub>  
U = unidentified peaks--x-ray pattern  
WA = wairakite, Ca(Al<sub>2</sub>Si<sub>4</sub>)O<sub>12</sub>·2H<sub>2</sub>O  
WO = wollastonite, CaSiO<sub>3</sub>  
X = xonotlite, Ca<sub>6</sub>Si<sub>6</sub>O<sub>17</sub>(OH)<sub>2</sub>

<sup>4</sup>Powder diffractometer x-ray analyses were used to determine the phases present.



## ABSTRACT

Potential new high temperature cementing compositions for geothermal wells have been investigated, primarily within the lime-magnesia-silica-water and lime-alumina-silica-water systems. The stabilities and phase equilibria of constituent phases have been determined, using reaction times varying from two to 98 days, with temperatures in the range up to 300-400°C, and pressures from 1400-10,000 psi (9.6-68.9 MPa).

Xonotlite, anorthite, boehmite, hydrogarnets, wairakite, x-phase or hexagonal anorthite, and truscottite are among the phases present in the system  $\text{CaO-Al}_2\text{O}_3\text{-SiO}_2\text{-H}_2\text{O}$ . Xonotlite, truscottite, talc, chrysotile, monticellite, and diopside are formed in the  $\text{CaO-MgO-SiO}_2\text{-H}_2\text{O}$  system. In the latter compositions, reaction is slower, and thus attainment of equilibrium is more difficult.

Viscosities of slurries, studies of reaction rates, determination of strength and microhardness, permeability, bond strength to rock, corrosiveness, and the effect of saline solutions generally comprise the major parts of the study. Other characterization tools used are x-ray diffraction, optical microscopy, SEM, microprobe, DTA, TGA, thermal expansion, thermal conductivity, and other analytical techniques.

## INTRODUCTION

The performance requirements of cements for geothermal wells are rather severe, including the demands of upper temperature limits which are beyond those usually met in deep oil wells. While modified calcium silicate-based cements have performed well at temperatures up to some 160°C (320°F) or higher (1-3), cements for geothermal wells should be stable up to about 400°C (752°F). This presents problems concerning long range stability, since the usual phases formed are not stable in the upper temperature regime. Recent attempts to extend the range of performance of calcium silicate based cements to higher temperatures have been carried out (4,5). While it has been generally accepted that for ordinary deep oil wells, cement compositions would be adjusted so that tobermorite would be formed as the stable binder; this phase decomposes above a maximum temperature which is a function of pressure (6,7) and composition (8,9) to yield the phases which are thermodynamically stable under the new conditions. Higher pressure increases the maximum thermal stability limit as does the substitution of  $Al^{3+}$  in the structure. However, the maximum stability temperature does not exceed 320°C at 20,000 psi (138 MPa) pressure (8), and is significantly lower at lower pressures. Xonotlite is stable to higher temperatures, and with high- $SiO_2$  ratios, truscottite (7,8) might be stable. Some mechanical problems concerning reactivity and conversion remained to be worked out.

In view of the range of wall rock compositions in geothermal areas, it is important, when determining long term compatibility of cementing materials, to explore a wider range of potential compositions, which could provide the necessary physical and mechanical properties, be technologically feasible for emplacement, and be durable in the chemical and thermal environment. The two major "systems" considered are  $CaO-Al_2O_3-SiO_2-H_2O$  (using a broader compositional range than for normal oil well cements) and  $CaO-MgO-SiO_2-H_2O$ . Work is in progress also to extend the above systems to greater complexities through use of other additives.

Recent studies of high temperature hydrothermal cements investigated the strength, various physical properties, and kinetics of reaction of some conventional as well as special cements (10,11), for the most part limited

to a maximum temperature of ca 250°C (12). While Portland cement compositions, pure calcium silicate compositions, or high-CaO calcium aluminosilicate compositions (13) have been rather extensively investigated, relatively little study has been made of compositions intermediate between high-alumina cements and silica. One compositional area within the CaO-Al<sub>2</sub>O<sub>3</sub>-SiO<sub>2</sub>-H<sub>2</sub>O system appeared to have considerable potential (11,14).

The second major system (obtained by adding MgO to the system CaO-SiO<sub>2</sub>-H<sub>2</sub>O), has been little studied for cement purposes except for asbestos-cement products, which are commercially autoclaved at temperatures up to ca 200°C, but for only short periods of time. The properties of these products are impressive, having high tensile strengths [up to 500 psi (34.5 MPa) flexural strength], imperviousness and dimensional stability (15,16) plus resistance to sulfate and other aggressive agents. Both manufacturing processes and uses are of course different, and if the C-M-S-H compositions prove thermally stable, they must also be adapted to technology for deep well cementing. There are some unknowns regarding phase equilibria, particularly in the low to intermediate temperature range (short term data on autoclaved asbestos materials suggest that the asbestos minerals are compatible with CSH phases such as tobermorite, xonotlite, or gyrolite). Some data on materials autoclaved for 2, 7, and 30 days at temperatures of 150-350°C [(CaO + MgO)/SiO<sub>2</sub> ratios of 0.5-2.5] indicated mutual compatibility of a serpentine phase and a calcium hydrosilicate (17). At 350°C, however, monticellite (anhydrous CaMgSiO<sub>4</sub>) was reported as stable instead, while previous hydrothermal synthesis of monticellite as low as 475°C had been reported (18). Other data are available on the properties of hydrothermal magnesium (calcium) hydrosilicates (19) at relatively modest temperatures.

Some incomplete data on phase stability at higher temperatures come from the mineralogical literature, concerned with contact metamorphism. The following reaction to synthesize tremolite asbestos: 5 talc + 6 alcite + 4 quartz = 3 tremolite + 6 CO<sub>2</sub> + 2 H<sub>2</sub>O, was placed at 440°C (at 2 kb, X<sub>CO<sub>2</sub></sub> = 0.5) (20). The lower temperature limit of tremolite's stability is not known; possibly tremolite is stable through the desired range. The hydrated magnesium silicate phases, serpentine (chrysotile, antigorite) and talc are stable within the 200-400°C temperature range at pressures up to 15-30,000 psi (103-207 MPa) (19).

Work has begun to explore new potential cementing compositions, concentrating upon determining the stability of the phases formed, and determining the most relevant physical and mechanical properties relevant to their emplacement and anticipated long range properties.

## EXPERIMENTAL PROCEDURES

### Materials

Mixtures within the CASH ( $\text{CaO-Al}_2\text{O}_3\text{-SiO}_2\text{-H}_2\text{O}$ ) and CMSH ( $\text{CaO-MgO-SiO}_2\text{-H}_2\text{O}$ ) systems were prepared using pure oxides, hydrated aluminosilicates, hydrated magnesium silicates, silicic acid, tripoli, 5  $\mu\text{m}$  quartz (Minusil), and commercially available cements, including two calcium-aluminate cements and a Class J cement. In addition a  $\text{B}_2\text{O}_3$  stabilized form of  $\beta\text{-C}_2\text{S}$  was also used as the starting material within the  $\text{CaO-SiO}_2$  portion of the ternary oxide diagrams shown in Figs. 1 and 2.

### Methods

Samples are mixed following either ASTM-C305 standards or the API standards. After mixing, the larger samples, cured as 2-inch by 1-inch diameter (50 x 25 mm) cylinders, are placed in a constant humidity chamber at greater than 95 percent relative humidity for 24 hours. These samples are then removed from their molds and placed in a Barnes 500 cc (75 x 250 mm) stainless steel autoclave. Samples are placed in a furnace, pressurized to the desired pressure, and allowed to equilibrate. Usually the temperature and pressure had equilibrated within the first 24 hours.

Samples which are prepared for testing within the standard 1/2-inch (12.7 mm) ID hydrothermal vessel were either put into crimped noble metal tubes (5 mm x 25 mm) in a dry state (in the presence of excess water which leaked into the tube from the pressure vessel) or in a few experiments the required water was emplaced within the sample and the noble metal tubes were sealed before hydrothermal treatment. In a few experiments the cement pastes were mixed with the desired w/s ratio, put into crimped metal tubes and also cured in the presence of excess  $\text{H}_2\text{O}$ .

Testing for microhardness was done on the Leitz microhardness tester using the Vickers indentation method with a 40X objective. Before small 3 mm samples were tested, they were embedded into epoxy, polished with 1-micron diamond paste, and coated with carbon. Cement samples which were 25 mm in diameter were merely polished and coated. Ten measurements were made on each sample and the mean and the standard deviation were calculated with the highest and the lowest values omitted.

Compressive strength measurements were made on a Tinius Olsen Testing Machine. Samples were sawed so the top and bottoms were parallel before testing.

Permeability measurements on the larger samples were made with pressurized (up to 800 psi) nitrogen gas flowing through the samples by measuring the displacement of water by the flowing gas (21). After the gas permeability measurements were made (using the Klinkenberg extrapolation method) these sample samples were epoxy-sealed into steel rings for measurement of water permeability. Water permeability was measured using pressurized water (2000 psi, 14 MPa) flowing through the sample.

## RESULTS

### Stability Relationships

Preliminary experiments using microhardness and compressive strength measurements as criteria for formation of cementing phases, led to the delineation of the areas between 45 and 55 percent  $\text{SiO}_2$  (near the x phase and anorthite stability field in the CASH system and near the xonotlite-chrysotile join in the CSMH system) as ones having potential geothermal application. It was necessary to determine detailed phase equilibria relations in this and surrounding areas in order to better understand the nature and behavior of these potential cements, particularly long term behavior.

Experiments were carried out between 250 and 400°C and 10,000 psi (68.9 MPa) in the presence of excess  $\text{H}_2\text{O}$  to map out phase relationships both above and below the critical point of  $\text{H}_2\text{O}$ . Initial mixtures were prepared from both oxides and from commercially available cements in order to establish phase relationships and to promote the ultimate use of these cements in geothermal wells. The two calcium aluminate cements (designated R and S) and a Class J cement were altered in their bulk chemistry by the addition of oxides (CaO and MgO) and various forms of  $\text{SiO}_2$  (5  $\mu\text{m}$  Minusil, tripoli, and silicic acid). The compositions studied are given in Figs. 1 and 2.

### Binary System CS(H)

Dry powdered samples within the CaO- $\text{SiO}_2$  system were inserted in noble metal tubes which were crimped and then cured hydrothermally in the presence of excess deionized water at a pressure of 10,000 psi (68.9 MPa) and temperature from 250 to 400°C for 10 days. For those mixtures using the starting materials listed in Table 1 which were cured at  $400 \pm 5^\circ\text{C}$ , xonotlite dehydrated to wollastonite ( $\beta\text{-CaSiO}_2$ ) +  $\text{H}_2\text{O}$  as had been previously reported (6,8). Wollastonite, formed as porous mats of large bladed crystals shown in Fig. 3, made the compositions more fragile than those compositions containing mostly xonotlite. The compositions formed after curing at 400°C included foshagite [ $\text{Ca}_4\text{Si}_3\text{O}_9(\text{OH})_2$ ] + xonotlite [ $\text{Ca}_6\text{Si}_6\text{O}_{17}(\text{OH})_2$ ] + a minor amount of wollastonite, cristobalite ( $\text{SiO}_2$ ), and dellaite [ $\text{Ca}_6\text{Si}_3\text{O}_{11}(\text{OH})_2$ ], indicating that full equilibrium in many cases had not yet been established. Of these, other than xonotlite, foshagite was the only compound which

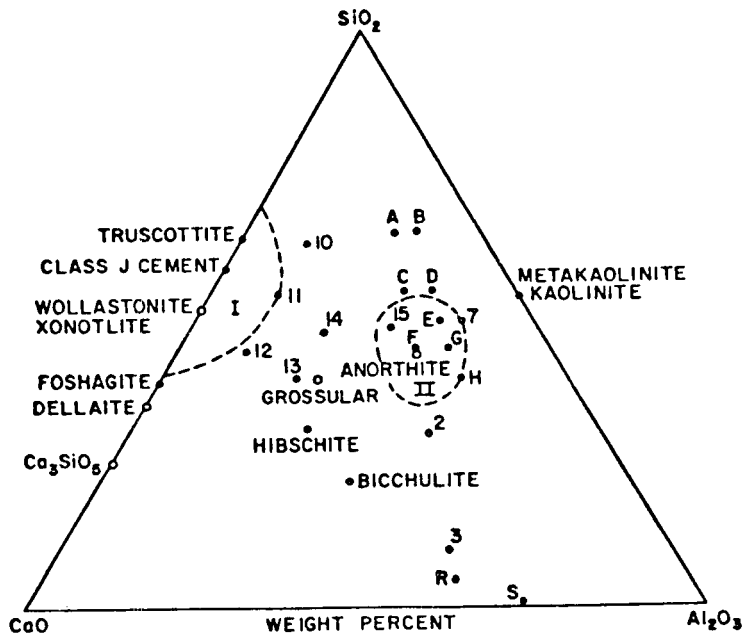


Figure 1. Compositions of starting materials of the product phases for the CAS(H) system.

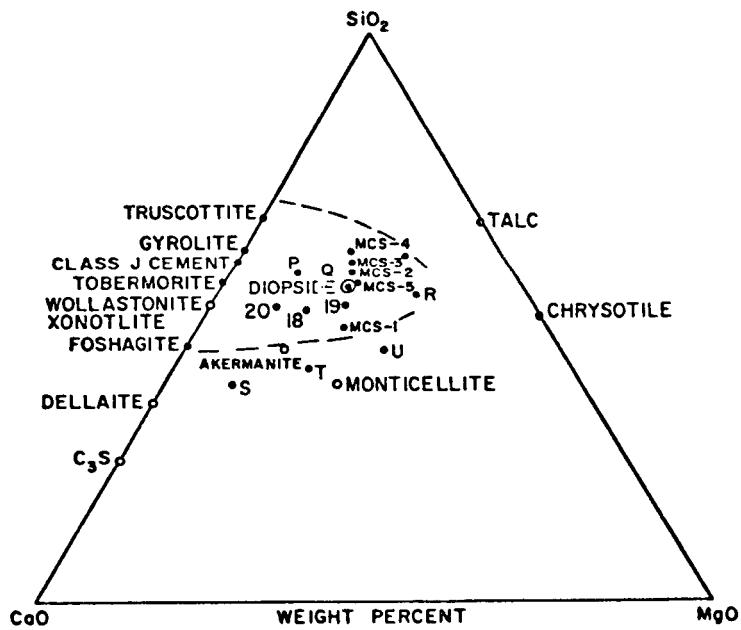


Figure 2. Compositions of starting materials of the product phases for the CMS(H) system.



TABLE 1

Runs used for Determinations of Phase Assemblages Crystallizing in a Portion of the Join CaO-SiO<sub>2</sub>-H<sub>2</sub>O<sup>1</sup>

Mole Ratio	Composition (weight %)		Starting Materials <sup>2</sup>	Temp. (°C±5°)	Pressure (MPa±1)	Time (days)	Phases Present at end of Run <sup>3,4</sup> m = minor amounts
	CaO	SiO <sub>2</sub>					
2:1	65.12	34.88	Oxides	400	68.9	7	DE + X
			β-C <sub>2</sub> S + T	400	"	7	X + mDE
			Oxides	350	"	7	DE + U
3:2	58.34	41.66	Oxides	400	68.9	3	X + F
			"	400	"	10	X + F
			β-C <sub>2</sub> S + T	400	68.9	3	X + F + mWO + mβ-C <sub>2</sub> S
			"	400	"	10	F + X + mWO + mCA
			"	400	172.	10	X
			"	400	17.2	10	F + WO + X
			"	350	68.9	10	F + X + CA
			"	300	"	10	F + X + SC + U
4:3	55.45	44.55	Oxides	400	68.9	3	X + WO + F
			"	400	"	10	X + WO + F
			β-C <sub>2</sub> S + T	400	"	3	F + X + WO + mβ-C <sub>2</sub> S
			"	400	"	10	X + F + WO
			"	400	172.	10	X
			"	400	17.2	10	W + X + F + mCA
			"	350	68.9	10	X + F + CA
			"	300	"	10	X + F + mSC
1:1	48.28	51.72	Oxides	400	68.9	3	X
			"	400	"	10	X + WO
			β-C <sub>2</sub> S + T	400	68.9	3	X + WO + β-C <sub>2</sub> S
			"	400	"	10	X + WO
			"	400	172.	10	X + WO
			"	400	17.2	10	WO
			"	350	68.9	10	X + mWO
			"	300	"	10	X
5:6	43.75	56.25	Oxides	400	68.9	3	X
			β-C <sub>2</sub> S + T	400	68.9	3	X + WO + CR + β-C <sub>2</sub> S
			"	400	"	10	X + WO
---	40.00	60.00	J	400	68.9	10	WO + X + CA
			"	350	"	10	X + TR + CA + SC
			"	300	"	10	X + TR + SC
			"	400	"	3	WO + mTR
2:3	38.36	61.64	Oxides	400	"	3	WO + mTR
			β-C <sub>2</sub> S + T	400	68.9	3	W + TR
3:5	35.90	64.10	Oxides	400	"	3	X + TR + WO
			"	400	"	10	WO + CR
			β-C <sub>2</sub> S + T	400	"	3	WO + TR + CR + β-C <sub>2</sub> S
			"	400	"	10	WO + TR
			"	350	"	10	X + TR + CA + SC
1:2	31.82	68.18	Oxides	400	68.9	3	TR + SC
			"	400	"	10	CR + AM
			"	400	"	10	X + WO + CR
			β-C <sub>2</sub> S + T	400	68.9	3	WO + CR

enhanced the cementitious properties. These reaction products were confirmed for all the starting materials used, with mixtures of  $\beta$ - $C_2S$  + tripoli being the most reactive. Abundant fine xonotlite needles made up the matrix surrounding the larger foshagite fibers with some wollastonite blades, shown in the lower left corner of Fig. 4.

For those mixtures hydrothermally cured at 250, 300, and 350°C and 10,000 psi, again the best cementitious compositions contained foshagite as fibers and xonotlite as fine needles. The fine interlocking needles of xonotlite prepared from  $\beta$ - $C_2S$  + tripoli with a bulk composition of 48 weight percent CaO + 52 weight percent  $SiO_2$  were indicative of some of the best cementing characteristics shown in Fig. 5. Truscottite [ $Ca_2Si_4O_9(OH)_2$ ] was present in the 250, 300, and 350°C cured products in varying amounts depending on the starting materials' silica content. Its presence in the mixtures was not obviously detrimental. Cristobalite was also present in the 300 and 350°C reaction products and not in the 250°C ones. At 400°C a few wollastonite blades were present.

#### Ternary System CAS(H)

The addition of up to 10 percent  $Al_2O_3$ , as boehmite [ $AlO(OH)$ ] in Region I (Fig. 1), 20 percent  $Al_2O_3$ , and 25-45 percent  $Al_2O_3$  in Region II, to the binary join CaO- $SiO_2$  in the presence of excess  $H_2O$  also affects the stability of the calcium-silicate phases formed (Table 2). Within Region I there were slight shifts in the d-spacings of both xonotlite and truscottite to smaller values and wollastonite appeared to be more stable than xonotlite down to temperatures of at least 390°C. The addition of 20 percent  $Al_2O_3$  resulted in the crystallization of the ternary hydrogarnets with compositions near grossular ( $Ca_3Al_2Si_3O_{12}$ ) from 400°C curing, and compositions near hibschite [ $Ca_3Al_2(SiO_4)_{3-x}(OH)_{4x}$ ] from 300°C curing. Triclinic anorthite was also present after both the 300 and 400°C and 10,000 psi hydrothermal treatment.

Within Region II mixtures prepared from two commercially available calcium aluminate cements with the addition of silica formed cementitious products near the anorthite composition. IR absorption spectrometry is presently being used for additional structural characterization of x-phase (a

modified hexagonal anorthite). The relatively small size crystals and dense clustering of the hexagonal plates of x-phase as shown in Fig. 6 are responsible for the favorable cementitious properties as compared with the large xonotlite, truscottite, and foshagite crystals present near the CaO-SiO<sub>2</sub> join.

Within Region II mixtures of  $\beta$ -C<sub>2</sub>S + metakaolinite + silica (50 wt. % SiO<sub>2</sub>, 13 wt. % CaO, 37 wt. % Al<sub>2</sub>O<sub>3</sub>) when hydrothermally treated produce triclinic anorthite with no x-phase at 400°C. At >300 to 400°C mostly triclinic anorthite and a sma-1 amount of x-phase were formed. These latter reaction products shown in Fig. 7 were not cementitious. Longer-term experiments are still in progress to determine if x-phase is stable relative to triclinic anorthite over the temperature range 250 to 400°C.

#### Ternary System CMS(H)

Mixtures listed in Table 3 were cured hydrothermally at 10,000 psi within the 250 to 400°C range. Dry samples were inserted in noble metal tubes (5 mm x 25 mm), crimped and cured in the presence of excess H<sub>2</sub>O; samples with a 0.45 w/s ratio were cured in sealed noble metal tubes for 7 to 10 days in conventional 1/2 inch ID hydrothermal pressure vessels.

The most interesting results within this system were that compositions at or near the diopside stability field showed the most favorable physical properties and highest strength characteristics after hydrothermal curing at 300 to 400°C for 7 to 98 days. Xonotlite formed after short time curing. As curing time increased the amount of xonotlite decreased and was replaced by diopside. At temperatures of 350°C mixtures of xonotlite and diopside produced a good cement. Below this temperature diopside was not present. For relatively short experiments (7 days) xonotlite, talc or chrysotile, traces of quartz,  $\beta$ -C<sub>2</sub>S, diopside, and either trace or major amounts of the carbonate containing phases were present. After 36 days curing xonotlite, chrysotile (also talc), and a trace of carbonate phase were present; after 63 days curing diopside appeared to become the predominant phase almost equal in intensity to xonotlite. In addition, a trace of monticellite was detected. Ninety-six to 98 days of curing produced the following phases: xonotlite, diopside, chrysotile, and a carbonate phase.

TABLE 2

Runs used for Determination of Phase Assemblages Crystallizing in a Portion of the System CaO-Al<sub>2</sub>O<sub>3</sub>-SiO<sub>2</sub>-H<sub>2</sub>O<sup>1</sup>

Mixture Number	Composition (weight %)			Starting Materials <sup>2</sup>	Temp. (°C±5°)	Pressure (MPa±1)	Time (days)	Phases Present at end of Run <sup>3,4</sup> m = minor amounts
	CaO	Al <sub>2</sub> O <sub>3</sub>	SiO <sub>2</sub>					
10	27	10	63	Oxides	400	68.9	10	TR + mWO + mCR
				"	350	"	"	TR
				"	300	"	"	TR
11	36	10	54	Oxides	400	68.9	10	WO + CR
				"	350	"	"	X + TR
				"	300	"	"	X + TR + mAH
12	45	10	45	Oxides	400	68.9	10	WO
				"	350	"	"	X
				"	300	"	"	X
13	40	20	40	Oxides	400	68.9	10	HG + AT
				"	400	172.	"	= HI
				"	400	17.2	"	= GR
14	32	20	48	Oxides	400	68.9	10	X + WO + AT
				"	400	172.	"	WO + X + AT
				"	400	17.2	"	WO + AT
15	21	30	49	Oxides	400	68.9	10	AT
				"	400	172.	"	AT
				"	400	17.2	"	AT
8	30	30	40	Oxides	400	68.9	10	AT + HG
2	25	45	30	Oxides	400	68.9	10	AT + BI + BO + CO
3	32	58	10	Oxides	400	68.9	10	BI + C <sub>4</sub> A <sub>3</sub> H <sub>3</sub> + CO + BO
7	10	40	50	Oxides	400	68.9	10	AT + AH + CR
E	13	37	50	S + Min	500	68.9	10	AH + Q
				"	400	"	"	AH + Q
				"	400	"	30	AH + Q
				"	400	172.	10	AH + Q
				"	400	17.2	10	AH + Q
				"	350	68.9	10	AH + Q
E	13	37	50	β-C <sub>2</sub> S + MK	400	6.9	10	AT
				"	400	68.9	30	AT
				"	400	17.2	10	AT + mAH
				"	350	68.9	10	AT + mAH
				"	300	68.9	10	AH + AT
				"	300	68.9	10	AH + AT
H	15	45	40	S + Min	400	68.9	10	AH + AT
				β-C <sub>2</sub> S + MK + BO	400	68.9	10	AT + BI + BO
A*	12	23	65	R + Min	390	20.7	4	Q + AH
B*	9	26	65	S + 5ZP + Min	380	20.7	10#	Q + AH + BO
C*	16	29	55	R + Min	390	20.7	4#	Q + AH
D*	12	33	55	S + 5ZP + Min	380	20.7	10#	AH + Q + BO
E*	13	37	50	S + M	400	9.65	3	AH + Q + BO
				"	365	9.65	6.5	AH + Q + WA
F*	19	36	45	R + Min	390	20.7	4	AH + Q
G*	14	41	45	S + 5ZP + Min	380	20.7	10#	AH + Q
R*	34	61	5	R	380	20.7	5	BI + C <sub>3</sub> AH <sub>6</sub> + BO surface BI + C <sub>3</sub> AH <sub>6</sub> + BO + Al <sub>2</sub> O <sub>3</sub> inside

#temperature maintained; pressure reduced to 1 MPa for half time of experiment.

It is concluded that the formation of the anhydrous phases including monticellite may be kinetically limited. The initial phases formed are the hydrates and platy minerals. In time these are followed by the development of the anhydrous phases, especially diopside. Traditionally these anhydrous phases are high temperature minerals. The present studies are at the lower limits of their stability regions. Scanning electron micrographs of the cured  $\beta$ - $C_2S$  + calcined chrysotile paste (Fig. 8) and a cured Class J cement + MgO + 5  $\mu$ m Minusil indicated the presence of fibrous and platy material respectively even though the x-ray diffraction data indicated nearly pure diopside. Diopside is usually blocky or prismatic. Possibly diopside formed as a pseudomorph after the initial fibrous chrysotile and xonotlite.

The MCS-5 composition (Fig. 2) after curing for 7 days at 300°C and 10,000 psi in a sealed noble metal tube showed evidence of zoning. The outside material was white and could be scraped from the bulk of the sample, revealing a stronger (harder) material beneath. The inner material consisted of xonotlite, scawtite, and a trace of talc and diopside; the outer material was xonotlite (much better crystallized--very sharp peaks), talc, and a trace of scawtite. The lack of scawtite in the outer material, and the corresponding increase in crystallinity of xonotlite suggested a possible link between crystallinity and the carbonate content.

The effect of scawtite and calcite upon the compressive strength and microhardness has yet to be determined. Values obtained to date seem to indicate acceptable and even superior strengths for the carbonate-containing cements. Should the effect of this presence prove to be inconsequential this would be extremely important when dealing with the design of plugging materials for carbonate-containing strata or in areas which have high  $HCO_3^-$  containing groundwater.

At this point it is still difficult to determine whether the critical point of water is a significant factor in these experiments. However, if the development of diopside is kinetically controlled, the reaction rate at 400°C should be greater, especially in the super-critical environment. The 300-400°C data for mixtures MCS-1 through 5 (Table 3) seem to indicate this possibility since trace amounts of diopside are usually detected at 400°C, but not at 300°C after 7 days.

TABLE 3

Runs used for Determination of Phase Assemblages Crystallizing in a Portion of the System CaO-MgO-SiO<sub>2</sub>-H<sub>2</sub>O

Mixture Number	Composition			Starting Materials <sup>2</sup>	Temp. (°C±5°)	Pressure (MPa±1)	Time (days)	Phases Present at End of Run <sup>3,4</sup> m = minor amount
	CaO	MgO	SiO <sub>2</sub>					
P	32	10	58	J + CC	400	68.9	10	X + WO
				"	350	"	"	X
				"	300	"	"	X
Q	24	20	56	J + CC	400	"	"	DI
				"	350	"	"	X + DI
				"	300	"	"	X + mCH
R	16	30	54	J + CC	400	"	"	DI + MO
				"	350	"	"	DI + X + CH
				"	300	"	"	X + CH
S	52	10	38	β-C <sub>2</sub> S + CC	400	"	"	DE + MO
				"	350	"	"	MO + mDE
				"	300	"	"	X + DE
T	39	20	41	β-C <sub>2</sub> S + CC	400	"	"	MO + DI
				"	350	"	"	MO + DI
				"	300	"	"	X + CH
U	26	30	44	β-C <sub>2</sub> S + CC	400	"	"	DI + MO
				"	350	"	"	MO + DI
				"	300	"	"	CH + X
MCS-1*	30	22	48	J + Min + MgO	400	"	7	X + CH + CA
MCS-2*	24	18	58	"	400	"	"	X + mCH + mSC
					300	"	"	X + mTA + mDI + mβ-C <sub>2</sub> S
MCS-3*	23	17	60	"	400	"	"	SC + TA + mQ + mβ-C <sub>2</sub> S + mX
					300	"	"	X + TA + mDI + mQ = mCH
MCS-4*	22	16	62	"	400	"	"	SC + TA + Q + mβ-C <sub>2</sub> S
					300	"	"	X + TA + DI + mQ + mCH
MCS-5*	26	19	51	"	400	"	"	SC + Q + TA + mβ-C <sub>2</sub> S
					300	"	"	X + TA + mCA + mDI + mCH
18*	34	15	51	J + MgO	400	"	"	X + SC + mTA + mDI inside
				"	400	"	"	X + TA + mSC surface
				"	400	"	36	X + CH + mCA
19*	28	20	52	J + Min + MgO	400	"	63	DI + X + CA + mCH + mMO
				"	400	"	96	X + CH + CA
				"	400	"	36	X + mCH + mCA
20*	38	10	52	J + MgO + CaO	400	"	63	DI + X + CH + mMO + mCA
				"	400	"	98	X + DI + CH + CA
				"	400	"	63	X + CH + CA
<u>Saturated NaCl used in mixing water:</u>								
MCS-1*	30	22	48	J + Min + MgO	400	"	7	DI + NaCl + MO + mX + mCA
					300	"	"	NaCl + SC + CH + Qm + X
MCS-2*	24	18	58	"	400	"	"	X + NaCl + TA + mDI + mCA
					300	"	"	X + NaCl + SC + mTA
MCS-3*	23	17	60	"	400	"	"	X + TA + NaCl + mDI + mCA
					300	"	"	NaCl + SC + TA + mQ + C + mDI + mDI
MCS-4*	22	16	62	"	400	"	"	NaCl + X + mTA + mDI + mCA
					300	"	"	NaCl + SC + Q + mTA
MCS-5*	26	19	55	"	400	"	7	DI + NaCl + mCA + mTA
					300	"	7	NaCl + X + SC + mCH
18*	34	15	51	J + MgO	400	"	63	X + DI + CA + mCH
				"	300	"	63	SC + X + CH
19*	28	20	52	J + Min + MgO	400	"	63	X + DI + CH + CA + mTA
				"	300	"	63	X + CH + mSC
20*	38	10	52	J + MgO + CaO	400	"	63	X + CA + CH + DI
				"	300	"	63	SC + X + CH + mDI

In addition to the deionized water runs, saturated brine was used as mixing solution for a number of experiments. For the most part results are nearly identical to the salt-free runs. One noteworthy difference, however, is that diopside begins to develop prominence at an earlier stage in the salt-containing runs. Even in the 7 day runs (Table 3) diopside begins to exhibit major proportions. It seems as if chloride complexing due to the presence of NaCl in solution allows more efficient mass transport resulting in more rapid reaction rates; or, simply, it increases the solubility.

#### Viscosity of Slurries

A Haake kotoviscometer, RV3, including a constant temperature circulator, has been put into operation. The unit as received contains a type MK-50 measuring head with a maximum torque of 0.49 newton-cm (50 cm-g). Two rotor sensor systems, SVI and SVIIP, are available for use, depending upon the substance being tested. The former is smooth-walled whereas the latter is serrated. The calculation factors for these sensor systems are given below. The torque/shear stress (y-axis) versus rotor speed/shear rate (x-axis) values are supplied to a Hewlett Packard X-Y recorder with a built-in time base.

Sensor System	SVI	SVIIP
Calculation Factors:		
A (Pa/scale grad.)	1.141	3.46368
M (min/s)	0.89	0.78
G (mPa·s/scale grad·min)	1282.06	4440.615
f ( $\cdot 10^{-4} \text{ cm}^{-3}$ )	253	768

where:  $G = \text{an instrument factor} = A/M \times 10^3 \text{ (mPa}\cdot\text{s/scale grad}\cdot\text{min)}$

$M = \text{sensor factor}$

$A = \text{shear stress factor}$

$\eta = \text{viscosity} = \frac{G \cdot S}{n} \text{ (mPa}\cdot\text{s) or (cp)}$

$S = \text{torque scale value (scale grad.)}$

$n = \text{rotational speed (rpm) 0 to } 1000 \text{ min}^{-1}$

Preliminary viscosity measurements were made on cement slurries without admixtures, including two calcium aluminate cement pastes ( $w/c = 0.45$ ), a Class C paste ( $0.56 w/c$ ), a type I paste ( $w/c = 0.30$ ), and a modified Class J cement paste ( $0.45 = w/c$ ), one mixed by hand and one mixed in a blender. The shear stress values,  $S$ , were measured up to a rotor speed,  $n$ , of 724 rpm using the serrated SVIIP sensor system. Using programmed shear increase rates of 400 and 100 rpm, gave the viscosities listed in Table 4. The low  $w/c$  ratio type I cement slurry increased in viscosity with time and in 5 minutes had exceeded the capacity of the instrument. The more water-rich class C cement slurry and both calcium aluminate slurries also increased in viscosity with time but not as much. On the other hand, the viscosity of the modified class J cement slurry decreased with time with the mixture mixed in the blender producing the most viscous mixture 45 minutes after the initial mixing. The viscosity of a  $\beta$ - $C_2S$  mixture decreased after 20 minutes, then the setting was abrupt.

Previous viscosity measurements made on a co-axial rotational Brookfield viscometer model 5X HBT showed that differences in the viscosities of slurries were related to systematic differences in total composition, different forms of added  $SiO_2$ , and different mixing times. The effect of varying the particle size of the added quartz produced higher viscosities of the samples with higher specific surface. With no admixture the viscosities were not much different for the deionized water versus saturated NaCl solutions. With a one percent addition of an admixture using deionized water the viscosity was reduced by at least a factor of four. Of the admixtures used a lignosulfonate-type retarder was found to be the most effective for a give concentration in reducing viscosity of the cement slurries. An increase of from 10 to 20 percent  $Al_2O_3$  reduced the viscosity whereas an increase of 10 to 20 percent MgO increased the viscosity by a factor of 5. Studies of the effects of superplasticizers, lignosulfonates, and oxides on viscosity are continuing.

The identification of the interrelationships between the retarding additive and the two different calcium-aluminate cements (designated R and S) have shown that there were significant differences in the behavior of the two cements using a lignosulfonate retarder.



TABLE 4

Compressive Strength and Microhardness Measurements for  
Modified Calcium Aluminate and Class J Oil Well Cement Samples

Sample	Starting Material	Compressive Strength kg/cm <sup>2</sup>	Microhardness kg/mm <sup>2</sup>
*A (Fig. 1)	R + Min	82	soft
*C (Fig. 1)	R + Min	127	--
*D (Fig. 1)	S + 5%P + Min	142	16.7 ± 4.3
*E (Fig. 1)	S + Min	311	30.66±11.5
*HYD-2	S + Min	306	17.02± 5.5
*F (Fig. 1)	R + Min	227	25.8 ±10.9
*G (Fig. 1)	S + 5%P + Min	144	21.6 ± 7.8
*R (Fig. 1)	R	576	48.4 ± 9.3
*19-J-400-3 (Fig. 2)	J + Min + MgO	-	25.0
*5-J-400	90% J + 10%MgO	341	19.17
*6-J-400	67% J + 23% Min + 10% MgO	203	13.04± 3.3
*6H-J-400	67% J + 23% Min + 10% MgO	163	10.82± 1.1
*18-J-400-96 (Fig. 2)	J + MgO	169	21.10± 2.1

TABLE 5

Haake Rotoviscometer, RV3, Viscosity Measurements with a MK-50 Measuring Head and a  
Serrated Rotor Sensor System, SVIIP

Cement Starting Materials	Water Solid	Viscosity (rpm)						Remarks
		Initial			20 min. wait			
		100	200	600	100	200	600	
Type I	0.30	2000	1200	815	2120	1350	off chart	5-min. wait period rather than 20 min. Mixed at >100 rpm
Ca-alum. S cement	0.45	1000	620	310	1130	1735	410	Mixed at >100 rpm
Ca-alum. S cement	0.45	400	230	150	1040	590	260	Mixed in blender at >10,000 rpm
Ca-alum. R cement	0.45	645	430	170	350	430	225	Mixed at >100 rpm
Class J oil-well cement	0.45	1890	1300	630	1830	1160	590	Mixed at >100 rpm
Class J oil-well cement	0.45	2040	1300	590	400	625	370	Mixed in blender at >10,000 rpm. About 300 cp at all speeds after 45 min.
β-C <sub>2</sub> S	0.50	1375	760	300	910	670	300	Mixed at >100 rpm
Class C cement	0.56	335	250	170	1245	755	280	Mixed at >100 rpm

## Properties

### Microhardness, Compressive Strength, and Permeability

Compressive strength measurements, using the Tinius Olsen Testing Machine, and microhardness measurements, using a Leitz miniload microhardness tester with the Vickers indenter, were used to characterize the strengths of the cured cements. Permeability measurements using both forced nitrogen gas at pressures up to 800 psi and forced deionized water at pressure of 2000 psi were made on these same cured neat pastes. Samples prepared with a saturated brine solution in the mixing water, in place of the deionized water, generally showed lower strength (as exhibited by the microhardness measurements) and a leaching of the cements was apparent when pressurized deionized water was used for the permeability measurements.

The data in the summary Table 5 shows the relationship between microhardness and compressive strength, therefore either may be used as a strength criterion. Additional permeability data have shown that measuring a gas permeability before measuring the water permeability has no detrimental effect (21), i.e. any damaging effects by the pressurized gas is not evident when the water pressurized water flows through the sample. Generally the water permeabilities are within an order of magnitude of the extrapolated gas permeability (water is an order of magnitude lower than the gas permeability).

### Cement-Rock Bonding

Various workers (22,23) have shown the feasibility of using a push-out test as a relative measure of bond strength. These investigators have used a modification of a punch and die apparatus in which a cement paste plug or steel rod is pushed out of either a host rock or a cement paste host, respectively. Present work is continuing on these approaches using a 3/4 inch central specimen of cured cement paste or steel rod embedded in various rock types or cement paste mixtures.

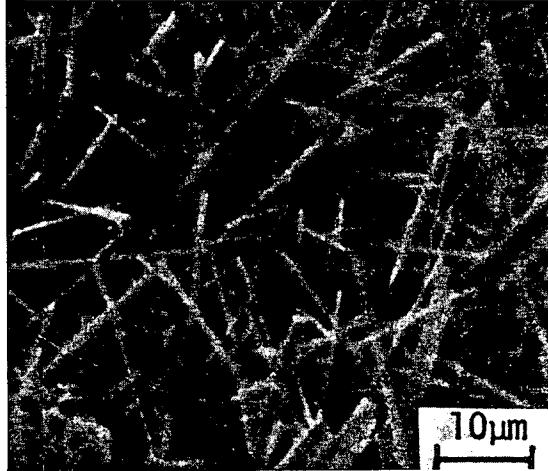


Figure 3. Mats of Wollastonite blades formed from 48% CaO, 52% SiO<sub>2</sub> cured at 400°C and 68.9 MPa for 10 days.

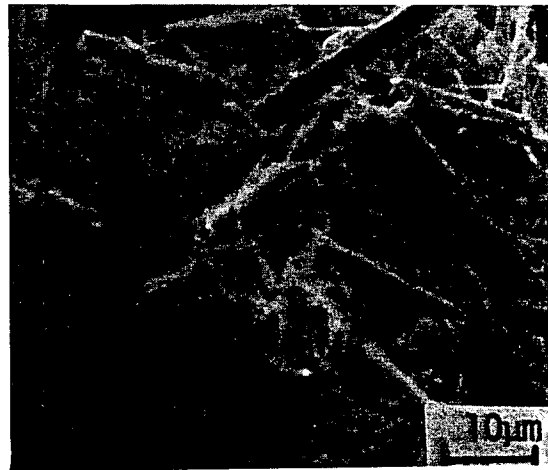


Figure 4. Large fibers of foshagite embedded in fine needles of xonotlite formed from 58% CaO, 42% SiO<sub>2</sub> cured at 400°C, 68.9 MPa for 10 days.



Figure 5. Interlocking needles of xonotlite formed from  $\beta$ - $C_2S$  + tripoli at 48% CaO, 52% SiO<sub>2</sub> cured at 350°C, 68.9 MPa for 10 days.

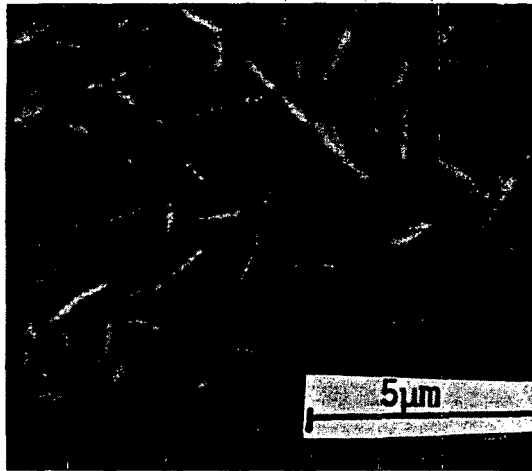


Figure 6. Hexagonal plates of x-phase formed from S calcium aluminate cement and 5  $\mu$ m minusil, 13% CaO, 37% Al<sub>2</sub>O<sub>3</sub>, 50% SiO<sub>2</sub> cured at 400°C, 68.9 MPa for 10 days.

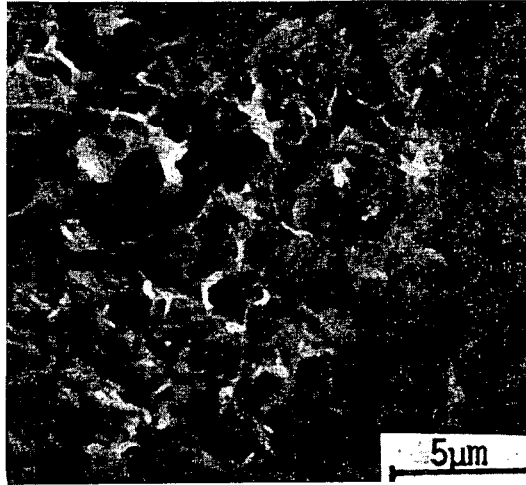


Figure 7. Mostly triclinic anorthite and some x-phase formed from  $\beta$ -C<sub>2</sub>S, metakaolinite, and silica cured at 400°C, 68.9 MPa, for 10 days.

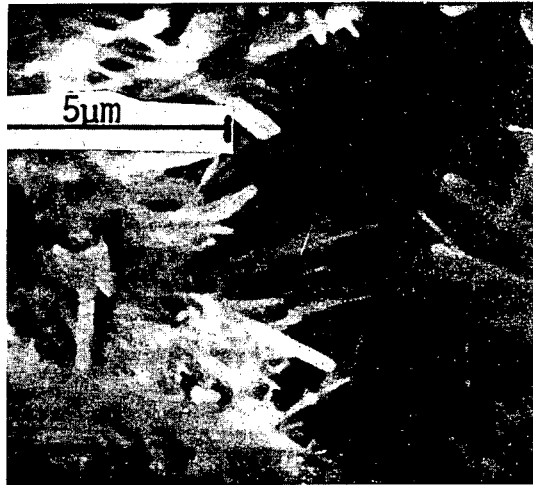


Figure 8. Nearly pure diopside formed from  $\beta$ -C<sub>2</sub>S and calcined chrsotile paste cured at 400°C, 68.9 MPa for 10 days.

## PERSONNEL

The research for this period has been under the direction of Dr. Della M. Roy with assistance from Drs. Michael Grutzeck and Elizabeth L. White. A graduate student, C. Langton, and research technicians G. Zimmerman and N. Hermanowicz have been involved in the research to various extents.

## REFERENCES

1. Ostroot, G. W., and Walker, W. A.: "Improved Compositions for Cementing Wells with Extreme Temperatures," Journal of Petroleum Technology, 277-284 (1961).
2. Kalousek, G. L.: "High Temperature Steam Curing of Concrete at High Pressure," Proc. Vth Intl. Symposium on the Chemistry of Cement, Tokyo, 1968, Vol. III, pp. 523-540 (1969).
3. Maravilla, S.: "A Hydrothermal Setting Cement for Cementing Ultra-deep, Hot Wells," Journal of Petroleum Technology, 1087-1094 (1974).
4. Eilers, L. H., and Root, R. L.: "Long Term Effects of High Temperature on Strength Retrogression of Cements," Soc. Pet. Eng. AIME, SPE 5871 (April 8-9, 1976).
5. Kalousek, G. L., and Chaw, S. Y.: "Reserach on Cements for Geothermal and Deep Oil Wells," SPE, 307-309 (December 1976).
6. Buckner, D. A., Roy, D. M., and Roy, R.: "Studies in the System  $\text{CaO-Al}_2\text{O}_3\text{-SiO}_2\text{-H}_2\text{O}$ . II. The System  $\text{CaSiO}_3\text{-H}_2\text{O}$ ," American Journal of Science 258, 132-147 (1960).
7. Roy, D. M., and Harker, R. I.: "Phase Equilibria in the System  $\text{CaO-SiO}_2\text{-H}_2\text{O}$ , Discussion," Proc. IVth. Intl. Symposium on the Chemistry of Cement, Washington, 1960, National Bureau of Standards, Monograph 43, 196-201 (1962).
8. Roy, D. M., and Johnson, A. M.: "Investigations of Stabilities of Calcium Silicate Hydrates at Elevated Temperatures and Pressures," Proc. Intl. Symposium on Autoclaved Calcium Silicate Building Products, Society of Chemical Industry, London, 114-120 (1965).
9. Diamond, S., White, J. L., and Dolch, W. L.: "Effects of Isomorphous Substitution to Hydrothermally Synthesized Tobermorite," American Mineralogist 51, 388-401 (1966).
10. Oyefesobi, S. O., and Roy, D. M.: "Hydrothermal Studies of Type V Cement-Quartz Mixes," Cement and Concrete Research 7, 803-810 (1976).
11. Oyefesobi, S. O., and Roy, D. M.: "Hydrothermal Studies of Special Types of Cement Mixed with Quartz," Cement and Concrete Research 7, 95-102 (1977).
12. Langton, C. A., Grutzeck, M. W., and Roy, D. M.: "Cement-Rock Interface at Elevated Temperatures and Pressures," Ceramic Bulletin 57, 324 (1978).
13. Roy, D. M., and Roy, R.: "Crystalline Solubility and Zeolitic Behavior in Garnet Phases in the System  $\text{CaO-Al}_2\text{O}_3\text{-SiO}_2\text{-H}_2\text{O}$ ," Proc. IVth Intl.

Symposium on the Chemistry of Cement, Washington, 1960, National Bureau of Standards, Monograph 43, Vol. I, 307 (1962).

14. Roy, D. M., White, E. L., Langton, C. A., and Zimmerman, K. G.: "Hydrated Calcium Aluminosilicate Cements for Hydrothermal Bonding," Cement and Concrete Research 8, 509-512 (1978),
15. Washa, G. C. (Chairman): "High Pressure Steam Curing Modern Practice, and Properties of Autoclaved Products," Report, ACI Committee 516, Journal of the Chemistry and Concrete Institute, 869-908 (August 1965).
16. Yang, Julie C.: "Autoclaved Asbestos Cement Products," Menzel Symposium on High Pressure Steam Curing," ACI Special Publication 32, 117-140 (1972).
17. Petrovic, J.: "The System  $\text{CaO-MgO-SiO}_2\text{-H}_2\text{O}$  from 150=350°C under Hydrothermal Conditions. I. Heterogeneous Mixtures," Silikaty 17 (4), 311-316 (in Slovak) (1973).
18. Roy, D. M.: "Subsolidus Data for the Join  $\text{Ca}_2\text{SiO}_4\text{-CaMgSiO}_4$  and the Stability of Merwinite," Mineralogical Magazine 31 (233), 187-195 (1956).
19. Roy, D. M., and Roy, R.: "Synthesis and Stability of Minerals in the System  $\text{MgO-Al}_2\text{O}_3\text{-SiO}_2\text{-H}_2\text{O}$ ," American Mineralogist 40, 147-178 (1955).
20. Slaughter, J., Kerrick, D. M., and Wall, V. J.: "Experimental and Thermodynamic Study of Equilibria in the System  $\text{CaO-MgO-SiO}_2\text{-H}_2\text{O-CO}_2$ ," American Journal of Science 275, 143-162 (1975).
21. Scheetz, B. E., White, E. L., Roy, D. M., and Zimmerman, K. G.: "Permeability Measurements on Cementitious Materials for Nuclear Waste Isolation," Paper AE6, Symposium on Science Underlying Radioactive Waste Management, Materials Research Society, Nov. 28 - Dec. 1 (1978), Proceedings, Plenum Press (in press).
22. Roy, D. M., White, W. B., Grutzeck, M. W., Sweet, J. R., and Oyefesobi, D.: "Borehole Plugging by Hydrothermal Transport," Final Report for Union Carbide Corp., ORNL-Sub-4091-3 (February 28, 1976).
23. Becker, H., and Peterson, G.: "Bond of Cement Compositions for Cementing Wells," Proc. 6th World Petroleum Congress, Frankfurt, Germany (June 10-26, 1963).





APPENDIX 4

SOUTHWEST RESEARCH INSTITUTE

6220 CULEBRA ROAD • POST OFFICE DRAWER 28510 • SAN ANTONIO, TEXAS 78284

HIGH-TEMPERATURE MATERIALS FOR USE  
IN THE CEMENTING OF GEOTHERMAL WELLS

TECHNICAL PROGRESS REPORT NO. 5  
October - December 1978  
SwRI Project No. 02-5083  
BNL Contract No. 427964-S


to

Brookhaven National Laboratory  
Upton, L. I., N.Y. 11973

January 15, 1979

APPROVED:

Prepared by:  
D. K. Curtice

  
U. S. Lindholm, Director  
Department of Materials Sciences



SAN ANTONIO, HOUSTON, TEXAS, AND WASHINGTON, D. C.

## ABSTRACT

A research program to develop improved cements for use in geothermal well completions was begun in October 1977 at Southwest Research Institute. This fifth quarterly technical progress report includes work accomplished during the period October - December 1978. Selection has been made of several formulations for use at 315°C and above. Physical testing of the various formulations has included compressive and bond strengths and permeability to water.

TABLE OF CONTENTS

	<u>Page</u>
I. INTRODUCTION	126
II. REVIEW AND EVALUATION	127
III. SwRI HIGH-TEMPERATURE CEMENT RESEARCH	128
A. Formulation Optimization	128
B. Physical Properties Evaluation	130
1. General	130
2. Compressive Strength	132
3. Bond Strength	133
4. Future Work	133
IV. CYCLICAL BOND TESTS OF SwRI 150°C CEMENT	134

## I. INTRODUCTION

In October 1977, Southwest Research Institute (SwRI) began a research program to develop an improved cement for use in high-temperature geothermal well completions. This report describes the research carried out during the fifth quarter of Brookhaven National Laboratory Contract No. 427964-S at SwRI.

During the period of October 1 to December 31, 1978, various formulations of hydrothermal cements have been studied to optimize those which will be pumpable at temperatures up to at least 315°C or higher and set with good compressive and bond strengths. Physical tests and long-term aging have continued.

A short-term test program has been added, to determine the effects of thermal cycling on one of the SwRI 150°C hydrothermal cements. This cement is for possible use in the completion of a hot dry rock geothermal well at Fenton Hill, New Mexico. Data indicates that even though the bond might be broken during the cooling down and reheat of these wells, the SwRI formulation will reheat the bond, maintaining good adhesion to the casing formation.

## II. REVIEW AND EVALUATION

We have continued to be alert for articles, etc., concerned with geothermal cementing, well completion and, generally, with all aspects of geothermal activities. However, it has become a very minor part of the research effort at this time.

### III. SwRI HIGH-TEMPERATURE CEMENT RESEARCH

#### A. Formulation Optimization

We have continued to search for the optimum formulation for use at 316°C and above. Table I gives the various recipes which will be useful at these temperatures. All of these gave us at least two hours pumping time at 316°C.

TABLE I  
 SwRI HYDROTHERMAL CEMENT FORMULATIONS  
 FOR USE AT 316°C AND HIGHER

<u>Ingredients</u>	<u>#60</u>	<u>#70</u>	<u>#80</u>	<u>#90</u>	<u>#100</u>	<u>#110</u>
Sand		50			50	
Flour	50	25	50	50	25	50
Britesil	10	10	10	10	10	10
Anhydrous Sodium Silicate	10	5	10	10	5	10
Bentonite	.5	3	.5	.5	3	.5
Al(OH) <sub>3</sub>	7					
Al <sub>2</sub> O <sub>3</sub>		5				
TiO <sub>2</sub>					8	
ZrO <sub>2</sub>			7			
La(OH) <sub>2</sub>						7
LaO <sub>2</sub>				7		
H <sub>2</sub> O	23	18	23	23	20	23



## B. Physical Properties Evaluation

### 1. General

We have continued to experiment with modifications to the various high-temperature formulations to respond better to placement and curing variables. However, the choice has been made to use either  $\text{Al}_2\text{O}_3$  or  $\text{ZrO}_2$  as the activation agent for temperatures of  $316^\circ\text{C}$ . Where necessary, in the future, if a longer pumping time than 2 hrs. might be necessary, we can make additions of one of several of the following oxides: lanthanum, hafnium or vanadium.

Curing and aging of our specimens has been done under simulated downhole geothermal conditions. This provides a more realistic and severe test of a cement to be used for completing a well with a bottom-hole temperature of  $316^\circ\text{C}$  and higher. We do not pre-cure or pre-set the specimens at a lower temperature and then expose them to the high heat for long-term aging. However, in many geothermal wells, it may be possible to cool the well down to  $150^\circ\text{C}$  or lower for periods of several hours. This would allow casing to be cemented without a flash set, or with few pumping problems. A cement with a high compressive strength would be required to withstand the force of an expanding casing upon reheating to the bottom temperatures.

The long-term exposure of specimens at  $316^\circ\text{C}$  has been done in a so-called static steam and brine environment. Enough liquid is placed in the autoclave to provide a fully saturated vapor condition. Other specimens are being cured presently, submerged in brine at  $316^\circ\text{C}$ . The brine solution used is a synthetic, simulating the "average" brine at the Mesa geothermal field as shown in Table II.

TABLE II

DISSOLVED SOLIDS CONTENT OF 5 EAST MESA WELLS, ppm

<u>Component</u>	<u>5-1A</u>	<u>5-1B</u>	<u>5-1C</u>	<u>6-1A</u>	<u>6-1B</u>	<u>Composite Average</u>
SiO <sub>2</sub>	201	130	130	128	220	162
Na	593	798	798	9,000	5,130	3,264
K	29	49	49	1,047	632	281
Ca	16	46	46	896	389	279
Mg	2	4	4	15	22	9
Cl	454	825	825	15,870	9,014	5,398
SO <sub>4</sub>	102	169	196	192	20	136
HCO <sub>3</sub>	331	705	717	126	305	437

2. Compressive Strength

One-inch cylinders and two-inch cubes have been made from several formulations, cured for periods of 14 and 28 days, and tested for compressive strength. Results of these tests after specimens were cured and aged in a saturated steam and/or brine environment are as shown in Table III. The Table is a summary of compressive and bond strength tests performed on various recipes and cured at the indicated times and temperatures. Each specimen number and type is an average of three specimens made according to the recipes shown in Table I.

TABLE III  
SUMMARY OF STRENGTH TESTS

<u>Specimen No.*</u>	<u>Activating Agent</u>	<u>Cure Time (days)</u>	<u>Compressive Strength psi</u>	<u>Shear Bond Strength psi</u>
60	Al(OH) <sub>3</sub>	28	3410	820
70	Al <sub>2</sub> O <sub>3</sub>	28	4156	1490
80	ZrO <sub>2</sub>	14	3650	1270
90	LaO <sub>2</sub>	28	1200	630
100	TiO <sub>2</sub>	14	1840	800
110	La(OH) <sub>2</sub>	14	848	**

NOTES:

All specimens were cured at 316°C and 2000 psi.

\* From Table I.

\*\* Cement did not harden sufficiently in 14 days.

### 3. Bond Strength

Shear bond strength tests have been made on specimens cured in steel cylinders. These measure 1-3/8-inch I.D. by 2-inches long, with a 1/2-inch steel pin centered by use of end plates. The slurry was poured into these molds and specimens cured in saturated steam/brine at 316°C/2000 psi for periods of from 14 to 28 days. Results are shown in Table III, as an average bond strength of three or four specimens.

The steel cylinders were machined from standard 1-3/8-inch ungalvanized pipe. No attempt was made to polish the inside of the pipe before filling with cement slurry. The 1/2-inch steel center pin was machined from 5/8-inch stock and polished with 600-grit paper.

### 4. Future Work

In the next quarter, the 28-day exposure tests will be completed on the zirconia recipe. Most, if not all, of the remaining permeability tests should also be completed during the sixth quarter. If it can be arranged, several hydraulic bond tests will be run on the alumina recipes.

We have noticed that the formulation using aluminum hydroxide without sand would not harden at 316°C after 48 hours curing time. Additions of fine silica sand provided a curing time of four hours at 316°C.

#### IV. CYCLICAL BOND TESTS OF SwRI 150°C CEMENT

A proposal was accepted for SwRI to perform certain tests on a 150°C formulation for possible application in the remedial cementing of the injection well at Fenton Hill near Los Alamos, New Mexico. The program consists primarily of a series of cyclical bond tests to try to simulate the cyclic conditions in the Hot Dry Rock (HDR) experimental well. Each cycle was about 48 hours long, cooling down from 200°C to 35°C, followed by reheating to 200°C, etc. A complete test was on the basis of 1, 3, and 7 cycles. Tests were run at 5000 psi, equivalent to the HDR well bottom-hole temperature. At the end of each sequence of cycles, the specimens were removed from the autoclave for the purpose of making bond and compressive strength tests, and then replaced for the next sequence of thermal cycling.

Test specimens were of two types:

- (1) Pipe-in-pipe, or steel rod-in-pipe, with cement in the annulus between pipes. This is our standard bond test.
- (2) Pipe-in-rock. This closely simulates the conditions downhole with the three different thermal coefficients to deal with. We believe that the 8-in. long sections were sufficient for obtaining good bond strength data.

Compressive strength and permeability tests will also be made on the cement after exposure to the cyclical conditions. These specimens will be removed at the end of the 1-, 3-, and 7-cycle sequences as in the above bond tests.

It has been our intention to show that our hydrothermal cement will form an excellent bond to the casing and rocks with good bond strengths. If the casing shrinks away from the SwRI cement, breaking the bond, then

expands again with an increase in heat flux, the cement bond will "heal" and nearly regain its maximum strength within 24 to 48 hours.

With the above thermal cycling tests, SwRI was asked to run curing tests at 80, 100, 125 and 150°C. This was prompted by the National Bureau of Standards (NBS) failing to obtain good curing properties on the SwRI 150°C cement formulation containing zinc oxide as the activator. A decision was made by SwRI to switch to the use of a higher temperature activation material, aluminum hydroxide. The NBS laboratory tests confirmed that the  $\text{Al(OH)}_3$  formulation cured properly and had good mechanical properties.

However, the LASL HDR test well had recovered thermally only to about a maximum of 150°C at the bottom of the casing (9600 ft.) and not much more than about 130°C at 9200 to 9400 feet depths. It became evident that the aluminum hydroxide formulation, because of the lower test hole temperature, might not set for possibly a week or more. Therefore, the series of curing tests were made at each of the above temperatures. Samples of cement were pulled at the end of 72 hours, and if not properly cured, every two or three days until a good cure was obtained or it was determined that the cement would take too long a time, i.e., 14 days, to harden. Table IV shows the results of this series of tests.

TABLE IV  
LONG-TERM CURING AT LOW TEMPERATURES

<u>Temp. (°C)</u>	<u>Length of Cure (Days)</u>	<u>Results</u>
80	12	Uncured, gelled
80	15	Firm, but only partially cured
100	12	Firm
100	15	Hard, but not completely cured
125	12	Hard cure - OK
150	5	Hard cure - OK

The results of the tests for bond strength on pipe and rock specimens are shown in Table V.

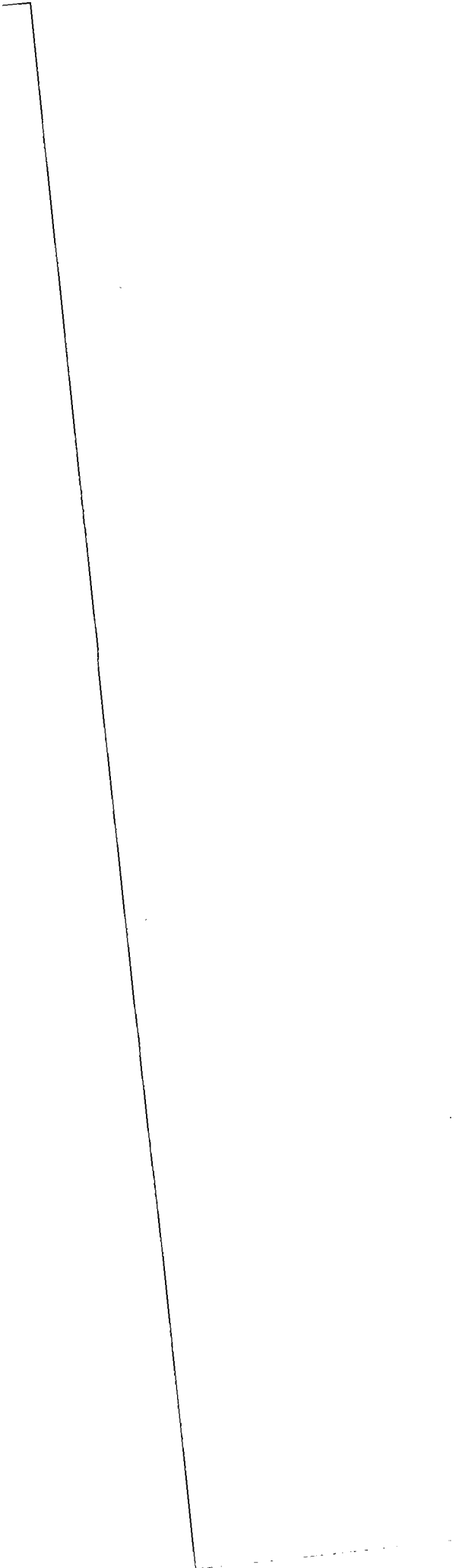
TABLE V  
SHEAR BOND TESTS

<u>Specimen</u>	<u>Cycles</u>	<u>Strength (psi)</u>
Rock	1	100
	3	72
	7	700
Rock	1	188
	3	130
	7	1068
Steel cylinder	1	86
	3	94
	7	not completed
	7	1242
	7	1258

Compressive strength tests of specimens cured with the above bond test specimens were 385 psi and 334 psi at the end of the 3 cycles. Measurements were not made after the first cycle. One specimen was tested at the end of the 7 cycles, with a strength of 3200 psi.

On December 19, 1978, a meeting was held at LASL, G4 Division, Los Alamos, New Mexico. At this meeting, members from LASL, NBS (Washington), and SwRI, discussed the above thermal tests and the tests performed at NBS. Because of the difficulties in resolving differences in curing tests, bond tests and other anomalous behavior, it was decided not to use the SwRI aluminum hydroxide formulation in the remedial cementing of the Fenton Hill test well. Further testing and studies will be performed as time and funds permit, to resolve the problems indicated above.





APPENDIX 5

BNL Contract 418691-S

PHOSPHATE BONDED GLASS  
CEMENTS FOR GEOTHERMAL WELLS

Technical Report No. 6  
October to December, 1978

from

Department of Materials and Chemical Engineering  
University of Rhode Island  
Kingston, Rhode Island

to

Process Technology Division  
Department of Applied Science  
Brookhaven National Laboratory  
Upton, New York, 11973

Contributors: T. J. Rockett  
N. Thakore  
S. J. Yuh

## I. Introduction

This report covers the work completed on contract 418691-S between October 1, 1978 and December 31, 1978. The tasks performed fall into two major groups. The first set of tasks are all related to the stability of silicate glasses in phosphate solutions, and the second set of tasks involve the equilibrium relationships in the system  $\text{CaO}-\text{Al}_2\text{O}_3-\text{P}_2\text{O}_5-\text{H}_2\text{O}$ .

These tasks were pursued to obtain basic information which will be used to design cement compositions to be tested for stability and strength at geothermal conditions. The overall goal is to generate a glass frit which when mixed with phosphoric acid will set to a cement. By understanding the corrosion of silicate glasses in phosphoric acid, a frit can be obtained which will interact at a controlled rate. By knowing the phases which form in the system  $\text{CaO}-\text{Al}_2\text{O}_3-\text{P}_2\text{O}_5-\text{H}_2\text{O}$  the composition of the glass may be tailored to yield a phase which when formed in the geothermal environment will remain stable.

## II. Glass Solubility

### a. Experimental Procedure

Details of the experimental procedure for the corrosion studies have been described in previous reports. Essentially, fibers are drawn from melts of various compositions and these are treated in the phosphate solutions for different times and the weight loss is measured.

The suspended fiber method was used to obtain weight loss data for (i) 50% SiO<sub>2</sub> glass in 30% and 50% H<sub>3</sub>PO<sub>4</sub> at 40°C and 90°C, (ii) 40% SiO<sub>2</sub> glass in 10% and 50% H<sub>3</sub>PO<sub>4</sub> at 40°C and 90°C and in 30% H<sub>3</sub>PO<sub>4</sub> at 65°C. This is a continuous weight change method. A single fiber is suspended from the bottom of a balance by a platinum wire such that the fiber is totally immersed in phosphoric acid placed inside an oven and maintained at a pre-determined temperature. Weight loss readings are made continuously. The data obtained are the weight loss of the fiber plus the buoyancy change due to reduced fiber volume. A correction for this is made by knowing the glass and the acid density. This method cannot be used if a silica film is formed on the surface because the density and porosity of the film are not known. Experiments were conducted on two series of glasses during this reporting period. Work was completed on the ternary glasses having the following formula XCaO: XAl<sub>2</sub>O<sub>3</sub>: 100-2X SiO<sub>2</sub> where X was varied from 20 to 30 weight percent. The second series of glasses was a sodium containing series with the general composition 7 Na<sub>2</sub>O: X CaO: X Al<sub>2</sub>O<sub>3</sub>: 93-2X SiO<sub>2</sub>. In this series the composition was varied from X = 16.5 weight percent to X = 26.5 weight percent. It should be mentioned that both of these series of glass contain about equal numbers of Ca<sup>++</sup> ions and Al<sup>+++</sup> ions.

b. Temperature Dependence of Corrosion

The corrosion rate of the ternary glasses has been determined at three temperatures. These values are shown in Table 1. Figure 1 reveals that if these data are plotted against reciprocal temperature a straight line is formed. From the extrapolation

TABLE 1

Temperature Dependence of Rate of Corrosion

40 SiO<sub>2</sub>:30 CaO:30 Al<sub>2</sub>O<sub>3</sub>

30% H<sub>3</sub>PO<sub>4</sub>

Temperature (°C)	Temperature (°K)	1/T (°K <sup>-1</sup> )	Rate of Dissolution of glass ( $\frac{\text{gms}}{\text{cm}^2\text{-hr}}$ )
40	313	0.00319	130.43 x 10 <sup>-4</sup>
65	338	0.00296	337.3 x 10 <sup>-4</sup>
90	363	0.00275	1156.5 x 10 <sup>-4</sup>

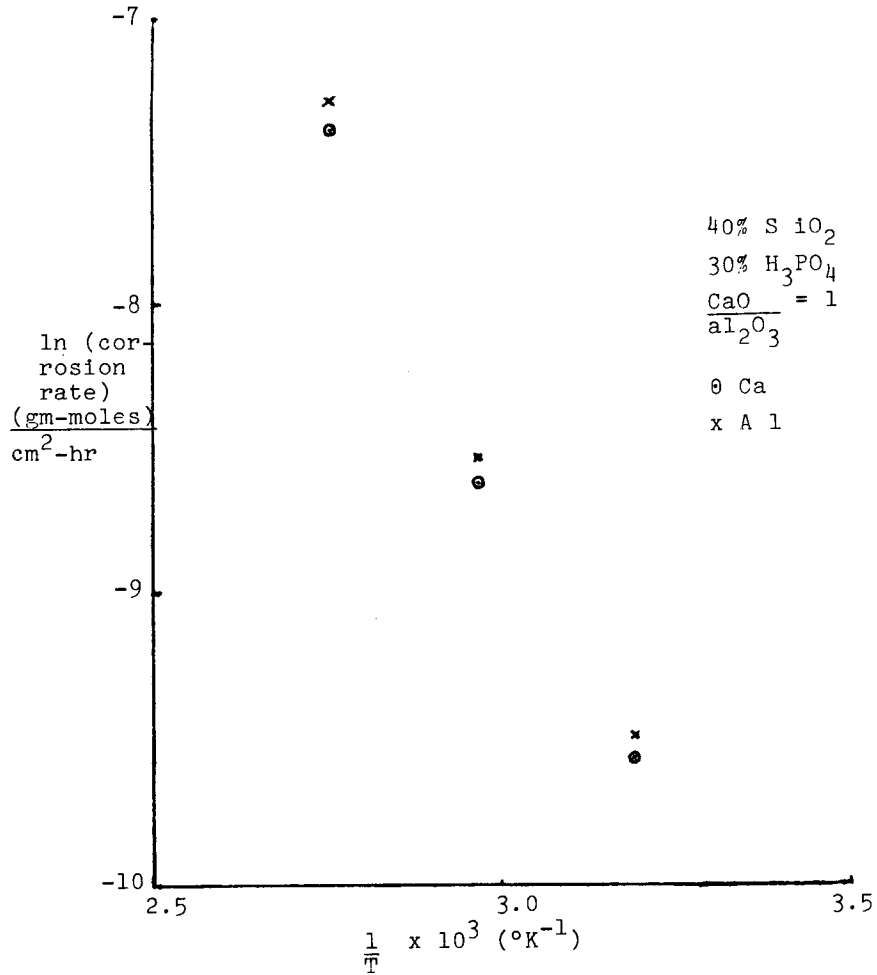


Figure 1. Activation energy determination.

of this line the corrosion rate of temperatures of 200°C and higher (those temperatures expected in a geothermal environment) may be found. Furthermore, this type of plot can be used to find an activation energy by measuring the slope of the corrosion curve.

Knowing the amount of  $\text{Ca}^{++}$  and  $\text{Al}^{+++}$  in the glass fibers, the glass dissolution rate can be converted to  $\text{Ca}^{++}$  and  $\text{Al}^{+++}$  extraction rates. These data are given in tables 2 and 3. Making the assumption that the breakdown mechanism for the glass is controlled by the rate at which the ion exchange reaction  $\text{H}^+(\text{solution}) + \text{Ion}(\text{glass}) \rightarrow \text{H}^+(\text{glass}) + \text{Ion}(\text{solution})$  takes place, the activation energy for this reaction can be calculated as follows:

1. The extraction rate for  $\text{Ca}^{++}$  can be given as

$$K_1 = Ae^{-\frac{E}{RT_1}}$$

where A is a constant, E is the activation energy for the reaction, R is the gas constant and  $T_1$  is the temperature.

2. The reaction rate,  $K_2$ , at a second temperature  $T_2$  is given as

$$k_2 = Ae^{-\frac{E}{RT_2}}$$

3. The ratio of the reaction rates at two different temperatures is

$$\frac{k_1}{k_2} = \frac{Ae^{-\frac{E}{RT_1}}}{Ae^{-\frac{E}{RT_2}}} = e^{-\frac{E}{RT_1} + \frac{E}{RT_2}}$$

4. Taking the natural log the following expression is obtained

$$\ln \frac{k_1}{k_2} = \frac{-E}{R} \left( \frac{1}{T_1} - \frac{1}{T_2} \right)$$

5. Using the value of the gas constant  $R = 1.987$  cal/deg. mole and the data from table 2, the activation energy can be found.

$$\ln \frac{6.98 \times 10^{-5}}{6.19 \times 10^{-4}} = \frac{-E}{1.987} \quad (.00319 - .00275)$$

and

$$E = 9.86 \text{ Kcal/mole}$$

An identical value will be found for  $Al^{+++}$ . The data from table 3 shows the values for K at different temperatures is the same as the values for calcium. This is because there are equal numbers of calcium and aluminum ions in the two glasses and the measured value-weight loss is assumed to result from a loss of calcium and aluminum at the same rates.

c. Corrosion of Sodium Containing Quarternary Glasses

The rate at which sodium containing glasses are broken down by phosphoric acid solutions has been determined for the compositions having the general formula  $7 Na_2O : X CaO : X Al_2O_3 : 93 - 2X SiO_2$ . The dissolution rates in the 30%  $H_3PO_4$  solution at  $40^\circ C$  are given in table 4. The data are plotted in figure 2.

As expected, the rates are higher for the sodium glasses with same silica concentrations. The drastic change in solubility near 50% silica is true of these glasses as was the case with the soda-free glasses. This drastic change supports the theory presented for the soda-free glasses that they undergo a phase separation

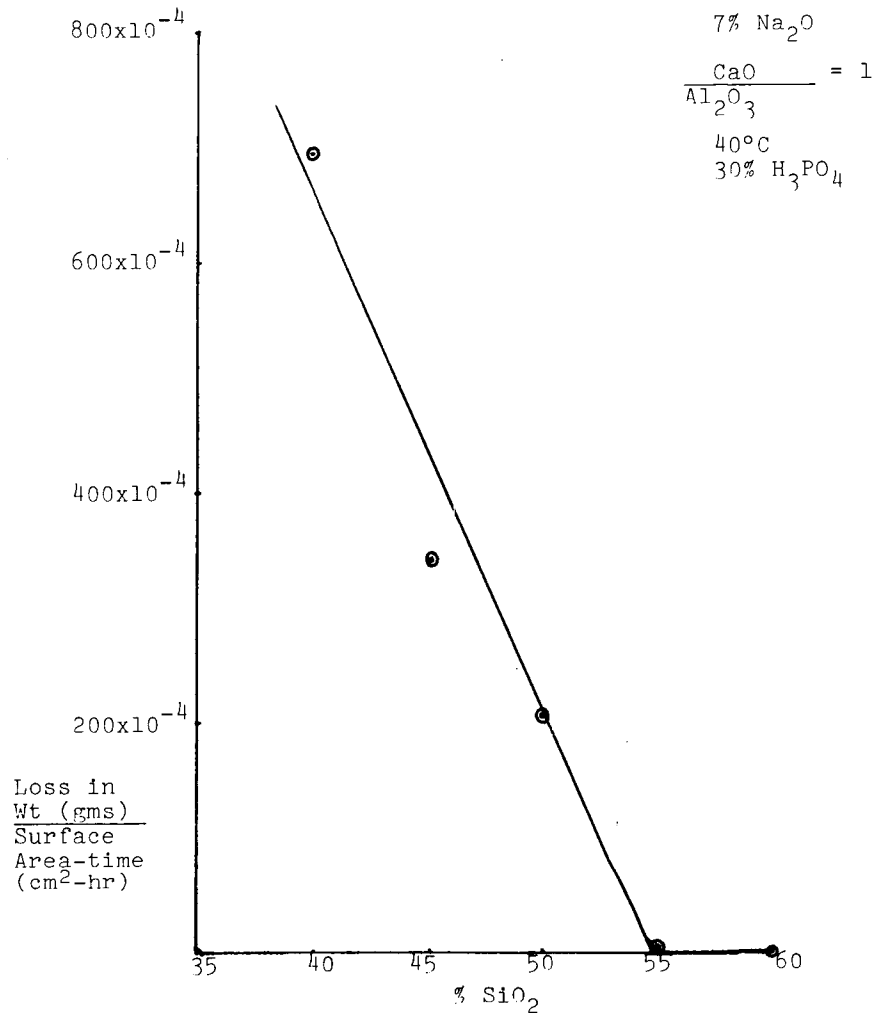


Figure 2. Corrosion rate of sodium containing glasses as a function of silica content.



Table 2  
Temperature Dependence of  
Calcium Extraction Rate

$\frac{1}{T}$ ( $^{\circ}\text{K}^{-1}$ )	Glass dissolution rate $\left(\frac{\text{gms}}{\text{cm}^2\text{-hr}}\right)$	$\text{Ca}^{2+}$ extraction rate $\left(\frac{\text{gm-moles}}{\text{cm}^2\text{-hr}}\right)$	$\ln(\text{Ca}^{2+}$ extraction rate)
0.00319	$130.43 \times 10^{-4}$	$6.98 \times 10^{-5}$	- 9.57
0.00296	$337.3 \times 10^{-4}$	$1.81 \times 10^{-4}$	- 8.62
0.00275	$1156.5 \times 10^{-4}$	$6.19 \times 10^{-4}$	- 7.39

Table 3  
Temperature Dependence of  
Aluminum Extraction Rate

$\frac{1}{T}$ ( $^{\circ}\text{K}^{-1}$ )	Glass dissolution rate $\left(\frac{\text{gms}}{\text{cm}^2\text{-hr}}\right)$	$\text{Al}^{3+}$ extraction rate $\left(\frac{\text{gm-moles}}{\text{cm}^2\text{-hr}}\right)$	$\ln(\text{Al}^{3+}$ extraction rate)
0.00319	$130.43 \times 10^{-4}$	$7.67 \times 10^{-5}$	- 9.48
0.00296	$337.3 \times 10^{-4}$	$1.98 \times 10^{-4}$	- 8.53
0.00275	$1156.5 \times 10^{-4}$	$6.80 \times 10^{-4}$	- 7.29

during cooling which greatly affects the corrosion behaviour. At higher silica concentrations a continuous silica phase is formed which contains dispersed glass units of sodium, calcium, aluminum and silica and which would be highly soluble but they are isolated from the solution by the insoluble silica network. At lower silica content, the glass structure is inverted. The continuous phase is very soluble releasing colloidal particles of a silica rich and insoluble phase to the corrosive liquid. The dimensions of the included units in both cases is the order of 30-50Å.

The major conclusion for geothermal cements is that corrosion rates can be controlled by varying the silica content. However, extreme care must be taken in designing the cement powder because a narrow range of compositions exist which separate the insoluble glasses from the extremely soluble glasses. On one side of this range, setting will be extremely rapid and on the other side, no cementing will be possible.

d. Effects of Acid Concentration on Corrosion Rate

The solubility of glass fibers of three different compositions was examined in the 10 weight percent phosphoric acid, 30 wt %  $H_3PO_4$  and 50 wt %  $H_3PO_4$ . The data are given in table 5 and figure 3 shows the trends.

The calcium aluminosilicate glass has a maximum dissolution rate in the 30% acid. The rate in 50% and 10% acid is virtually the same. The trend is repeated at 90°C with the 30% rate being twice that of the 10% and 50% rates. The increase from 10 to 30 can be explained by the increase in  $H^+$  activity. The drop-off at 50% is probably caused by the extreme phosphate ion

Table 4

Dissolution Rate With Silica Concentration  
In Sodium Calcium Aluminosilicate Glasses

Temperature = 40°C

Solution = 30% H<sub>3</sub>PO<sub>4</sub>

<u>% SiO<sub>2</sub></u> <u>in the glass</u>	<u>Dissolution rate</u> <u>(gms/cm<sup>2</sup> - hr)</u>
60	0
55	3.30 x 10 <sup>-4</sup>
50	204.8 x 10 <sup>-4</sup>
45	343.95 x 10 <sup>-4</sup>
40	692 x 10 <sup>-4</sup>

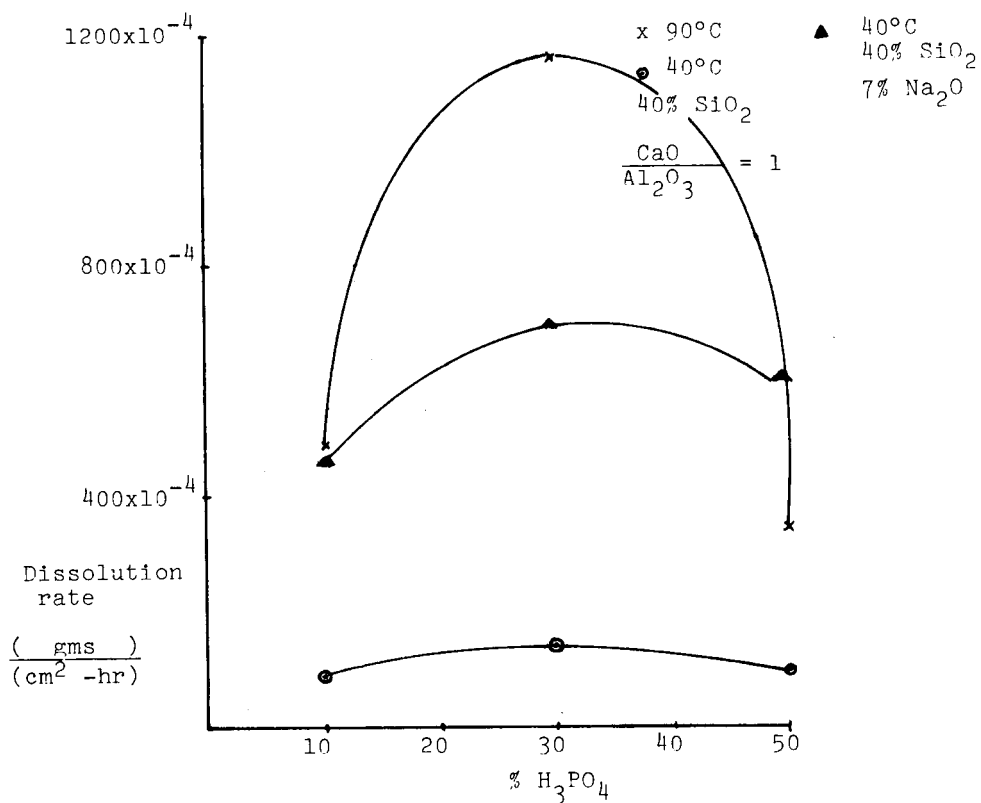


Figure 3. Effect of acid concentration on corrosion rate of 40% SiO<sub>2</sub> glass.

TABLE 5

Effect of Acid Concentration  
on Rate of Corrosion

Glass = 20 CaO:30 Al<sub>2</sub>O<sub>3</sub>:40% SiO<sub>2</sub>

Temperature = 40°C

<u>Acid Concentration</u> wt % H <sub>3</sub> PO <sub>4</sub>	<u>Rate</u> $\left(\frac{\text{gms}}{\text{cm}^2\text{-hr}}\right)$
50	93.82 x 10 <sup>-4</sup>
30	130.4 x 10 <sup>-4</sup>
10	89.35 x 10 <sup>-4</sup>

40% SiO<sub>2</sub>

90°C

<u>Acid Concentration</u> wt % H <sub>3</sub> PO <sub>4</sub>	<u>Rate</u> $\left(\frac{\text{gms}}{\text{cm}^2\text{-hr}}\right)$
50	341.59 x 10 <sup>-4</sup>
30	1156.5 x 10 <sup>-4</sup>
10	493.5 x 10 <sup>-4</sup>

50% SiO<sub>2</sub>

40°C

<u>Acid Concentration</u> wt % H <sub>3</sub> PO <sub>4</sub>	<u>Rate</u> $\left(\frac{\text{gms}}{\text{cm}^2\text{-hr}}\right)$
50	9.59 x 10 <sup>-4</sup>
30	11.29 x 10 <sup>-4</sup>

TABLE 5 (CONTINUED)

Effect of Acid Concentration  
on Rate of Corrosion

50% SiO<sub>2</sub>

90°C

<u>Acid Concentration</u> wt% H <sub>3</sub> PO <sub>4</sub>	<u>Rate</u> ( $\frac{\text{gms}}{\text{cm}^2\text{-hr}}$ )
50	82.03 x 10 <sup>-4</sup>
30	145.1 x 10 <sup>-4</sup>

40% SiO<sub>2</sub>

7% Na<sub>2</sub>O

$\frac{\text{CaO}}{\text{Al}_2\text{O}_3} = 1$

40°C

<u>Acid Concentration</u> wt% H <sub>3</sub> PO <sub>4</sub>	<u>Rate</u> ( $\frac{\text{gms}}{\text{cm}^2\text{-hr}}$ )
50	551.68 x 10 <sup>-4</sup>
30	692 x 10 <sup>-4</sup>
10	493 x 10 <sup>-4</sup>

concentration which could form insoluble species at the corroding interface.

The same trend is observed for the glasses containing sodium oxide, and it is presumed that a mixed ion effect is responsible for the low rates observed in the 50% solution. These glasses will be tested for cementing properties and the cement behaviour will be related to the solubility properties.

### III. The System CaO-Al<sub>2</sub>O<sub>3</sub>-P<sub>2</sub>O<sub>5</sub>-H<sub>2</sub>O

The phase relations in the quaternary system CaO-Al<sub>2</sub>O<sub>3</sub>-P<sub>2</sub>O<sub>5</sub>-H<sub>2</sub>O are under investigation at 200°C to determine which phases are stable at these conditions. The technique for sealing calcium aluminate powders and phosphoric acid liquids in glass tubes and holding in furnaces until equilibrium is reached has been discussed in previous reports. The equilibrium phases are identified by X-ray diffraction analysis and by optical microscopy.

Thus far, two sections have been examined in the system - the water - P<sub>2</sub>O<sub>5</sub> - 50 Al<sub>2</sub>O<sub>3</sub>:50 CaO plane and the water - P<sub>2</sub>O<sub>5</sub> - 25 Al<sub>2</sub>O<sub>3</sub>:75 CaO plane. The results are presented in table 6 and the data are plotted in figures 4 and 5. The 75% CaO:25 Al<sub>2</sub>O<sub>3</sub> plane shows increased solubility of solids in the 30% phosphoric acid solution. The crystalline phases stable at 200°C are berlinite and monetite. No evidence for crandallite or any other calcium-aluminum phosphate compounds has been found. This investigation will also be continued during the coming quarter.

Table 6

Results of experiments made in the system

CaO-Al<sub>2</sub>O<sub>3</sub>-P<sub>2</sub>O<sub>5</sub>-H<sub>2</sub>O at 200°C

No.	Composition wt %			Time (hrs)	Phases Present
	50% CaO: 50% Al <sub>2</sub> O <sub>3</sub>	P <sub>2</sub> O <sub>5</sub>	H <sub>2</sub> O		
45-1	2.0	9.8	88.2	70	AlPO <sub>4</sub> + liq + Vap
45-2	4.0	9.6	86.4	96	AlPO <sub>4</sub> + Liq + Vap
45-3	6.0	9.4	84.6	120	AlPO <sub>4</sub> + Liq + Vap
45-4	8.0	9.2	82.8	120	AlPO <sub>4</sub> + Liq + Vap
45-5	10.0	9.0	81.0	120	AlPO <sub>4</sub> + X* + Liq + Vap
45-6	2.0	29.4	68.6	72	AlPO <sub>4</sub> + Liq + Vap
45-7	4.0	28.8	67.2	72	AlPO <sub>4</sub> + Liq + Vap
45-8	6.0	28.2	65.8	66	AlPO <sub>2</sub> + Liq + Vap
45-9	8.0	27.6	64.4	72	AlPO <sub>4</sub> + CaHPO <sub>4</sub> + Liq + Vap
45-10	10.0	27.0	63.0	66	AlPO <sub>4</sub> + CaHPO <sub>4</sub> + Liq + Vap
45-11	2.0	49.0	49.0	18	Liq + Vap
45-12	4.0	48.0	48.0	95	Liq + Vap
45-13	6.0	47.0	47.0	72	AlPO <sub>4</sub> + X* + Liq + Vap
45-14	8.0	46.0	46.0	95	AlPO <sub>4</sub> + X* + Liq + Vap
45-15	10.0	45.0	45.0	95	AlPO <sub>4</sub> + X* + Liq + Vap

\*X : unidentified phase, probably formed on cooling

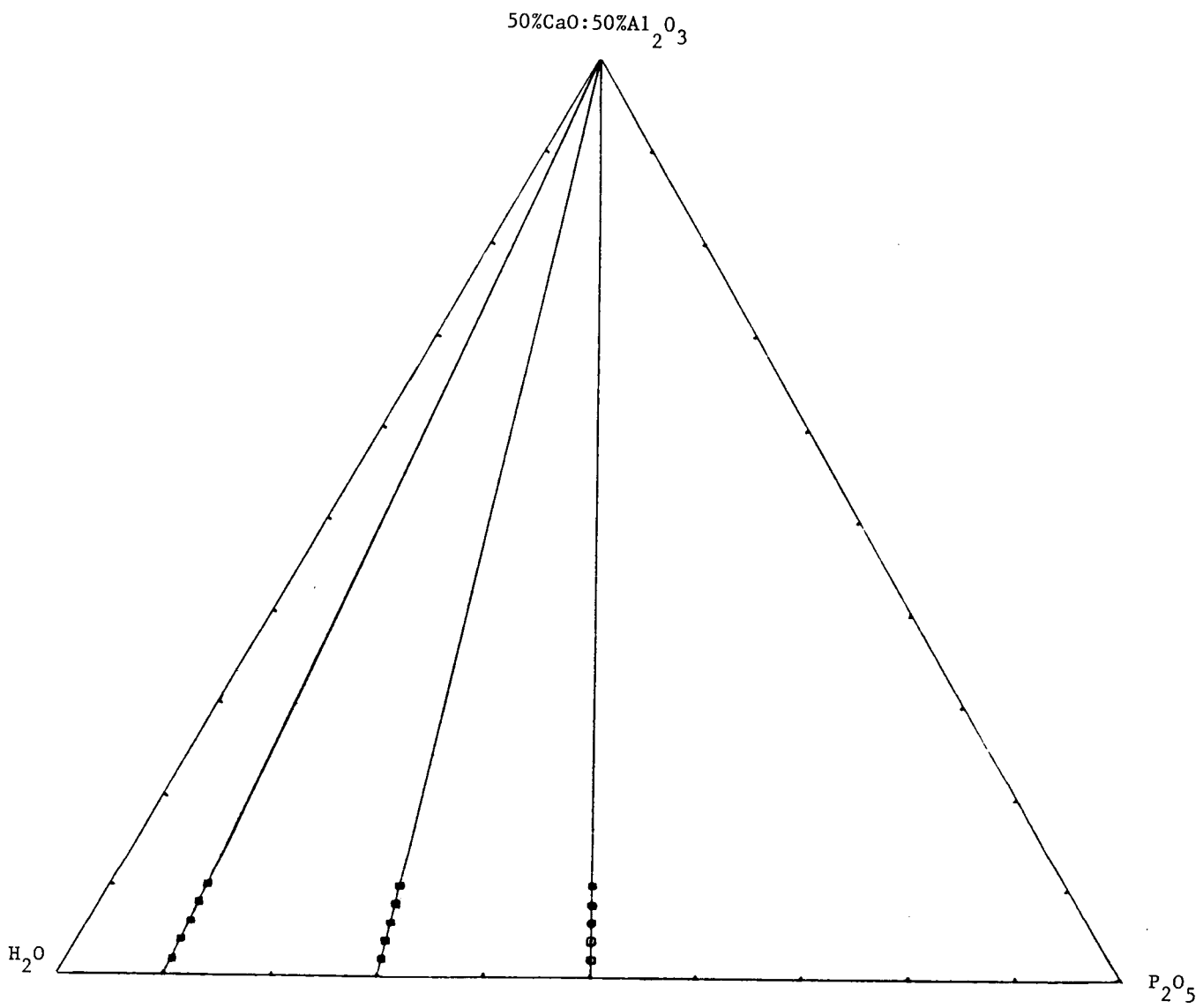


Figure 4. Compositions of firings made in the system CaO-Al<sub>2</sub>O<sub>3</sub>-P<sub>2</sub>O<sub>5</sub>-H<sub>2</sub>O.



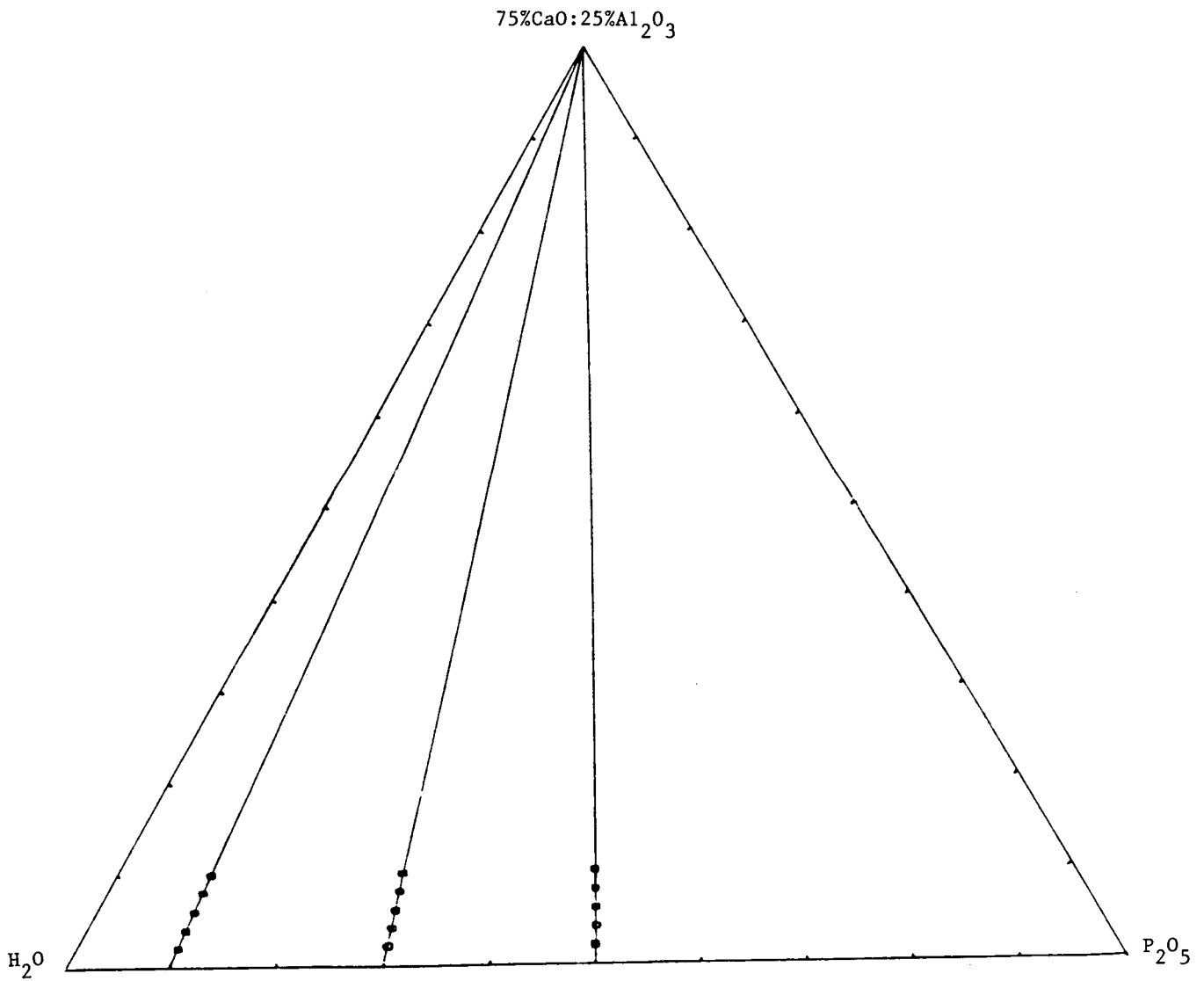


Figure 5. Compositions of firings made in the system  $\text{CaO}-\text{Al}_2\text{O}_3-\text{P}_2\text{O}_5-\text{H}_2\text{O}$ .